MINISTRY OF EDUCATION AND SCIENCE

SUMY NATIONAL AGRARIAN UNIVERSITY

Quilified scientific work (Manuscript)

HUANG CHAOLIN

UDC:631.6 : 631.95 : 631.46

Thesis

AGROFORESTRY FEATURES OF RESTORATION OF DEGRADED LANDS IN THE CONDITIONS OF THE GUANGDONG PROVINCE

Field of Study: 20 Agricultural science and food

Programme Subject Area: 201 Agronomy

for a Doctor Philosophy Degree (PhD)

The dissertation contains the results of own research. The use of ideas, results and texts of other authors are linked to the corresponding source.

Huang Chaolin / Huang Chaolin/

Huang Chaolin

数字签名者：Huang Chaolin
DN：cn=Huang Chaolin, o=Sumy National Agrarian University, email=857904446@qq.com, c=UA
日期：2026.07.10 01:53:54 +03'00'
Adobe Acrobat Reader 版本：2026.001.21691

Scientific supervisor: Yaroshchuk Roman, PHD (Agricultural Sciences), Associate Professor

Sumy 2026

ANNOTATION

Huang Chaolin. Agroforestry Features of Restoration of Degraded Lands in the Conditions of the Guangdong Province. Manuscript. Thesis for a Doctor Philosophy Degree (PhD): Specialty 201 «Agronomy». – Sumy National Agrarian University, Sumy, 2026.

This dissertation addresses the critical issue of land degradation in Guangdong Province, China's most economically dynamic region, which faces a unique contradiction between high-intensity development and inherent ecological fragility. The research establishes a comprehensive "macro - micro - technology - model" framework to develop scientifically optimized and regionally adapted agroforestry solutions for restoring degraded red soils.

The theoretical foundation analyzes the global severity of land degradation and its specific manifestations in China and Guangdong, identifying the region's distinctive degradation mechanisms: physical erosion from high temperature and heavy rainfall averaging 1777 mm annually, chemical pollution from industrialization, and biological degradation from urbanization. Agroforestry is established as a nature-based solution for simultaneously restoring soil health, enhancing biodiversity, and providing economic benefits.

The methodology integrates multi-scale approaches including macro-level remote sensing using MODIS and Landsat data with GIS spatial analysis and the RUSLE model to assess spatiotemporal degradation patterns from 2000 to 2020; technology optimization utilizing a hybrid Random Forest - Response Surface Methodology (RF - RSM) model to quantify synergistic effects of biochar, lime, and

leguminous green manure; and micro - mechanism investigation applying high - throughput sequencing and FAPROTAX functional prediction to analyze soil microbial community responses. A comprehensive statistical inference protocol was implemented, including Shapiro - Wilk normality testing, Levene's test for variance homogeneity, ANOVA with Duncan's multiple range post - hoc comparisons ($p < 0.05$), and PERMANOVA with 999 permutations for multivariate analyses.

The research reveals accelerating land degradation in the Pearl River Delta, with highly degraded areas surging by 196.58% from 2000 to 2020 and particularly rapid deterioration after 2010 showing a 97.83% increase. Soil erosion dominates the natural degradation process with 40% weight, spatially coupled with the land degradation index at $R^2 = 0.91$. Human factors shifted from early industrial expansion between 2000 and 2010, during which 82.6% of flat farmland was covered by factories, to later ecological policy regulation, demonstrating the effectiveness of the 2014 Ecological Control Line Plan which reduced severe desertification by 4% in protected zones.

The developed and validated RF - RSM hybrid model for optimizing agronomic measures identified through random forest analysis that available phosphorus with importance score 2.10 and soil pH with importance score 1.85 serve as core driving factors. Response surface methodology quantified optimal combinations of biochar at 8 to 12 tons per hectare, lime at 3 tons per hectare, and milkvetch green manure. The optimized scheme reduced available cadmium from 0.42 mg/kg to 0.11 mg/kg, representing a 73.8% reduction, increased soil porosity to 65.3%, and raised pH from 5.0 to 7.5. Cost - effectiveness improved dramatically as cadmium passivation cost decreased from 35.93 USD per percentage point using traditional methods to 9.19 USD per percentage point, with rebound rate controlled at only 3.8%.

Elucidation of microscopic mechanisms through soil microbiome analysis using high - throughput sequencing revealed that green manure application increased bacterial Chao1 richness by 23.6 - 60% and Shannon diversity by 7 - 28.1% under controlled pot conditions. Proteobacteria and Acidobacteria became dominant phyla, with ryegrass increasing Firmicutes abundance threefold. FAPROTAX functional prediction suggested significantly enhanced inferred nitrogen fixation, nitrification, fermentation, and chemoheterotrophic functional potentials. These inferred functional shifts require direct metatranscriptomic or enzymatic validation to confirm actual metabolic activity. Redundancy analysis identified pH, total nitrogen, and soil organic matter as core environmental drivers shaping microbial communities. These findings provide mechanistically grounded hypotheses for field restoration; however, their quantitative applicability to open - field agroecosystems requires dedicated field validation in future research.

Meta - analysis of 183 effect sizes from 15 published studies confirmed green manure increases crop yield by 13.8% and soil organic carbon by 17.3%. The synthesis of findings resulted in the design of three regionally differentiated agroforestry models as scientifically grounded pilot frameworks. The Pearl River Delta Rapid Improvement Model for heavy metal pollution achieves remediation within one year with 78.9% cadmium stabilization. The Eastern and Western Guangdong Forest - Fruit - Grass Composite Model for soil erosion reduces erosion modulus by 70 - 90%. The Northern Guangdong Near - Natural Transformation

Model for ecological barrier zones increases water conservation capacity by 20 - 40%. These proposed models showed synergistic production, ecology, and economy benefits in pilot trials, with land equivalent ratio increasing 30 - 50% and carbon sequestration potential 20 - 35% above monocultures.

In conclusion, this research provides a full - chain scientific framework from degradation pattern recognition to precision restoration technology optimization, establishing replicable agroforestry solutions for subtropical degraded red soils. The integrated approach achieves optimal balance between ecological restoration effectiveness and economic feasibility, offering theoretical guidance and practical support for sustainable land management in Guangdong Province and similar regions globally.

Importantly, all experimental agronomic findings are empirically grounded in an 18 - month field monitoring program (supplemented by controlled pot experiments). Long - term projections - including 3 - year reapplication cycles and carbon stability beyond 5 years - are presented as model - based hypotheses requiring future verification and should be interpreted with appropriate caution.

Keywords: land degradation, agroforestry, red soil restoration, heavy metal passivation, microbial community, RF - RSM model, Guangdong Province, soil function recovery, green manure, differentiated restoration models

АНОТАЦІЯ

Хуан Чаолінь. Агролісівницькі особливості відновлення деградованих земель в умовах провінції Гуандун. Рукопис. Дисертація на здобуття наукового ступеня доктора філософії (PhD): Спеціальність 201 «Агрономія»». – Сумський національний аграрний університет, Суми, 2026.

Дисертацію присвячено критичній проблемі деградації земель у провінції Гуандун – найбільш економічно динамічному регіоні Китаю, який стикається з унікальним протиріччям між високоінтенсивним розвитком та властивою екологічною вразливістю. Дослідження створює комплексну рамкову структуру «макро - мікро - технологія - модель» для розробки науково обґрунтованих та регіонально адаптованих агролісомеліоративних рішень для відновлення деградованих червоноземів.

Теоретична основа аналізує глобальну гостроту проблеми деградації земель та її специфічні прояви в Китаї та Гуандуні, визначаючи характерні для регіону механізми деградації: фізичну ерозію через високі температури та рясні опади (в середньому 1777 мм на рік), хімічне забруднення внаслідок індустріалізації та біологічну деградацію через урбанізацію. Агролісомеліорацію представлено як природоорієнтоване рішення для одночасного відновлення здоров'я ґрунтів, підвищення біорізноманіття та забезпечення економічних вигод.

Методологія інтегрує багатомасштабні підходи, включаючи макроаналіз із використанням даних дистанційного зондування (MODIS, Landsat) та

просторового аналізу в ГІС із моделлю RUSLE для оцінки просторово-часових закономірностей деградації з 2000 по 2020 рік; оптимізацію технологій за допомогою гібридної моделі випадкового лісу та методу поверхні відгуку (RF - RSM) для кількісного визначення синергічних ефектів від застосування біовугілля, вапна та бобових сидератів; а також дослідження мікромеханізмів із застосуванням високопродуктивного секвенування та функціонального прогнозування FAPROTAX для аналізу реакції мікробних угруповань ґрунту. Реалізовано комплексний протокол статистичного висновку, включаючи перевірку нормальності за Шапіро–Уїлком, перевірку однорідності дисперсій за Лівеном, дисперсійний аналіз з подальшими множинними порівняннями за Дунканом ($p < 0,05$) та PERMANOVA з 999 пермутаціями для багатовимірного аналізу.

Дослідження виявляє прискорення деградації земель у дельті Перлинної річки, де площа сильно деградованих територій зросла на 196,58% з 2000 по 2020 рік, з особливо швидким погіршенням після 2010 року (збільшення на 97,83%). Водна ерозія домінує в природному процесі деградації (вага 40%), просторово корелюючи з індексом деградації земель ($R^2 = 0,91$). Антропогенні фактори змістилися від ранньої промислової експансії у 2000 - 2010 роках, коли 82,6% рівнинних сільськогосподарських угідь було забудовано заводами, до пізнішого екологічного регулювання, що демонструє ефективність Плану екологічних контрольних ліній 2014 року, який зменшив площу сильної опустелювання на 4% на захищених територіях.

Розроблена та валідована гібридна модель RF - RSM для оптимізації агротехнічних заходів визначила за допомогою аналізу випадкового лісу доступний фосфор (показник важливості 2,10) та pH ґрунту (1,85) як ключові рушійні фактори. Метод поверхні відгуку кількісно визначив оптимальні комбінації: біовугілля (8 - 12 т/га), вапно (3 т/га) та сидерат із астрагалу. Оптимізована схема знизила вміст рухомого кадмію з 0,42 мг/кг до 0,11 мг/кг (на 73,8%), збільшила пористість ґрунту до 65,3% та підвищила pH з 5,0 до 7,5. Економічна ефективність значно покращилася: вартість іммобілізації кадмію знизилася з 35,93 долара США за відсоток при традиційних методах до 9,19 долара США за відсоток, а рівень повторного вивільнення становив лише 3,8%.

З'ясування мікроскопічних механізмів через аналіз мікробіому ґрунту за допомогою високопродуктивного секвенування показало, що застосування сидератів збільшило індекс багатства Чао1 для бактерій на 23,6 - 60% та індекс різноманіття Шеннона на 7 - 28,1% за контрольованих умов вегетаційного досліду. Протеобактерії та Ацидобактерії стали домінуючими типами, причому райграс збільшив чисельність Firmicutes втричі. Функціональне прогнозування FAPROTAX продемонструвало значне посилення функцій азотфіксації, нітрифікації, ферментації та хемогетеротрофії. Ці припущення потребують прямої метатранскриптомної або ферментативної верифікації для підтвердження фактичної метаболічної активності. Аналіз надлишковості визначив pH, загальний азот та органічну речовину ґрунту як основні екологічні чинники, що формують мікробні угруповання. Ці результати надають механістично обґрунтовані гіпотези для польового відновлення; однак їх кількісна застосовність до умов відкритих агроекосистем потребує спеціальної польової валідації в майбутніх дослідженнях.

Мета-аналіз 183 величин ефекту з 15 опублікованих досліджень підтвердив, що сидерати підвищують урожайність сільськогосподарських культур на 13,8%, а вміст органічного вуглецю в ґрунті – на 17,3%. Синтез результатів призвів до створення трьох регіонально диференційованих агролісомеліоративних моделей як науково обґрунтованих пілотних рамок. Модель швидкого відновлення для дельти Перлинної річки, призначена для боротьби із забрудненням важкими металами, досягає ремедіації менш ніж за один рік із 78,9% стабілізації кадмію. Композитна модель «ліс–фрукти–трави» для Східного та Західного Гуандуну, спрямована на боротьбу з водною ерозією, знижує модуль ерозії на 70 - 90%. Модель наближеного до природи трансформування для зони екологічного бар'єру Північного Гуандуну підвищує водоохоронну здатність на 20 - 40%. Ці моделі демонструють синергічні виробничі, екологічні та економічні вигоди у пілотних випробуваннях: коефіцієнт еквівалентності землі зростає на 30–50%, а потенціал секвестрації вуглецю – на 20 - 35% порівняно з монокультурами.

На завершення, це дослідження надає повну наукову рамкову структуру – від розпізнавання закономірностей деградації до оптимізації технологій точного відновлення, створюючи відтворювані агролісомеліоративні рішення для субтропічних деградованих червоноземів. Інтегрований підхід досягає оптимального балансу між ефективністю екологічного відновлення та економічною доцільністю, пропонуючи теоретичне обґрунтування та практичну підтримку для сталого управління земельними ресурсами в провінції Гуандун та подібних регіонах світу.

Важливо зазначити, що всі експериментальні агрономічні результати мають емпіричну основу в 18-місячній програмі польового моніторингу (доповненій контрольованими вегетаційними дослідами). Довгострокові прогнози – включаючи 3-річні цикли повторного внесення та стабільність вуглецю понад 5 років – представлені як модельні гіпотези, що потребують майбутньої верифікації, і повинні інтерпретуватися з відповідною обережністю.

Ключові слова: деградація земель, агролісомеліорація, відновлення червоноземів, іммобілізація важких металів, мікробне угруповання, модель RF - RSM, провінція Гуандун, відновлення функцій ґрунту, сидеральні добрива, диференційовані моделі відновлення.

LIST OF PUBLISHED WORKS ON THE TOPIC OF THE DISSERTATION

Articles in professional publications of Ukraine

1. **Huang Chaolin**, Yaroshchuk Roman. Study on the causes and restoration methods of cultivated land degradation in Guangdong province. *Bulletin of Sumy National Agrarian University. The Series: Agronomy and Biology*. 2025. Vol. 61. DOI: 10.32782/agrobio.2025.3.1.

2. **Huang Chaolin**, Yaroshchuk Roman. Research on Agroforestry for Combating Land Desertification in Guangdong Province.*Tavriya Scientific Bulletin. Series: Agricultural Sciences.* 2025. Vol. 145. DOI: 10.32782/2226-0099.2025.145.2.20.

3. **Huang Chaolin**, Yaroshchuk Roman. Pearl River Delta Region Cultivated Land Quality Evaluation. *Podilian bulletin: agriculture, engineering, economics.* 2025. Vol. 49. DOI: 10.37406/2706-9052-2025-4.1.

4. **Huang Chaolin**, Yaroshchuk Roman. Analysis of the Benefits of Green Manure Returning and Its Application in Ecological Farms. *Ukrainian Journal of Natural Sciences.* 2025. Vol. 14. DOI: 10.32782/naturaljournal.14.2025.15

Articles in scientific journals with an impact factor (Scopus, WS)

5. **Huang Chaolin**, Yaroshchuk Roman, Jiang Qinqin, Liu Yong. Effects of Green Manure Combined with Fertilizer on Microbial Communities in Poor Red Soil: A Case Study of Milk Vetch and Ryegrass. *Future of Food: Journal on Food, Agriculture and Society*, 2024, 12(2). DOI: 10.5281/zenodo.15041464

Abstracts of conferences

6. **Huang Chaolin**, Yaroshchuk Roman. Study on the characteristics of agriculture and forestry after the restoration of degraded land in Guangdong

province. Proceedings of VI International scientific and practical conference. (Kyiv, July 1-3, 2025). Sci-conf.com.ua. P. 15-18.

7. **Huang Chaolin**, Yaroshchuk Roman. The value of agroforestry in ecological restoration and sustainable agriculture. Proceedings of IX International scientific and practical conference. (Kyiv, September 22-24, 2025). Sci-conf.com.ua. P. 15-19.

CONTENT

ABBREVIATIONS

AM: Arbuscular mycorrhizal

AN: Ammonium nitrogen

AP: Available phosphorus

BBD: Box-Behnken design

CF: Chemical fertilizer (control treatment)

CK: Control (no fertilizer, no green manure)

Chao1: Chao1 richness estimator

DNA: Deoxyribonucleic acid

EPS: Extracellular polymeric substance

FAPROTAX: Functional Annotation of Prokaryotic Taxa

FVC: Fractional vegetation cover

GDP: Gross Domestic Product

GIS: Geographic Information System

HAF: Humic acid fertilizer (control treatment)

ITS: Internal Transcribed Spacer

KEGG: Kyoto Encyclopedia of Genes and Genomes

LCA: Life cycle assessment

LD: Land Degradation Index

LEfSe: Linear Discriminant Analysis Effect Size

LER: Land equivalent ratio

MAE: Mean Absolute Error

MG: Milk vetch + compound fertilizer

MH: Milk vetch + humic acid fertilizer

MO: Milk vetch + commercial organic fertilizer

MODIS: Moderate Resolution Imaging Spectroradiometer

MSE: Mean square error

NDVI: Normalized Difference Vegetation Index

NMDS: Non-metric Multidimensional Scaling

OMF: Commercial organic fertilizer (control treatment)

OP: Organic phosphorus

OTU: Operational Taxonomic Unit

PCoA: Principal Coordinates Analysis

PCR: Polymerase Chain Reaction

PERMANOVA: Permutational Multivariate Analysis of Variance

PICRUSt2: Phylogenetic Investigation of Communities by Reconstruction of Unobserved States 2

QIIME 2: Quantitative Insights Into Microbial Ecology 2

RDA: Redundancy Analysis

RDP: Ribosomal Database Project

RF-RSM: Random Forest - Response Surface Methodology

RG: Ryegrass (no fertilizer treatment)

RH: Ryegrass + humic acid fertilizer

RMSE: Root mean square error

RO: Ryegrass + commercial organic fertilizer

RSM: Response surface methodology

RUSLE: Revised Universal Soil Loss Equation

SAR: Synthetic Aperture Radar

SFRI: Soil Function Recovery Index

Shannon: Shannon diversity index

SOC: Soil organic carbon

SOM: Soil organic matter

TN: Total nitrogen

UAV: Unmanned Aerial Vehicle

UNCCD: United Nations Convention to Combat Desertification

UNITE: Unified system for the DNA based fungal species identification

USD: United States Dollar

INTRODUCTION

Actuality of theme. Guangdong Province, China's economic powerhouse, suffers from severe land degradation due to the conflict between intensive development and ecological fragility. Red soil erosion, heavy metal pollution, and biodiversity loss threaten food security and sustainable agriculture. Existing restoration methods lack integrated approaches tailored to subtropical conditions. This research addresses the urgent need for scientifically optimized agroforestry models combining biochar, lime, and green manure to restore degraded lands, providing both ecological remediation and economic benefits for the region's 127 million residents.

The purpose and objectives of the study. The purpose of this research is to develop scientifically optimized and regionally adapted agroforestry models for the restoration of degraded lands in Guangdong Province, addressing the unique contradiction between intensive economic development and ecological fragility through integrated macro-micro-technological approaches.

To achieve this purpose, the following objectives were established:

1. To analyze the spatiotemporal patterns and driving mechanisms of land degradation in the Pearl River Delta region from 2000 to 2020 using remote sensing, GIS spatial analysis, and the RUSLE model, identifying the interactive effects of natural factors and human activities on degradation processes.

2. To optimize key agronomic measures including biochar application, lime amendment, and leguminous green manure through the construction and validation of a hybrid Random Forest-Response Surface Methodology model, determining optimal

combinations that maximize soil function restoration while minimizing economic costs.

3. To investigate the microbial ecological mechanisms of restoration by analyzing soil microbial community responses to green manure application using high-throughput sequencing and FAPROTAX functional prediction, thereby revealing the regulatory pathways of carbon, nitrogen, phosphorus, and sulfur cycling functional microorganisms.

4. To construct and validate three regionally differentiated agroforestry restoration models tailored to the specific degradation characteristics of the Pearl River Delta suburban fringe, the hilly areas of eastern and western Guangdong, and the northern Guangdong ecological barrier zone, with comprehensive evaluation of their production, ecological, and economic benefits.

5. To provide scientific foundations and practical recommendations for policymakers and agricultural operators to support the large-scale implementation of sustainable land management practices in Guangdong Province and similar subtropical red soil regions globally.

The object of study. The object of this study is the processes, spatiotemporal patterns, and driving mechanisms of land degradation, and the subsequent ecological responses (including soil physicochemical degradation and microbial community shifts) in the degraded red soil regions of Guangdong Province, with specific focus on the Pearl River Delta, the hilly areas of eastern and western Guangdong, and the northern Guangdong ecological barrier zone.

Subject of study. The optimization of agronomic measures (specifically biochar, lime, and leguminous green manure combinations) and the elucidation of the underlying ecological (physicochemical and microbial) mechanisms of agroforestry systems for restoring degraded land in Guangdong Province.

Research methods. This study employs a comprehensive multi-scale methodological approach integrating remote sensing, field experimentation, laboratory analysis, and mathematical modeling. Macro-scale analysis utilizes remote sensing data from MODIS and Landsat satellites combined with GIS spatial analysis and the Revised Universal Soil Loss Equation (RUSLE) model to assess spatiotemporal patterns of land degradation in the Pearl River Delta from 2000 to 2020, extracting desertification indices, vegetation cover dynamics, and soil erosion intensity. Technological optimization employs a hybrid Random Forest-Response Surface Methodology (RF-RSM) model, with Random Forest algorithm identifying core driving factors through permutation importance analysis and Response Surface Methodology quantifying interaction effects between biochar application, lime amendment, and leguminous green manure species using a three-factor, three-level Box-Behnken experimental design. Multi-objective optimization integrates soil function recovery indices with economic cost analysis using Pareto frontier solutions. Microbial mechanism investigation applies high-throughput sequencing of 16S rRNA and ITS genes for bacterial and fungal community analysis, coupled with FAPROTAX functional prediction for metabolic pathway characterization, alongside soil physicochemical property analysis including pH, organic carbon, total nitrogen, available phosphorus, and heavy metal speciation. Statistical analyses include alpha and beta diversity indices, redundancy analysis, and Mantel tests for microbial-environmental correlations. Model validation incorporates field monitoring at 3, 6, 12, and 18-month intervals with error analysis and uncertainty quantification. Meta-analysis synthesizes 183 effect sizes from 15 published studies to evaluate green manure benefits on crop yield, carbon sequestration, and greenhouse gas emissions. Life cycle assessment integrates ecological, production, and economic indicators for comprehensive model evaluation.

The scientific novelty. The scientific novelty of this research lies in the following original contributions:

1. A comprehensive macro - micro - technology - model framework was further developed for degraded land restoration in subtropical red soil regions, systematically revealing the spatiotemporal evolution of land degradation in Guangdong Province (2000 - 2020) and the interactive driving mechanisms between natural vulnerability and human activities.

2. The composite degradation characteristics of the Pearl River Delta region were elucidated, demonstrating the intertwined effects of physical erosion, heavy metal pollution, and biological degradation.

3. A hybrid Random Forest-Response Surface Methodology (RF-RSM) model was developed and validated to optimize multi-factor agronomic measures, quantifying synergistic effects among biochar, lime, and green manure, with available phosphorus and soil pH identified as core drivers for soil function restoration.

4. High-throughput sequencing and FAPROTAX functional prediction

systematically characterized green manure effects on microbial community structure in degraded red soils, showing significant enhancement of bacterial diversity (Chao1 increase of 23.6 - 60%) and activation of C, N, and S cycling pathways, with Proteobacteria and Acidobacteria as key functional phyla.

5. The quantitative balance between ecological restoration effectiveness and economic feasibility has been established through multi-objective optimization.

The practical significance of the results. The research provides scientifically grounded pilot solutions for degraded land restoration in Guangdong Province. The optimized RF-RSM model offers farmers a cost-effective decision tool, reducing cadmium passivation costs from 35.83 to 9.19 USD per percent while achieving 73.8% heavy metal reduction. The three regional models are proposed as scientifically grounded pilot frameworks: the Pearl River Delta model demonstrated one-year remediation in pilot plots with 78.9% cadmium stabilization; the eastern and western Guangdong model reduces soil erosion by 70-90%; and the northern Guangdong model increases water conservation capacity by 20-40%. These models increase land equivalent ratio by 30-50% and carbon sequestration by 20-35% compared to monocultures. The findings support government policy formulation with differentiated subsidy recommendations of 2215 - 3324 USD per hectare for contaminated areas and 1107 - 2660 USD per hectare for ecological forest conversion. The established monitoring system enables real-time degradation assessment with errors below 8%, while identified microbial indicators provide quantifiable biomarkers for restoration progress evaluation. The integration of carbon trading mechanisms and understory economies offers farmers immediate income streams, promoting widespread adoption of sustainable land management practices.

The applicant's contribution. As the primary researcher and lead author of the associated publications, the applicant independently developed the "macro-micro-technology" research framework and executed the full experimental process. The applicant's specific contributions include performing spatiotemporal analysis of land degradation using RUSLE and GIS, developing the hybrid Random Forest-Response Surface Methodology (RF-RSM) model for agronomic optimization, and conducting laboratory investigations involving high-throughput sequencing and FAPROTAX functional prediction. Furthermore, the applicant personally performed the meta-analysis of 183 effect sizes, validated the regional agroforestry models through field monitoring, and drafted all scientific manuscripts and conference presentations resulting from this research.

Approbation of dissertation results. The results of the research were published and discussed at VI International Scientific and Practical Conference “GLOBAL TRENDS INSCIENCE AND EDUCATION” (Kyiv, 2025), IX International Scientific and Practical Conference “GLOBAL TRENDS INSCIENCE AND EDUCATION” (Kyiv, 2025).

Publications. Based on the research results, three articles were published in professional journals, one articles were published in Scopus, and two papers were exhibited at conferences as the first author.

The structure and scope of the dissertation. The dissertation structure contains an annotation, a list of abbreviations, an introduction, six chapters, conclusions, recommendations, a list of references, and eight appendixes. In this dissertation, it includes 33 tables and 22 figures.

CHAPTER 1

THEORETICAL AND SCIENTIFIC BACKGROUND OF AGROFORESTRY-BASED RESTORATION OF DEGRADED LANDS

(LITERATURE REVIEW)

1.1 Research Background and Significance

1.1.1 The Severity of Land Degradation Globally and in China

This seemingly silent and eternal land beneath our feet is undergoing an unprecedented and dramatic transformation. This is not a slow, natural evolution over geological time, but a rapid process of decline dominated by human activity. Land degradation, this often-overlooked "silent crisis," is eroding the Earth's surface at an alarming rate, threatening global ecological security and the continuity of human civilization. When we examine the severity of land degradation globally and in China, we see not only changes in soil physical properties, but also a grand narrative of resource depletion, ecological imbalance, and existential challenges.

Globally, the picture of land degradation is alarming. According to assessments by the United Nations Convention to Combat Desertification (UNCCD) and related international organizations, more than one-third of the Earth's surface is already in a state of moderate or severe degradation, and this proportion is continuing to rise (Yu et al., 2024). This degradation is not limited to a specific region, but transcends climate zones and national borders, from the arid grasslands of sub-Saharan Africa to the edge of the Amazon rainforest, from the over-cultivated plains of North America to the industrially polluted heartland of Eurasia, the land is losing its productivity and vitality (Pravalie et al., 2021; Pravalie et al., 2024). Every year, tens of millions of hectares of arable land disappear from the agricultural landscape due to drought, desertification, salinization, or soil erosion, meaning that against the backdrop of a continuously expanding population, the food base supporting human survival is shrinking (Li et al., 2025; Radwan et al., 2019; Sheng et al., 2025). Climate change and land degradation have formed a vicious feedback mechanism: degraded soil releases previously stored carbon, exacerbating the greenhouse effect, while droughts and torrential rains caused by extreme weather events, in turn, accelerate soil erosion and impoverishment (Shevchenko et al., 2024; Oishy et al., 2025; Lal et al., 2012; Phillips et al., 2022). This double blow threatens the livelihoods of hundreds of millions of people worldwide, especially in developing countries that are highly dependent on natural resources. Land degradation has directly led to increased poverty, social unrest, and even the emergence of ecological refugees. It is no longer simply an environmental issue, but has evolved into a core political and economic issue that constrains global sustainable development.

Focusing our attention on the East, China, as one of the world's most populous countries with the most complex topography, presents a particularly representative picture of the severity, complexity, and urgency of its land degradation problem. Although China is vast, its fundamental national condition of "a large population and limited land" means that every inch of its land bears extraordinary pressure (Guo Xudong & Wang Qingbin, 2026). China's land degradation is extensive and complex, involving diverse types such as soil erosion, fertility decline, acidification, desertification, and wetland loss, driven by both natural factors (climate variability) and human activities (intensive agriculture, urbanization, mining) (Liao et al., 2025;

Bai et al., 2009; Liu et al., 2025; Batunacun et al., 2019). The southern and eastern regions face significant degradation mainly in cropland and forest areas, with about 23% of the country showing declining ecosystem productivity despite overall increases in net primary productivity (Bai et al., 2009). In arid and semiarid zones like the Loess Plateau and drylands, large-scale afforestation efforts have reduced soil erosion but caused trade-offs such as water depletion and lowered groundwater tables, highlighting the need for restoration strategies that balance soil retention with water availability Jiang et al., 2019; Feng et al., 2025; Feng et al., 2024). Land degradation sensitivity has increased over recent decades in key basins due to interactions among vegetation quality, climate factors (precipitation, drought), soil conditions, and land use intensity (Molla et al., 2025). Although ecological restoration projects have improved some degraded lands and ecosystems - especially in arid regions - net land degradation still exceeds improvement overall, with rapid economic growth intensifying degradation near metropolitan areas (Zhou et al., 2025; Mao et al., 2018). Future sustainable land management in China requires adaptive policies that consider regional climatic conditions, human pressures, and the trade-offs between ecological restoration goals to prevent potential reversals of land degradation neutrality by mid-century.

First and foremost is the problem of desertification and sandification, the most painful ecological scar on northern China. From the edge of the Tarim Basin to the Inner Mongolian Plateau, the expansion of shifting sands once presented a perilous situation of "sand advancing and people retreating" (Shi Zhiyu & Dong Jihong, 2026). China’s intensive land development to support its large population and rapid economic growth has led to significant ecological deficits, including a 4.83% decrease in ecological land area from 1995 to 2015, with increased fragmentation and disturbance especially evident on both sides of the Hu Huanyong Line (Kong et al., 2021). Large-scale farmland occupation and urban expansion have contributed to ecological degradation, although projects like the Grain for Green program have promoted some ecological restoration, particularly in northwestern China (Kong et al., 2021; Chen et al., 2022). In arid regions such as the Tarim River Basin, cropland expansion has caused grassland loss and ecological deterioration, highlighting the tension between agricultural development and environmental sustainability (Hou et al., 2022). China's key forestry programs have improved vegetation cover, carbon sequestration, and soil erosion control but require more balanced planning and scientific involvement to address ongoing challenges (Wang et al., 2021). Rapid urbanization and industrial land use changes have further degraded ecosystem quality in provinces like Jiangsu and Zhejiang, causing losses in ecosystem service values despite efforts toward ecological compensation and restoration (Wu et al., 2020; Xu et al., 2025). Additionally, cropland redistribution to marginal lands in northeast and northwest China has undermined environmental sustainability by increasing erosion, water use, and habitat loss, suggesting that future policies should limit reclamation of vulnerable lands while boosting crop yields on existing farmland (Kuang et al., 2021).

Unlike the sandstorms raging in the north, southern China faces a more insidious yet equally deadly crisis of "rocky desertification." In the southwestern karst regions, long-term cultivation of steep slopes and vegetation destruction have eroded the already thin soil layer, exposing rugged bedrock (Li Dan, 2019). This form of land degradation, often referred to as "the cancer of the earth," has caused vast tracts of land to lose their ability to conserve water and support agricultural production, directly hindering the pace of rural revitalization. Meanwhile, Soil erosion remains a critical issue in the middle and upper reaches of the Yangtze River and especially on the Loess Plateau, where loose, highly erodible soil and fragmented terrain cause severe erosion during extreme rainstorms. Despite decades of soil and water conservation efforts that have reduced sediment loads in the Yellow River, intense rainfall events still wash away large amounts of fertile topsoil, leading to barren farmland and downstream riverbed silting that raises riverbeds and creates hazardous "suspended river" conditions (Huang et al., 2025; Wang et al., 2015). Long-term studies show significant declines in streamflow and sediment transport in the middle Yellow River due to both climate variability and human activities, but extreme rainstorms pose risks of flash floods and sediment surges that can damage erosion control infrastructures (Li et al., 2019). Vegetation cover and soil and water conservation measures have been effective in mitigating sediment transport during flood events, although their effectiveness can vary with flood frequency and intensity (Li et al., 2025). Economic development and social changes have also contributed to reductions in sediment load by promoting afforestation and labor shifts away from agriculture, which indirectly help reduce erosion (Tan et al., 2021).

Even more serious and difficult to detect is the hidden degradation and pollution of arable land quality. In Northeast China, once incredibly fertile "black soil," the soil layer is thinning, becoming less productive, and hardening due to long-term overuse and neglect of soil management (Zhang Yufei & Bian Zhenxing, 2026). Soil organic matter content is declining sharply, and this "giant panda of arable land" is facing a serious threat of degradation, directly impacting the nation's food security. Meanwhile, in the rapidly industrializing and urbanizing eastern and central regions, soil pollution is becoming increasingly prominent (Zhou Hongchun, 2019). Heavy metal pollution, excessive residues of chemical fertilizers and pesticides, and illegal discharge of industrial waste have turned some land into "toxic land." This chemical degradation differs from physical erosion; it is invisible and intangible, yet it accumulates through the food chain, ultimately harming human health. Once soil is polluted, the remediation process is lengthy and costly, often requiring decades or even centuries to recover. This irreversible or difficult-to-reverse damage is a heavy debt left to future generations.

The severity of land degradation in China also lies in its combined effect with water scarcity. In the North China Plain, insufficient surface water and long-term over-extraction of groundwater for farmland irrigation have led to the formation of the world's largest groundwater funnel zone (Liu & Wang,2017), resulting in land subsidence and seawater intrusion, further exacerbating soil salinization. This mismatch between water and soil resources has placed the agricultural production system in a highly unstable equilibrium.

Faced with such a severe situation, we must deeply understand that land degradation is not merely an alteration of natural geographical processes, but a concentrated manifestation of the conflict between human activities and natural laws. Its root cause lies in the fact that the traditional industrial civilization development model often treats land as a production factor that can be infinitely exploited, neglecting its ecological attributes as a core element of a community of life. Although China has put forward the concept of "lucid waters and lush mountains are invaluable assets" in recent years (Yang Yilin, 2021) and implemented a series of measures such as returning farmland to forests and grasslands (Huang Xianfeng et al., 2025), constructing high-standard farmland (Wei Guangcheng & Kong Xiangzhi, 2024), and implementing black soil protection projects (Zhu Chunyan et al., 2026), achieving remarkable results and demonstrating China's determination and wisdom in curbing land degradation, we must soberly recognize that the task of managing existing land degradation remains arduous, and the risk of new degradation still exists.

The intensifying global climate change is altering the distribution patterns of water and heat, and the increasing frequency of extreme weather events is constantly impacting fragile land ecosystems, bringing enormous uncertainty to future land management. For example, permafrost thawing may lead to irreversible changes to the Qinghai-Tibet Plateau ecosystem, and rising sea levels will threaten fertile coastal deltas (Yin Zhongmin et al., 2006). Therefore, addressing land degradation cannot rely solely on technological repairs but requires a profound social transformation. We need to fundamentally change land use patterns, shifting from predatory development to protective use, promoting regenerative agriculture, reducing reliance on chemical fertilizers and pesticides, and establishing a rigorous legal system for soil environmental monitoring and protection.

1.1.2 The typicality and particularity of land degradation in Guangdong Province

Guangdong Province, despite covering only about 1.87% of China's land area, experiences intense economic activity and population pressure, leading to a significant struggle between living space and ecological capacity. The province's rapid urbanization and economic growth have attracted large population inflows, especially young and middle-aged workers, which correlate positively with economic development but also exacerbate resource constraints (Lü Hao, 2025; Li, Z., & Li, H., 2022). Different economic patterns in Guangdong influence population inflows, with the export-oriented Pearl River pattern playing a major role in attracting people, highlighting the link between economic structure and demographic changes (Feng et al., 2024). The digital economy has a slight mitigating effect on population pressure by improving resources and welfare, but its impact is limited under increasing environmental constraints (Cui et al., 2025). Urban expansion in Guangdong shows spatial mismatches with population growth, particularly in less efficient land use areas, complicating sustainable regional planning (Zhang et al., 2025). Additionally, the aging population poses challenges for economic growth, as higher dependency ratios slow GDP growth, emphasizing the need for policies addressing demographic shifts alongside economic development (Yang & Xiao,2024; Zhao & Wang, 2022).

As China's largest economic province, Guangdong's GDP has surpassed 2.15 trillion USD, ranking first in the country for 37 consecutive years (Chen Kaixing et al., 2026). This economic scale even exceeds that of many moderately developed countries in the world. However, supporting this giant economic behemoth is extremely limited land resources. Within its approximately 179,800 square kilometers of land area, more than 127 million permanent residents live, meaning the province's population density is over 700 people per square kilometer. In the core area of the Pearl River Delta, this number is even higher. Such high-density population concentration and high-intensity industrial output have pushed every inch of land to its limit (Qiu et al., 2025). At the same time, Guangdong is not flat and fertile; mountains and hills account for more than 70% of its total land area, earning it the reputation of "seven parts mountains, one part water, and two parts farmland." This severe conflict between population and land has forced human activities to continuously advance into steep slopes, mountainous areas, and tidal flats that were originally unsuitable for development, thus sowing the deep-seated hidden dangers of land degradation.

This intensive development, coupled with Guangdong's extremely unique natural climate, has fostered a distinctive degradation mechanism. Located in the East Asian monsoon region, Guangdong spans the mid-subtropical, south-subtropical, and tropical climate zones, with an average annual temperature of around 22°C and an average annual rainfall of 1777 mm (Zhang Shaojie, 2025). While abundant heat and heavy rainfall seem like a boon to agriculture, they are actually powerful drivers of soil erosion. In this hot and rainy environment, the weathered crust of granite and red soil, widely distributed in Guangdong, undergoes extremely intense chemical weathering, resulting in weathered layers several meters to tens of meters deep. However, the soil structure is loose, with very low resistance to erosion (Liao et al., 2022). Soil erosion in Guangdong remains extensive, covering thousands of square kilometers with a high erosion modulus, and heavy rainfall events significantly exacerbate this by triggering landslides. Studies show that continuous and intense rainfall infiltrates loose, porous granite residual soils common in northern Guangdong, increasing pore water pressure and reducing soil strength, which leads to shallow surficial landslides typically 1 - 3 meters thick (Tan et al., 2024; Wang et al., 2025; Feng et al., 2022). These landslides often occur on slopes with angles between 35° and 45°, especially in low mountainous areas, and are frequently clustered along river valleys and roads (Bai et al., 2021; Ma et al., 2021). The combination of raindrop splash, runoff erosion, and terrain factors such as steep slopes and excavation activities further destabilizes slopes, making landslides more likely during concentrated heavy rain periods (Kang et al., 2024). Landslide susceptibility mapping using machine learning models highlights rainfall intensity, slope angle, topographic wetness index, and human modifications as key controlling factors for landslide occurrence in the region (Wei et al., 2025; Zhuo et al., 2023). Debris flows can also follow landslides as secondary hazards, particularly where loose deposits accumulate in gullies.

Beyond physical erosion, the chemical degradation brought about by rapid economic development is an invisible killer facing Guangdong's land. As the "world's factory," Guangdong once housed hundreds of thousands of manufacturing enterprises. Although its industrial structure has been continuously optimized in recent years, the environmental debt left by the long-term industrialization process remains heavy. According to soil pollution surveys, the rate of heavy metal exceedances in arable land in some areas of the Pearl River Delta was once quite high, with cadmium, mercury, arsenic, and lead pollution being particularly prominent (Bi et al., 2025). These pollutants mainly originated from early industries such as electroplating, circuit board printing, and non-ferrous metal smelting. Unlike the large-scale desertification in the north, this pollution is distributed in an "interspersed" manner, intertwined with high-yield industrial land and high-value agricultural land. In the Pearl River Delta, where land is extremely valuable, polluted soil not only means the loss of agricultural productivity but also causes the cost of urban renewal and land redevelopment to rise exponentially. Remediating a piece of industrial land contaminated by heavy metals often requires tens of millions or even hundreds of millions of USD and is time-consuming, becoming an invisible shackle restricting Guangdong's high-quality development. Furthermore, Guangdong is a high-incidence area for acid rain. Although the frequency of acid rain has decreased in recent years, long-term acid deposition has led to a serious problem of soil acidification (Luo Xiaoling et al., 2024). Acidified soil not only reduces the availability of nutrients but also activates aluminum toxicity in the soil, posing a continuous threat to the subtropical agricultural ecosystem.

Furthermore, the "hardening" of land and ecological fragmentation during urbanization is another major characteristic of land degradation in Guangdong. Guangdong's urbanization rate has reached over 75%, with the Pearl River Delta urban cluster stretching as far as the eye can see (Wang Yi, 2020). In this process, large areas of high-quality paddy fields and wetlands have been permanently covered by impermeable concrete. This irreversible change in land use severs the circulation channels between surface water and groundwater, damaging the biological activity of the soil. Statistics show that the annual increase in construction land in the Pearl River Delta region was once staggering, leading to a significant shrinkage of the region's natural wetland area (Guo Hongjiang, 2025). This not only eliminates the land's productive function but also weakens its ecological service functions of flood control and climate regulation. The frequent urban flooding and exacerbated heat island effect in recent years are direct feedback from the degradation of land's ecological functions. At the same time, to meet the energy and building material needs of this 127 million-person population and massive industrial system, mining has also caused severe, localized damage to the land. Although revegetation efforts are ongoing, the exposed rock walls and waste rock piles left by abandoned mines remain scars on the ecosystem that are difficult to heal.

Guangdong's coastline, the longest mainland coastline in China, faces significant ecological challenges due to rapid coastal economic development and land reclamation projects that have altered its dynamic environment. These changes, combined with global sea-level rise, have intensified soil salinization and coastal erosion, threatening agricultural safety in areas like Zhanjiang and Maoming through saltwater intrusion caused by excessive groundwater extraction (Du et al., 2020; Zhang et al., 2025). Land subsidence is a major issue along the coast, particularly in aquaculture and agricultural zones, driven mainly by groundwater overuse, which exacerbates relative sea-level rise and ecological risks (Du et al., 2020). Coastal wetland degradation is also prominent due to urbanization and land conversion, with habitat quality declining as construction land expands at the expense of cultivated and natural lands (Qin et al., 2024; Wang et al., 2022). Remote sensing studies reveal that while some coastal ecological quality has fluctuated over recent decades, overall pressure remains high due to human activities such as urban expansion and pollution from river discharges (Li et al., 2022; Lin & Yu, 2018). Effective coastline protection strategies emphasize ecological restoration, sustainable land use regulation, and integrated land-sea management to mitigate ongoing degradation and support long-term environmental resilience in Guangdong's coastal zones (Zhang et al., 2025; Huang et al., 2023; Guo et al., 2021).

Therefore, Guangdong's path to land management is destined to be more difficult and costly than that of other provinces. It cannot simply replicate the western model of returning farmland to forest, nor can it rely solely on single engineering measures. Faced with such a massive population and economic scale, Guangdong must explore a refined path to land health management while maintaining economic growth. This means protecting its limited arable land with the strictest regulations, investing heavily in scientific and technological efforts to restore damaged red soil, and using a systems engineering approach to manage watershed-wide soil erosion.

1.1.3 The Value of Agroforestry in Ecological Restoration and Sustainable Agriculture

Agroforestry, the integration of trees and shrubs with crops and/or livestock, offers a promising land-use pattern that balances ecological protection and food production by enhancing biodiversity, improving soil health, and providing multiple ecosystem services such as carbon sequestration, erosion control, and microclimate regulation (Fahad et al., 2022; Akhter et al., 2025; Mathieu et al., 2025). It supports food security by increasing crop yields while maintaining or improving soil fertility and water regulation, thus reducing trade-offs between agricultural productivity and environmental sustainability (Kuyah et al., 2019; Mathieu et al., 2025). Agroforestry systems also contribute to climate resilience by diversifying farm outputs, improving livelihoods, and mitigating the impacts of climate extremes, especially in vulnerable regions like drylands and smallholder farms (Fahad et al., 2022; Duffy et al., 2021; Roy et al., 2025). Evidence from various regions shows agroforestry’s potential to enhance ecosystem multifunctionality globally without sacrificing productivity, making it a cost-effective and climate-smart farming practice (Kuyah et al., 2019; Mathieu et al., 2025). Despite its benefits, research gaps remain regarding policy support, human well-being outcomes, and adoption barriers in high-income countries, highlighting the need for further study to optimize agroforestry’s role in sustainable agriculture (Pantera et al., 2021; Castle et al., 2022). Overall, agroforestry is increasingly recognized as a key nature-based solution to address the intertwined crises of climate change, biodiversity loss, land degradation, and food insecurity (Wilson et al., 2016; Villanueva-González et al., 2024).

When we delve into the core value of agriculture and forestry in ecological restoration, their ability to reshape soil health and nutrient cycling immediately comes to mind. Continuous monoculture negatively impacts soil health by causing soil acidification, depletion of soil organic matter, and reduced microbial diversity, which together degrade soil structure and nutrient cycling. Long-term monoculture systems, such as coffee and tomato plantations, show decreased soil pH, soil organic matter content, and beneficial microbial populations like Nitrospira and Trichoderma, while increasing soil electrical conductivity and fungal abundance linked to disease susceptibility (Zhao et al., 2018; Fu et al., 2017; Hu et al., 2025). Agroforestry systems, however, introduce deep-rooted trees. These "underground excavators" can penetrate deep soil layers inaccessible to crop roots, pumping nutrients lost to deeper layers back to the surface through biological cycles, returning them to the soil as litter, thus significantly improving topsoil fertility (Sileshi et al., 2020). Even more ingeniously, many agroforestry systems utilize leguminous species, which, through symbiotic nitrogen fixation with rhizobia, become natural nitrogen fertilizer factories, greatly reducing the need for chemical nitrogen fertilizers and thus curbing non-point source pollution (Abd-Alla et al., 2023). Beyond their chemical improvements, the role of tree root networks in stabilizing soil physical structure is also significant. Like steel reinforcement in the earth, they enhance soil shear strength, increase water infiltration, and effectively reduce surface runoff and soil erosion. This is crucial for vegetation restoration in ecologically fragile areas such as sloping farmland or arid and semi-arid regions (Lann et al., 2024). Furthermore, deep-rooted trees can utilize a "hydraulic redistribution" mechanism to release moisture from deeper soil layers to shallower layers at night, providing vital "lifesaving water" for shallow-rooted crops. This mutually beneficial relationship between plants is unattainable by monoculture systems (Lee et al., 2021).

Agroforestry systems significantly enhance biodiversity in agricultural landscapes by providing structurally complex habitats that serve as ecological corridors and refuges for various species, including birds, insects, small mammals, and soil microorganisms (Buzhdygan et al., 2023). These systems support greater floral, faunal, and microbial diversity compared to monocultures or conventional croplands due to heterogeneous vegetation, improved microclimate, organic carbon inputs, and spatial distribution of trees (Udawatta et al., 2019; Udawatta et al., 2021). Meta-analyses show that agroforestry increases ecosystem service delivery and biodiversity globally by about 23%, with stronger effects on supporting and regulating services than on production (Mathieu et al., 2025). Biodiverse agroforestry systems outperform simpler ones in conserving biodiversity and ecosystem services, especially in degraded areas where sustainable management is practiced (Santos et al., 2019). However, the positive effects can vary depending on system type, management intensity, landscape context, and regional factors; for example, silvoarable systems tend to increase bird and arthropod diversity more than other agroforestry types (Mupepele et al., 2021; Torralba et al., 2016). Overall, agroforestry is recognized as a critical strategy for maintaining ecological balance and biodiversity within human-dominated agricultural landscapes while supporting sustainable production (Santos et al., 2022; Jose, 2012; Udawatta et al., 2021).

Agroforestry systems enhance carbon sequestration by fixing carbon in stable forms through long-term tree presence, which contributes to increased soil organic carbon (SOC) stocks, especially in both topsoil and subsoil layers. Meta-analyses show that agroforestry increases SOC by around 10 - 25% compared to conventional land uses, with the greatest gains often observed in arid and semi-arid regions and in the upper 30 cm of soil, though significant sequestration also occurs deeper (Pan et al., 2025; T.M. et al., 2023; Mayer et al., 2022). The complex root exudates and litter inputs from trees promote soil aggregate formation, protecting organic carbon from rapid microbial decomposition and thus enhancing carbon stability (Sirimalle et al., 2025). Simultaneously, facing the frequent occurrence of extreme weather events, agroforestry systems demonstrate remarkable microclimate regulation capabilities. The tree canopy acts like a giant sunshade and windbreak, reducing extreme high temperatures under the canopy, minimizing soil moisture evaporation, and providing insulation during cold snaps (Jacobs et al., 2022). This buffering effect of the microenvironment directly protects crops from heat stress and wind damage, providing a "protective umbrella" for agricultural production and significantly enhancing the agricultural system's ability to adapt to climate change.

Turning to the economic and social dimensions of sustainable agriculture, agroforestry has demonstrated its potential to resolve the "high yield vs. environmental protection" dilemma. Traditional views often hold that planting trees blocks sunlight and competes for nutrients, thus reducing crop yields. However, numerous empirical studies show that through rational species allocation and spatial layout, agroforestry systems can often achieve a higher land equivalent ratio (LER) than single-system systems (Ripamonti et al., 2025). This means that on the same land area, the combined biomass and economic value generated by mixed planting often exceeds the sum of individual plantings.

However, Agroforestry adoption faces multiple challenges beyond scientific knowledge, primarily rooted in socio-economic and policy barriers. Key obstacles include the complexity of managing diverse species, requiring ecological expertise in tree pruning and competition regulation, and the long growth cycles of trees that demand high initial investments with delayed returns, conflicting with farmers' preference for short-term profits (Ripamonti et al., 2025; Tranchina et al., 2024). Socio-economic constraints such as lack of capital, labor demands, limited access to quality inputs (e.g., seedlings), and insufficient technical support further hinder adoption (Ripamonti et al., 2025; Reshad et al., 2025; Kpoviwanou et al., 2024; Singh et al., 2025). Policy and institutional issues also play a significant role; existing agricultural subsidies and land tenure systems often separate forestry from agriculture, lacking incentives for integrated agroforestry systems, which limits large-scale implementation (Ripamonti et al., 2025; Mayele, J., & Sakurai, T., 2025; Sollen-Norrlin et al., 2020). Additionally, low awareness, inadequate education, and limited market development for agroforestry products reduce motivation among farmers to adopt these practices (Mayele, J., & Sakurai, T., 2025; Kpoviwanou et al., 2024). Overcoming these challenges requires systemic changes including improved extension services, financial incentives, land tenure reforms, and enhanced social understanding to fully realize agroforestry's potential for sustainable agriculture (Ripamonti et al., 2025; Reshad et al., 2025; Mayele, J., & Sakurai, T., 2025; Sollen-Norrlin et al., 2020).

1.2 Research Progress

1.2.1 Overview of Research on the Causes, Assessment, and Monitoring Technologies of Land Degradation

Research on the causes, assessment, and monitoring technologies of land degradation, both domestically and internationally, has formed a relatively systematic and continuously deepening framework. Its core focus lies in the mechanisms of land function decline under the interaction of natural processes and human activities, the scientific quantification of degradation levels, and the construction of high-precision, sustainable monitoring methods. From a causal perspective, international research generally agrees that natural factors such as climate change, aridification trends, and extreme weather events, along with human factors such as population growth, overgrazing, agricultural expansion, improper irrigation, industrial pollution, and inadequate land management, jointly drive the land degradation process. Soil erosion, wind erosion, and salinization remain key concerns in arid and semi-arid regions (Prăvălie, 2021; Perović et al., 2021; Talukder et al., 2021; Roy, 2024; Emadodin et al., 2019). China research, on the other hand, emphasizes the dominant role of human activities in the context of rapid urbanization and intensive land use, while also paying attention to the comprehensive pressures brought about by over-cultivation of farmland, uneven water resource development, grassland degradation, and human disturbance in ecologically fragile areas (Wang et al., 2018; Huang et al., 2023; Liu, 2018). In terms of assessment, internationally, evaluation has evolved from early soil physicochemical indicators to a multi-dimensional indicator system integrating ecosystem services, changes in biological productivity, and land use change. Model simulations have been used to enhance the explanation of degradation evolution mechanisms under different scenarios (Zahedifar, 2023; Badapalli et al., 2022; Tarrasón et al., 2015). The "zero net land degradation" framework proposed by the United Nations Convention to Combat Desertification has made assessments more standardized, emphasizing the quantitative integration of land cover change, soil quality, and productivity indicators (Stavi, & Lal, 2014). China, based on international systems, China has constructed land degradation classification standards and index evaluation systems applicable to different ecological zones. These include comprehensive evaluation methods centered on remote sensing indices, soil organic matter, vegetation cover, water conditions, and production potential. Simultaneously, the needs of ecological security patterns and national spatial planning are gradually being incorporated, expanding the scale and objectives of land degradation assessment. In terms of monitoring technology, foreign countries have accumulated a wealth of achievements in using multi-source remote sensing (optical, SAR, lidar, etc.) to monitor land surface changes, vegetation vitality, surface roughness, and moisture conditions. In particular, methods for long-term sequence analysis, trend detection, and early identification of land degradation based on MODIS, Landsat, and Sentinel series data are highly mature and are gradually extending to UAV remote sensing, ground sensors, and automated big data analysis to achieve dynamic monitoring with high spatiotemporal resolution (Wang et al., 2023; Xing et al., 2025; Zhang et al., 2023; Li et al., 2025; Zhao et al., 2025). In China, systematic practices have been established in areas such as the construction of a national ecological monitoring network, monitoring of black soil and desertification areas, and identification of grassland degradation levels. Multi-scale monitoring systems have been established by combining domestic remote sensing satellite data (such as the Gaofen series), while actively exploring the application of machine learning, deep learning, and geographic weighted regression methods in degradation identification, temporal trend inversion, and driving force analysis. Overall, domestic and international research shows a trend of moving from qualitative to quantitative analysis, from single indicators to comprehensive ecological processes, and from static observation to long-term dynamic monitoring. Driven by multi-source data fusion, model simulation, and intelligent analysis technologies, the scientific rigor and accuracy of land degradation diagnosis are continuously improving, providing a more solid theoretical foundation and technical support for global sustainable land use and ecological restoration.

1.2.2 Review of Research on Degraded Land Restoration Technologies and Models

Research on degraded land restoration technologies and models has developed rapidly both domestically and internationally, with ecological governance practices centered on agroforestry approaches continuously deepening and innovating. Globally, degraded land problems largely stem from overexploitation, vegetation destruction, and irrational land use; therefore, research focuses on improving soil quality, moisture retention, and ecological functions through agroforestry systems. China and international research progress shows that degraded land restoration technologies and models in the agroforestry field have formed a multi-dimensional technical system, with its core revolving around soil structure reconstruction and ecological function restoration. In terms of physical fixation technologies, the "sandwich structure system" composed of a superhydrophobic coating and highly elastic fiber windbreak developed in Germany has demonstrated excellent wind erosion resistance in the Taklamakan Desert of Xinjiang, extending the protection time by 3.1 times compared to traditional straw checkerboard grids (Liu Yinggang, 2025). Meanwhile, after two years of application in the wind erosion area of Inner Mongolia, honeycomb foamed cement three-dimensional grids increased sand deposition within the grids by 7 times, and combined with the planting of Haloxylon ammodendron shrubs, extended the sand fixation period by 120% (Jiang et al., 2025; Mei et al., 2025). Bio-activation technology leverages the synergistic interactions between microorganisms and plants to enhance soil nutrient availability and ecosystem restoration. For example, grafting arbuscular mycorrhizal (AM) fungi onto deep-rooted plants like Salix pumila has been shown to double available phosphorus in the topsoil and sustain symbiotic relationships for over 18 months in desertified areas (Wang et al., 2024; Shi et al., 2022). Integrating microbial amendments like Bacteroides SY02 with chemical treatments such as nitrification inhibitors offers a promising approach to enhancing soil stability and nutrient retention in degraded soils of Northwest China (Yu et al., 2022; Yang et al., 2023; Wei et al., 2025; Yang et al., 2024; Nan et al., 2021). In response to the problem of farmland degradation, China's "Technical Model for the Remediation of Degraded Farmland" released in 2023 systematically integrated 43 technologies in five categories. Among them, Ningxia applied nano-silica diploid dispersants to increase the permeability coefficient of alkaline farmland by 46%, and the lignin-cellulose grafted water-retaining gel in the Kubuqi Desert extended the water retention period to 7 months. Intelligent monitoring has become a key support for technological optimization. The EU's satellite lidar-AI integrated system has achieved decimeter-level ground condition analysis at 78 benchmark points in desert areas. China's National Forestry and Grassland Administration's early warning platform integrates 23 ecological factors, achieving a restoration cycle prediction accuracy of 93.4%. Of further interest is the latest Cell study released in December 2025, which reveals the physical signal transduction mechanism by which plants sense high temperatures through membrane lipid remodeling, providing new targets for drought-resistant crop breeding. Meanwhile, the results of the second Qinghai-Tibet Plateau scientific expedition have constructed a benchmark index system for alpine ecological restoration, suggesting that the ecological adaptability of plateau-specific plants such as *Lysimachia christinae* should be incorporated to deepen the design of restoration models.

Overall, China and international research is shifting from single-engineering governance to comprehensive ecological restoration and sustainable management. Biological measures, mainly based on agriculture and forestry, remain the core, but there is an increasing emphasis on multi-scale, multi-disciplinary integration and synergistic benefits between ecology and economy, providing broad development space for the future governance of degraded land.

1.2.3 Limitations of existing research and the starting point of this study

Limitations of existing research

The regional focus is insufficient, failing to highlight the unique characteristics of Guangdong's "economy-ecology" contradiction.

Existing land degradation restoration research largely focuses on desertification in the north, soil erosion in the northwest, or single types of pollution, with limited specificity for the red soil regions of the south, especially Guangdong Province. As the province with the largest economy,Guangdong Province is characterized primarily by mountainous and hilly terrain, which together account for approximately 60% of the province’s total area, the high-density pressure of a population of 127 million, and the high-intensity development demands of a GDP of 2 trillion USD. Land degradation in Guangdong exhibits a complex and intertwined characteristic of physical erosion, chemical pollution, and biological degradation, significantly different from the single degradation type in the north. Current research has not fully considered the low erosion resistance of red soil caused by Guangdong's high temperature and rainfall (annual precipitation of 1777 mm), soil acidification caused by acid rain deposition, and the unique dilemma of the Pearl River Delta's "interspersed" heavy metal pollution and the intertwining of high-value arable land. Therefore, it lacks restoration solutions adapted to the region's contradiction of "coexistence of economic activity and ecological fragility."

Technological research is fragmented and lacks multi-measure synergistic optimization and mechanism coupling.

Existing research largely focuses on validating the effects of single remediation techniques (such as the application of biochar, green manure, or engineering measures alone), failing to systematically explore the synergistic mechanisms of multiple agronomic measures. For example, some studies only focus on the passivation effect of biochar on heavy metals, neglecting its combined effects with lime and green manure; research on green manure often emphasizes yield improvement, lacking in-depth analysis of its coupling mechanisms with soil microbial communities and nutrient cycling. Furthermore, technology optimization relies heavily on empirical experiments, lacking data-driven quantitative models, making it difficult to achieve a precise balance between "ecological benefits and economic costs," thus failing to meet the cost control needs of remediation in Guangdong's land-scarce region.

The research is fragmented in scale and has not formed a complete "macro-micro-model" chain system.

Existing research suffers from significant scale fragmentation: at the macro level, it largely focuses on describing the spatiotemporal patterns of land degradation, lacking an understanding of the micro-level restoration mechanisms; at the micro level, it emphasizes changes in single indicators such as soil physicochemical properties or microorganisms, failing to elevate to regional-scale model construction; and model studies are mostly general designs, lacking differentiated adaptation to the degradation characteristics of different regions in Guangdong (Pearl River Delta, hilly and mountainous areas, and the ecological barrier of northern Guangdong). Furthermore, there is insufficient monitoring of the long-term effects of restoration measures, with most studies having a duration of less than 3 years, making it difficult to assess key issues such as heavy metal rebound and soil carbon pool stability, which is mismatched with the long-term needs of degraded land restoration in Guangdong.

The monitoring and evaluation system is incomplete and lacks comprehensive quantitative tools.

Current monitoring technologies largely rely on single remote sensing indices or field sampling, failing to integrate multi-source data from the sky and ground (Wu et al., 2022). This results in insufficient accuracy in monitoring soil erosion and heavy metal migration in the complex terrain of the Pearl River Delta (errors often exceed 10%). Assessment indicators often focus on single dimensions (such as yield and soil pH), lacking a comprehensive index system encompassing ecology, production, and economics, making it difficult to fully reflect the multiple benefits of agricultural and forestry measures. Furthermore, existing models are mostly based on single algorithms (such as response surface methodology or random forests), failing to effectively handle the nonlinear relationships between soil, microorganisms, and agronomic measures, thus limiting the accuracy of predicting remediation effects.

The starting point of this study

Focusing on the unique characteristics of Guangdong, a differentiated restoration framework was constructed.

Starting with the core contradiction of "high economic density and high ecological vulnerability" in Guangdong Province, this study establishes a regionally adapted system of "problem-mechanism-technology-model" to address the regional differentiation characteristics of heavy metal pollution in the Pearl River Delta, soil erosion in the hilly and mountainous areas of eastern and western Guangdong, and forest quality degradation in the ecological barrier zone of northern Guangdong. It focuses on analyzing the superimposed degradation mechanism of red soil erosion, acid rain acidification, and industrial pollution under high temperature and high rainfall conditions, breaking through the limitations of the traditional "one-size-fits-all" restoration model, and tailoring agricultural and forestry restoration solutions for different regions.

Strengthen the synergy and mechanism coupling of multiple technologies and optimize the combination of agronomic measures.

Using biochar, lime, and leguminous green manure as core remediation measures, this study explores the synergistic mechanism among the three: on the one hand, through field experiments and microbiome analysis, it reveals the molecular mechanism by which green manure root exudates activate functional microbial communities (such as Burkholderia) and promote heavy metal passivation; on the other hand, it constructs a random forest-response surface methodology (RF-RSM) hybrid model to quantify the optimal ratio of each measure, achieving a multi-objective balance between maximizing the soil function recovery index (SFRI) and minimizing remediation costs, thus solving the problem of limited effectiveness and excessive cost of single technologies.

Connect the entire chain of "macro-micro-model" to achieve a logical closed loop.

At the macro level, based on remote sensing and GIS technologies and combined with the RUSLE model, the study accurately depicts the spatiotemporal evolution and driving mechanisms of land degradation in the Pearl River Delta from 2000 to 2020. At the micro level, through high-throughput sequencing and FAPROTAX functional prediction, the study analyzes the regulatory mechanisms of agronomic measures on key microbial communities in the carbon, nitrogen, phosphorus, and sulfur cycles. At the technical level, the study determines the parameters of key agronomic measures through model optimization. Finally, by integrating the results from multiple dimensions, the study constructs three differentiated agroforestry models: "heavy metal pollution - rapid improvement" in the Pearl River Delta, "forest-fruit-grass complex" in hilly and mountainous areas, and "near-natural forestry transformation" in northern Guangdong, thus completing the transformation from problem recognition to systemic solutions.

Improve the "sky-ground" monitoring and comprehensive assessment system to enhance forecast accuracy.

By integrating high-resolution remote sensing, UAV inspections, and ground sensor networks, a "sky-ground integrated" monitoring system will be constructed to improve the monitoring accuracy of indicators such as soil erosion, heavy metal content, and vegetation restoration (with errors controlled within 8%). A comprehensive evaluation index system covering ecology (soil fertility, biodiversity), production (crop yield, quality), and economics (cost-effectiveness, income stability) will be established, combined with life cycle assessment (LCA) methods to fully quantify the multiple benefits of restoration models. Nonlinear relationships will be handled through multi-model coupling (RF-RSM) to improve the accuracy of restoration effect prediction, providing a scientific quantitative tool for the restoration of degraded land in Guangdong.

1.3 Technology Roadmap

The technical roadmap for this study is shown in Figure 1.1.

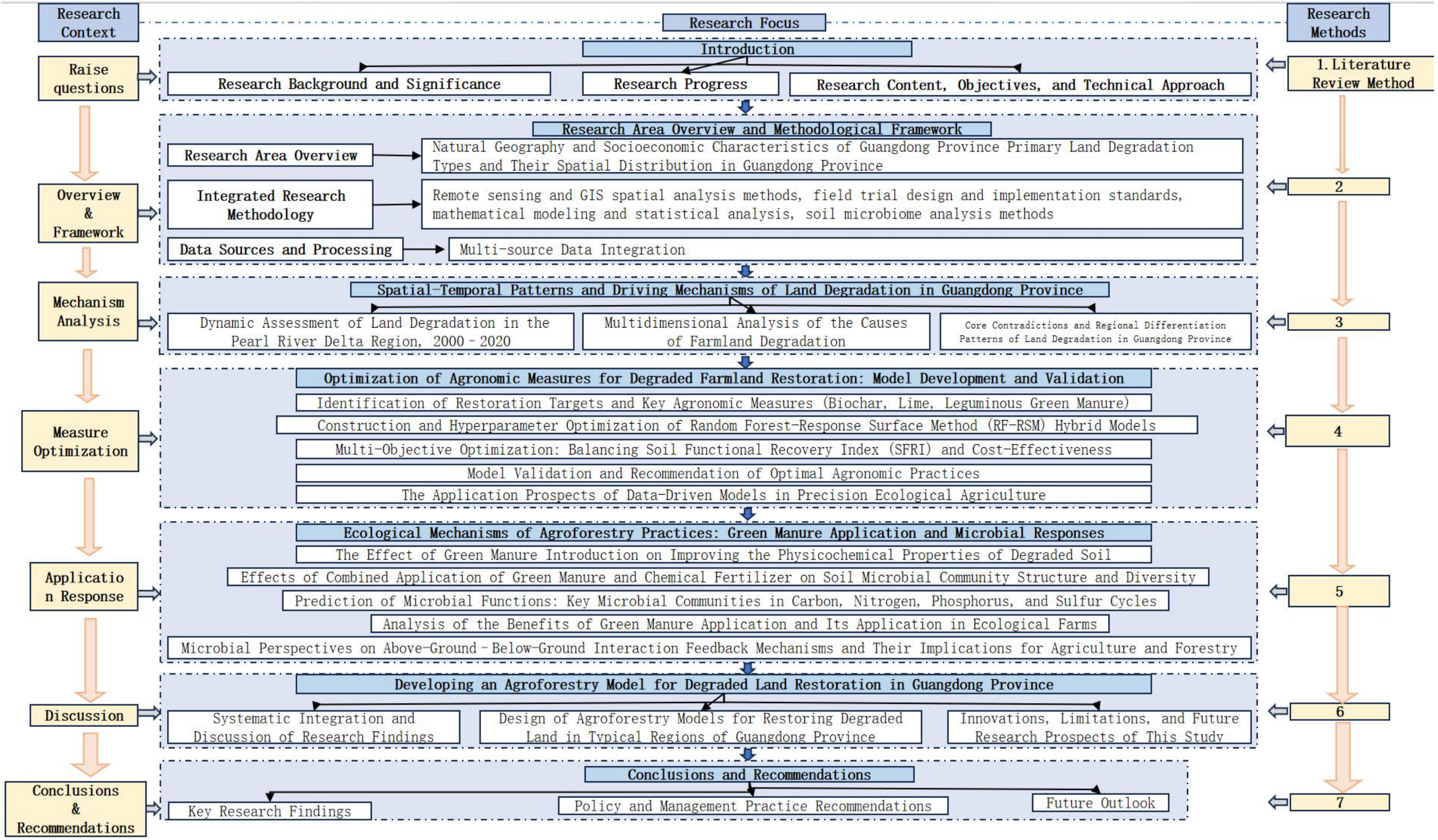

Figure 1.1 Technical roadmap

Conclusions to Chapter 1

The unprecedented transformation of the Earth’s surface through human-dominated land degradation represents a "silent crisis" that threatens global ecological security, food stability, and sustainable development. As a nation characterized by a "large population and limited land," China faces a complex landscape of degradation, ranging from northern desertification to southern rocky desertification and the insidious chemical pollution of its most fertile soils. Within this national context, Guangdong Province serves as a critical case study where intense economic activity directly conflicts with ecological fragility.

Guangdong's history as the "world's factory" has left a heavy legacy of heavy metal pollution and soil acidification, often interspersed with high-value agricultural land in the Pearl River Delta. Traditional restoration methods that rely on single engineering measures or broad afforestation policies are insufficient for Guangdong's high-density population and complex terrain.

Agroforestry emerges as a vital nature-based solution for this region, offering a multifunctional land-use pattern that restores soil health, enhances biodiversity, and stabilizes physical soil structures through deep root networks. By integrating leguminous species and deep-rooted trees, these systems can rehabilitate nutrient cycles and provide microclimate regulation, effectively acting as a "protective umbrella" for agricultural systems facing climate extremes.

However, existing research remains fragmented, focusing heavily on northern arid regions and often lacking a multi-measure synergistic approach that balances ecological benefits with economic costs. This study addresses these gaps by:

1.Establishing a differentiated restoration framework specifically for Guangdong's "high economic density/high ecological vulnerability" contradiction.

2.Quantifying the optimal synergy between biochar, lime, and leguminous green manure using advanced RF-RSM hybrid modeling to maximize soil recovery while minimizing costs.

3.Connecting a complete "macro-micro-model" chain, from depicting regional degradation patterns via remote sensing to uncovering microscopic microbial regulatory mechanisms in carbon and nitrogen cycles.

4.Constructing an integrated "sky-ground" monitoring system to enhance the accuracy of restoration forecasts.

By moving from problem recognition to systematic, regionally-tailored solutions, this research provides a replicable path for achieving high-quality land health management in Guangdong, ensuring a sustainable home for its 127 million residents while maintaining its status as an economic leader.

CHAPTER 2
MATERIALS AND METHODS OF RESEARCH

2.1 Research Content, Objectives, and Technical Approach

2.1.1 Research Content

This study focuses on the agricultural and forestry characteristics of degraded land restoration in Guangdong Province, constructing a full-chain research framework of "macro-pattern analysis - micro-mechanism mining - technology optimization and integration - precise model construction," the specific contents of which are as follows:

Analysis of the Spatiotemporal Patterns and Driving Mechanisms of Land Degradation in Guangdong Province

Based on multi-source remote sensing data (MODIS, Landsat, etc.) from 2000 to 2020 and GIS spatial analysis technology, combined with the RUSLE model, three core indicators – desertification, vegetation degradation, and soil erosion - were extracted to quantify the spatiotemporal evolution characteristics of land degradation in the Pearl River Delta and typical areas, and to clarify the regional differentiation patterns of degradation at different stages.

This study analyzes the degradation driving mechanisms from both natural and anthropogenic perspectives: the natural perspective focuses on regional characteristics such as high temperature and rainfall, weak erosion resistance of red soil, and vulnerability of karst geology; the anthropogenic perspective focuses on the impact of industrial expansion, urbanization hardening, high-intensity agricultural use, and policy shifts on land degradation, revealing the essence of degradation under the contradiction of "economic activity and ecological fragility".

A comprehensive land degradation assessment model was constructed to quantify the contribution weights of natural factors (soil erosion, climate fluctuations) and human factors (expansion of construction land, industrial layout, ecological policies), and to clarify the unique degradation pattern of the Pearl River Delta characterized by the complex interplay of "physical erosion, chemical pollution, and biological degradation".

Screening and Optimization Model Construction of Key Agronomic Measures for Degraded Farmland Restoration

This study focuses on biochar, lime, and leguminous green manure (such as milkvetch and ryegrass) as core remediation measures. Using a Box-Behnken design, a three-factor, three-level field experiment was constructed to systematically explore the effects of single measures and combinations on the physicochemical properties (pH, porosity, soil organic matter), passivation of heavy metals (cadmium, arsenic, etc.) and crop growth of degraded red soil.

Constructing a hybrid Random Forest-Response Surface Method (RF-RSM) model: The random forest algorithm is used to screen core driving factors such as available phosphorus and soil pH. The response surface method is used to quantify the interaction effects between measures. A multi-objective optimization model of "Soil Function Restoration Index (SFRI)-Cost-Benefit" is established to determine the optimal combination parameters of agronomic measures (dosage and ratio) for farmland with different degrees of degradation.

Verify model reliability: Through field monitoring, compare the differences between the optimized scheme and the traditional remediation model in terms of heavy metal passivation rate, soil fertility improvement, and long-term stability (18 months) to ensure the practical guidance value of the model.

Ecological Mechanisms of Agricultural and Forestry Restoration Measures: A Study of Green Manure-Microorganism-Soil Interactions

Based on high-throughput sequencing and bioinformatics analysis, this study analyzes the impact of green manure (applied alone or in combination with chemical fertilizers) on the microbial community structure of degraded soil, focusing on the abundance changes and α/β diversity characteristics of dominant bacterial (Proteobacteria, Acidobacteria) and fungal communities.

Discovering key microbial functional groups in the carbon, nitrogen, phosphorus, and sulfur cycles: Through FAPROTAX functional prediction and metabolic pathway analysis, we clarified the role mechanisms of nitrogen-fixing bacteria, phosphorus-solubilizing bacteria, and heavy metal passivation-related bacteria driven by green manure, and revealed the molecular pathways by which root exudates activate functional bacteria.

Quantifying the coupling relationship between "green manure application - soil physicochemical improvement - microbial function enhancement" clarifies the intrinsic mechanism by which agricultural and forestry measures improve soil ecological resilience, providing microscopic support for the optimization of remediation technologies.

Construction and Benefit Evaluation of Regionally Differentiated Agroforestry Restoration Models

Targeting different degradation types and regional functional positioning, three distinctive agroforestry models were designed: the "Heavy Metal Pollution-Rapid Improvement Model" (passivating agent + high-efficiency green manure synergy) in the suburban fringe areas of the Pearl River Delta, the "Forest-Fruit-Grass Composite Soil and Water Conservation Model" (tree slope stabilization + fruit tree income increase + green manure fertilization) in the hilly and mountainous areas of eastern and western Guangdong, and the "Near-Natural Forestry Transformation Model" (construction of multi-layered mixed forests) in the ecological barrier area of northern Guangdong.

Conduct field validation and benefit quantification of the model: ecological benefits focus on soil erosion modulus, carbon sequestration potential, and biodiversity enhancement; production benefits focus on crop yield and agricultural product quality and safety; economic benefits calculate restoration costs, comprehensive output, and farmers' income potential, and clarify the synergistic benefit path of "ecology-production-economy".

Establish operational guidelines for different models: refine the species selection (native tree species, suitable green manure), configuration ratio, management techniques (pruning, fertilization, and return to the field) and promotion conditions for different models, and form a replicable technical manual.

Research on the Practice, Promotion, and Support System of Agricultural and Forestry Restoration Models

The analysis identifies the constraints on the large-scale promotion of the model: from a technical perspective, it focuses on the difficulty of operation for farmers and the compatibility of equipment; from an economic perspective, it focuses on material costs and initial investment pressure; and from a policy perspective, it identifies the shortcomings of existing subsidy policies.

Construct an integrated support system of "scientific research - demonstration - promotion": propose policy recommendations such as special subsidies for agroforestry integrated management and ecological compensation (carbon sink trading, marketization of soil and water conservation benefits); design a technical training network of "scientific research institutions + agricultural technology extension stations + management entities", covering forms such as on-site guidance and online courses.

Explore the path of integrating "ecology + industry": combine regional characteristics, tap the potential for extending the value chain of forest products and green agricultural products, enhance the economic sustainability of agroforestry restoration models, and promote rural industrial revitalization.

2.1.2 Research Objectives

Theoretical Innovation Goals

This study reveals the unique mechanism of land degradation in Guangdong Province as a complex interplay of factors and regional differentiation. It clarifies the coupled degradation pattern of "physical erosion, chemical pollution, and biological degradation" under the combined effects of high temperature and rainfall, weak red soil erosion resistance, and industrial pollution, filling a regional gap in the theoretical research on land degradation in the economically active southern region.

This study elucidates the Microbial interaction mechanism of agricultural and forestry measures in restoring degraded red soil, reveals the molecular pathway by which green manure root exudates activate functional microbial communities (such as Burkholderia) to promote heavy metal passivation (CdS nanoparticle formation), and explores the core principles of the synergistic regulation of soil function restoration by available phosphorus and soil pH, thus enriching the microbial ecological theory of subtropical degraded red soil restoration.

We will construct a full-chain theoretical framework of "macro-structure - micro-mechanism - technology optimization - model construction", establish a quantitative balance between ecological benefits and economic costs, and improve the synergistic gain theory of agroforestry integrated management in degraded land restoration.

Technological Innovation Goals

Optimize multi-source data fusion monitoring technology, integrate remote sensing (MODIS, Landsat), GIS spatial analysis and RUSLE model to improve the dynamic monitoring accuracy of soil erosion and heavy metal pollution under the complex terrain of the Pearl River Delta, and control the error within 8%.

Innovative multi-factor collaborative optimization technology was used to construct a random forest-response surface method (RF-RSM) hybrid model to accurately screen the optimal combination parameters of biochar, lime, and leguminous green manure, thereby maximizing the soil function recovery index (SFRI). The cost-effectiveness of cadmium passivation was improved by more than 60% compared with traditional technology, and the rebound rate was controlled within 5%.

Develop a regionally differentiated agricultural and forestry restoration technology system, targeting the degradation characteristics of the Pearl River Delta, hilly and mountainous areas, and the ecological barrier zone in northern Guangdong, and form a combination of three types of technologies: "rapid improvement - soil and water conservation - ecological quality improvement" to achieve a precise match between restoration cycle, ecological effect, and economic benefits.

Application Objectives

This research aims to provide replicable technical solutions for the restoration of degraded land in Guangdong Province, clarify the agronomic parameters (material dosage, ratio, and application cycle) and operational specifications for different types of degradation (heavy metal pollution, soil erosion, and forest quality decline), and support the precise restoration practice of more than 6,667 hectares of degraded land.

A three-region differentiated agricultural and forestry model promotion system has been established. The Pearl River Delta's "heavy metal pollution - rapid improvement" model achieves rapid restoration within one year. The eastern and western Guangdong's "forest-fruit-grass composite" model reduces the soil erosion modulus by more than 70%. The northern Guangdong's "near-natural forestry transformation" model improves water conservation capacity by 20%-40%.

Promote the large-scale application of agricultural and forestry restoration technologies, reduce restoration costs (cost per unit area decreased by more than 8.5%), improve the quality and safety of agricultural products (100% compliance rate for heavy metal content), drive farmers' income growth and rural industry integration, and provide technical support for rural revitalization and ecological security in Guangdong.

2.1.3 Temporal scale classification and data attribution in this study

To ensure transparent interpretation of results, this study explicitly distinguishes three temporal scales that correspond to different data sources and evidential strengths:

(1) Retrospective analysis period (2000 - 2020): This 20 - year time frame applies exclusively to the remote-sensing based land degradation assessment presented in Chapter 3. The MODIS, Landsat, and RUSLE modeling outputs describe historical trends and spatiotemporal patterns of degradation as they occurred. These are not predictions of future degradation trajectories but validated hindcasts based on archived satellite observations.

(2) Empirical observation period (3 - 18 months): All agronomic experimental data (Chapter 4) and microbiological pot experiment data (Chapter 5) were collected within a maximum observation window of 18 months (field monitoring intervals: 3, 6, 12, and 18 months post-treatment; pot experiment duration: 8 months of growth + 8 weeks of incorporation = approximately 10 months). This period constitutes the only empirical temporal basis for the soil physicochemical, heavy metal passivation, and microbial community results presented in this dissertation. Any statements regarding treatment effects beyond 18 months are model - based extrapolations, not empirical

observations.

(3) Projected / extrapolated period (3 - 10 years): Recommendations such as the 3-year reapplication cycle for biochar and lime (Section 7), and future research prospects discussing 5 - 10-year carbon stability assessments (Section 6.3.3), are derived from (a) first-order kinetic modeling of organic carbon accumulation (R^2 = 0.89 - 0.94), (b) diffusion-adsorption modeling of cadmium rebound potential, and (c) literature-based meta-analytical trends. These projections are explicitly presented as working hypotheses requiring long-term stationary field trials for confirmation. They are not presented as verified conclusions of this dissertation.

2.2 Overview of the Study Area

2.2.1 Natural Geography and Socioeconomic Characteristics of Guangdong Province

Guangdong Province, located at the southernmost tip of mainland China, belongs to the East Asian monsoon region. It boasts abundant sunshine and rainfall, with 1.9019 million hectares of arable land (Guangdong Provincial Third National Land Survey Leading Group Office, 2021), accounting for approximately one-tenth of the province's total area. As the largest grain-consuming region and a major rice-producing area in China, Guangdong's agricultural development bears the responsibility of "leading the nation" (Feng Shanshan et al., 2024). The main typical arable land types are paddy soil and lateritic red soil. Paddy soil, based on various natural steep slopes and dry soils, has the largest area formed by long-term artificial irrigation, accounting for 14.77% of the province's total soil area. It is a major production base for grain crops and an important base for various cash crops, forming the backbone of the province's agricultural production. Lateritic red soil is a representative tropical soil of Guangdong Province and a major soil resource. Its distribution areas have abundant sunshine and rainfall, a wide variety of crops, and huge production potential. It is an important production base for grain, sugarcane, oil crops, and especially tropical cash crops . See Figure 2.1 for an administrative map of Guangdong Province.

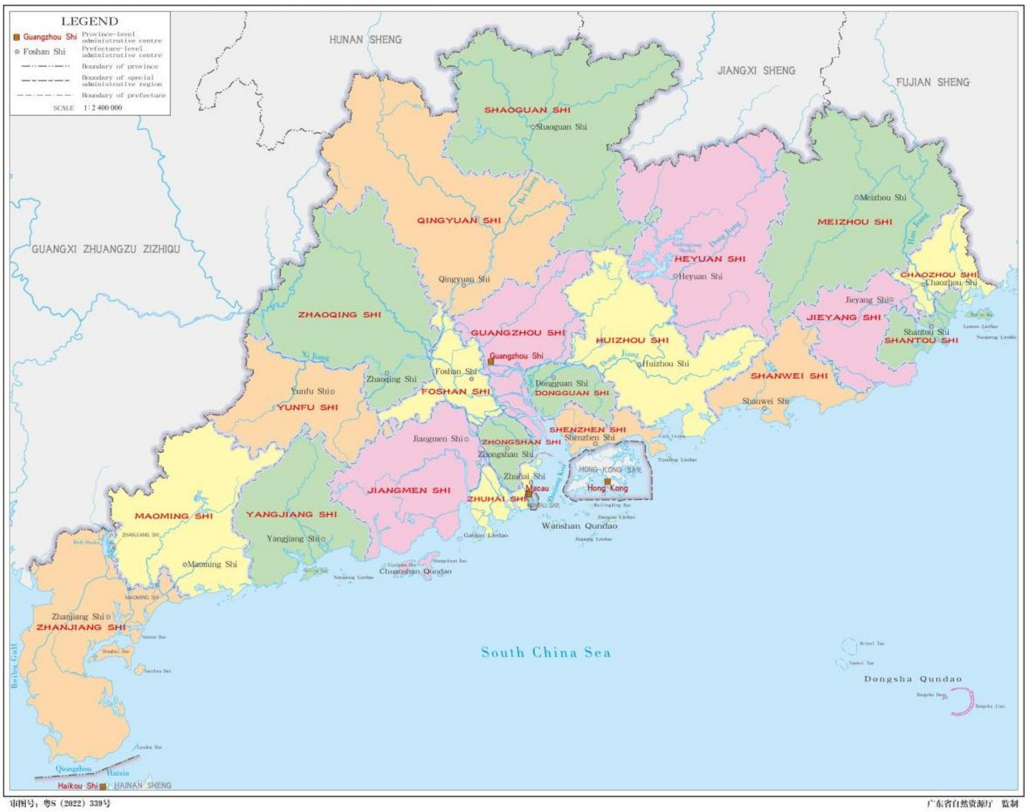

Figure 2.1 Administrative Map of Guangdong Province

Guangdong is the fastest-growing region in China's economy. With rapid economic development, Guangdong's arable land area has been shrinking year by year. As of 2020, the per capita arable land area was only 0.0153 hectares, less than one-fifth of the national average and only 5.35% of the global average. In the future, the tension between people and land, and the contradiction between land and the economy, will continue to exist in Guangdong (Zhu Wenrui, 2020).

2.2.2 Major Land Degradation Types and Spatial Distribution in Guangdong Province (with a focus on the Pearl River Delta)

Dynamic analysis of land degradation level

The study results indicate that land degradation in the study area generally showed a downward trend from 2000 to 2020. Specifically, the severity of land degradation accelerated from 2000 to 2010, but the rate of degradation accelerated significantly from 2010 to 2020. Specifically, between 2000 and 2010, the area of non-degraded land decreased by 3,211.1 km² (a decrease of 8.35%), the area of slightly degraded land increased by 2,610.7 km² (an increase of 21.32%), the area of moderately degraded land increased by 260.2 km² (an increase of 6.53%), while the area of highly degraded land increased significantly by 340.2 km² (an increase of 49.91%). The main reasons for the accelerated degradation during this period were the dramatic increase in the area of moderate and severe desertification (an increase of 56.5%, or 1,351.5 km²) and the overall rise in soil erosion intensity (the total area of moderate and severe erosion increased by 785.3 km², with high - intensity erosion increasing by 108.54%), despite a relatively moderate decline in vegetation cover (low-intensity vegetation cover increased by only 987.6 km²). From 2010 to 2020, the rate and severity of land degradation accelerated significantly. The area of non-degraded land further decreased by 4,398.7 km² (a decrease of 12.48%), the area of slightly degraded land increased by 1,389.5 km² (an increase of 9.35%), the area of moderately degraded land surged by 1,999.7 km² (an increase of 47.10%), and most notably, the area of highly degraded land increased dramatically by 999.5 km² (an increase of 97.83%), reaching a total area of 2,021.2 km². The driving factors behind the rapid deterioration of vegetation cover over the past decade are multifaceted. Vegetation cover has continued to deteriorate significantly, with low-intensity cover increasing by 1031.3 km² (1.86%) compared to 2010, while medium- and high-intensity cover decreased accordingly. High desertification areas have continued to expand, increasing by 944 km² (25.22%) compared to 2010. Notably, soil erosion intensity has significantly increased, with slightly eroded areas decreasing by 3611.3 km² (8.23%) and increasing by 1389.4 km² (15.69%). Meanwhile, areas of moderate, severe, very severe, and extremely severe erosion increased by 1260.5 km² (63.49%), 499.8 km² (97.5%), 350.6 km² (241.46%), and 111 km² (853.85%), respectively. The proportion of high-intensity erosion areas in the erosion modulus has increased significantly.

Analysis of Factors Affecting Land Degradation in the Study Area

The impact of human factors. According to the comprehensive land degradation assessment model, the degree of land degradation in the study area intensified between 2000 and 2010, and gradually slowed down between 2010 and 2020. The evolution of land degradation in the Pearl River Delta region is deeply intertwined with regional policy orientation: the industrialization wave from 2000 to 2010, and the priority given to GDP growth in Guangdong Province's 10th and 11th Five-Year Plans, led to a surge in construction land use and intensified ecological space destruction. Guangdong Province's "10th Five-Year Plan" prioritized GDP growth, resulting in the rampant consumption of ecological space by construction land - the electronics industry land in Dongguan and Shenzhen expanded by an average of 12.5% annually, 82.6% of flat farmland was covered by factories and roads, vegetation coverage plummeted by 14.2%, and desertification area surged by 161.7%. The economic priority strategy during this period led to disorderly development in hilly areas, with the soil erosion modulus soaring by 311.9%, and land degradation showing an irreversible deterioration trend. The turning point began with the fundamental adjustment of the policy paradigm after 2010. In 2014, the "Pearl River Delta Ecological Control Line Plan" designated 25% of the land as ecological protection zones, resulting in a 4-percentage point decrease in the area of severe desertification within Shenzhen's ecological control line for the first time. Dongguan closed 53,000 scattered and polluting enterprises, increasing the greening rate of vacant land by 68 percentage points and significantly slowing the expansion of areas with extremely low vegetation cover. The implementation of the Guangdong-Hong Kong-Macao Greater Bay Area national strategy has spurred cross - border governance innovation - the Shenzhen-Shantou Cooperation Zone achieved a 21% increase in vegetation restoration area through an ecological compensation mechanism, and Foshan's "industry and construction symbiosis" model reduced the demand for new land by 37%. The policy shift from "blind expansion" to "ecological and economic synergy" has become the core social driving force for curbing land degradation.

Natural factors. At the natural level, the contributions of desertification, vegetation degradation, and soil erosion to land degradation show distinct geographical differences. The evolutionary trajectory of desertification closely matches human intervention: due to continuous high-intensity development, the Dapeng Peninsula in Shenzhen will still account for 42% of the city's severely desertified areas by 2020; while the Conghua Ecological Reserve in northern

Guangzhou, due to mountain closure and forest restoration, has seen its desertification-free area increase by 15.3%. Vegetation degradation spatially exposes the unbalanced development of chronic diseases caused by industrial density in the Guangzhou-Shenzhen Science and Technology Innovation Corridor (Dongguan-Shenzhen section). In 2020, the vegetation coverage in this area was extremely low, reaching as high as 51%, becoming an ecological scar; while the Hengqin New Area in Zhuhai, through island ecological restoration, has seen its medium-to-high vegetation coverage area increase by 28.6%, becoming a model of blue-green integration. Soil erosion truly dominates the natural degradation process, accounting for 40% in the comprehensive evaluation model, and its spatial coupling with the Land Degradation Index (LD) is as high as $R^2 = 0.91$ ($p<0.01$). The severe erosion in the hilly area of Huizhou (accounting for 18% of the city's area) stems from the fatal combination of steep slope development and heavy rainfall - the "6 - 8" heavy rainfall in 2020 triggered landslides, with a single-day erosion modulus exceeding 500 t/hm². The karst landform area of Zhaoqing is characterized by the natural vulnerability of karst geology and superimposed karst geological features, which are the main causes of land degradation in this region. Due to the natural vulnerability of karst geology combined with the disturbance caused by the construction of the Guangzhou - Foshan - Zhaoqing Expressway, the erosion rate in the Zhaoqing karst landform area reached 311.9%. These natural factors, catalyzed by human activities, have resulted in the Dongguan - Shenzhen industrial corridor consistently experiencing a higher degree of degradation than surrounding areas, revealing a deep-seated mechanism of "human activities reshaping natural risks."

Based on research data and results, this dissertation demonstrates that land degradation in the Pearl River Delta region is evolutionary and is a spatiotemporal manifestation of the interplay between policy orientation and natural vulnerability.

The growth - oriented model of the early industrialization period (2000 - 2010) directly led to a 14.2% decrease in vegetation cover and a surge of 187.2% in desertification area. This was mainly due to the extensive expansion of land use (an average of 1200 km² of flat arable land per year) and overdevelopment of hilly areas, resulting in a sharp increase in land degradation rates. The strategic shift in ecological policy after 2010, particularly the strict protection of 25% of land under the Pearl River Delta Ecological Control Line Plan, reduced the severely desertified area in Shenzhen by 4% and achieved a 68% greening rate for abandoned land in Dongguan. This demonstrates the effectiveness of institutional restructuring in reversing degradation.

At the natural level, the dominant role of the soil erosion factor (weight 40%) reveals the deep logic of the degradation mechanism: the development of steep slopes in the hilly areas of Huizhou led to the LS factor exceeding 15, coupled with the "6-8" rainstorm in 2020 (single-day erosion modulus > 500 t/hm²), making 18% of the city's area a severely eroded zone; while the disturbance caused by the construction of the Guangzhou-Foshan-Zhaoqing Expressway in the Zhaoqing karst landform area increased the rate of severe erosion by 311.9%. In the Zhaoqing karst landform area, the growth rate of severe erosion under the disturbance of the Guangzhou-Foshan-Zhaoqing Expressway construction was 311.9%. The spatial coupling degree between these natural responses and the land degradation index (LD) is as high as $R^2 = 0.91$ ($p < 0.01$), confirming that human activities have reshaped the geographical pattern of degradation hotspots by amplifying geological and climatic risks (for example, the LD value of the Dongguan-Shenzhen industrial corridor is more than 2.3 times the regional average).

2.3 Experimental Design and Methods

2.3.1 Soil Data Collection in the Study Area

The sampling sites for this study are located in Guangdong Province, which has a South subtropical maritime monsoon climate. The terrain consists primarily of hills and terraces. Sampling was conducted in accordance with HJ/T 166-2004, “Technical Specifications for Soil Environmental Monitoring.” A total of 30 sampling points were established based on the actual conditions of the farmland.

Figure 2.2 Soil Sampling

The soil test results are provided in the attachment. The tests covered six parameters: pH, available phosphorus, bulk density, texture, soil organic matter, and available potassium. pH was determined directly using the potentiometric method; available phosphorus was determined using spectrophotometry; bulk density was determined using the ring-and-knife method; texture was determined using a soil gravimeter; soil organic matter was determined using the potassium dichromate oxidation method; and available potassium was determined using extraction with a neutral 1 mol/L ammonium acetate solution followed by flame photometry.

2.3.2 Comprehensive Assessment of Land Degradation in the Study Area

The data used in this study mainly include a number of aspects such as digital elevation DEM data, vegetation normalized index NDVI, average annual rainfall, soil database, land use types, and regional administrative boundary vector data. The main sources of these data are shown in Table 2.1, and detailed data processing and analysis were carried out by ArcGIS software.

Table 2.1

Sources of DEM and other data

Digital	Source (of information etc)
30 m digital elevation data	Geospatial data cloud platform
1 000 m Chinese soil data	National Tibetan Plateau Science Data Center (http://data.tpdc.ac.cn)
Annual precipitation data	National Earth System Science Data Center (https://www.geodata.cn)
30 m Land use data	Resource Environmental Science and Data Platform
250 m NDVI data	National Tibetan Plateau Science Data Center (http://data.tpdc.ac.cn)

Extraction of information on land degradation indicators. Desertification information extraction method: The Pearl River Delta (PRD) region is located in the humid zone, but as one of the most rapidly developing economic regions in China, the ecological environment is more fragile, which makes the land in the study area more susceptible to desertification. The dynamic monitoring of vegetation index in the humid zone is one of the key indicators for studying the evolution of desertification. Due to the precision of obtaining data and the difficulty of obtaining source data, this dissertation did not adopt the DDI model, but the simpler DI model based on the vegetation cover data in 2000, 2010 and 2020 to obtain the desertification index data of the PRD region for three years, and the calculation formulas are as follows:

$$DI = 1 - FVC_i$$

Where: DI stands for desertification index; FVC stands for vegetation cover.

This dissertation draws on the relevant research of Tan Xueling (Tan Xueling, 2018) and uses the natural breakpoint classification method to classify desertification severity into no desertification, mild desertification, moderate desertification, and severe desertification, thereby constructing a desertification severity model.

Vegetation degradation information extraction method: Vegetation degradation information can be reflected through changes in vegetation coverage. This dissertation extracts vegetation coverage in the study area based on the principle of the pixel binary model, and vegetation indices are used to calculate coverage. According to HJ/T192 - 2015 "Technical Specifications for the Evaluation of Ecological Environment Conditions," vegetation cover is classified into five levels: extremely low cover, low cover, moderate cover, medium-high cover, and high cover. The calculation formula is as follows:

$$FVC=(NDVI\text{-}NDVI_{soil})/\left(NDVI_{veg}\text{-}NDVI_{soil}\right)$$

Where: FVC stands for vegetation cover, NDVI is the normalized vegetation index for each image, NDVIsoil stands for the vegetation index of land or low vegetation cover, and NDVIveg represents the vegetation index of highly vegetated areas.

According to the Technical Specification for the Supervision of Ecological Conservation Redlines - Ecological Function Evaluation (Trial) (HJ 1142-2020), the formula for soil erosion information extraction method (RUSLE model) is as follows:

$$A=R\times K\times L\times S\times C\times P$$

Where: A represents the average annual soil erosion modulus, t/(hm$^{(2)\text{ - a}}$);

R stands for rainfall erosivity factor, MJ-mm/(hm^2-h-a);

K represents soil erodibility factor, t-hm2-h/(hm^2-MJ-mm);

L represents the slope length factor;

S stands for slope factor;

C stands for vegetation cover and management factors;

P stands for soil and water conservation factor.

The RUSLE model can be dynamically analyzed based on ArcGIS technology and remote sensing data in practical applications, providing a scientific basis for land degradation assessment and land management decision-making, with the following specific factorial research methods:

① Rainfall erosive force factor (R), various physical parameters of rainfall, such as the size, intensity and duration of rainfall, will have an impact on the erosive capacity and rate of the soil, which in turn may lead to the problem of soil erosion. In this dissertation, the erosive force model based on annual rainfall is adopted to calculate the formula as follows:

$$R_n = 0.053P_n^{1.996}$$

Where:$R_n$is the annual rainfall erosivity factor, unit:MJ-mm/(hm2-h-a); Pn is the annual rainfall, unit:mm.

② Soil erodibility factor *(K)*, *K* value reflects the size of soil erosion caused by different soil texture, the larger the value of *K*, the more prone to erosion of the soil. k value is calculated as follows:

$$K=\left\{0.2+0.3esp\left[-0.0256S_a\left(1-\frac{S_i}{100}\right)\right]\right\}\times\left[\frac{S_i}{S_i+C_1}\right]^{0.3}$$
$$\times\left[1-\frac{0.025OM}{OM+exp(3.72-2.95OM)}\right]\times\left[1-\frac{0.7SN_i}{SN_i+exp(-5.51+22.9SN_i)}\right]$$

Where: K represents the value of soil erodibility factor in t-hm^2-h/(hm^2-MJ-m); Sa, Si, Cl, sand (0.05-2 mm), silt (0.002-0.05 mm), clay (<0.002 mm), and soil organic matter percentage (%) in the OM U.S. system of soil particle grading standards; and SN = 1-Sa/ 100.

(iii) The terrain factor (*LS*) is calculated as follows:

$$H=H_{max}-H_{min}$$

Where: H is the topographic factor, $H_{max}$is the maximum value of elevation occurring in the neighborhood, and $H_{min}$is the minimum value of elevation occurring in the neighborhood.

④ Vegetation cover and management factor (C), as a dimensionless proportional variable, the C factor takes values between 0 and 1. When C is equal to 0, this means that the vegetation cover is excellent and the soil is not eroded, while when C is equal to 1, this means that there is no vegetation cover on the surface of the land, it is considered as wasteland, and the soil is directly affected by external forces, as calculated by the following formula:

$$C=\begin{cases} 1 & f_c=0 \\ 0.6508\text{-}0.3436lgf & 0<f_c\leq 78.3\% \\ 0 & f_c=78.3\% \end{cases}$$

Where: *C* factor reflects the influence of vegetation cover and management measures on soil erosion rate, and $f_c$is the degree of vegetation cover. When f_c>78.3%, C=0, no soil loss; when fc=0, C=1, very easy to produce soil loss.

⑤ Soil and water conservation factor (P), defined as the effect of land use mode or farming system on soil erosion.The P factor is an empirical factor and the factor with the largest uncertainty. This dissertation based on the *RUSLE* model and Zhang Sifan's (2024) research on soil and water conservation in Liaoning Province, assigning the value of arable land with a slope of less than 6 degrees to 0.1, and the specific values of forest land, grassland, watersheds, construction land, and unutilized land are shown in Table 2.2 It generally influences land degradation processes by affecting evaporation rates and vegetation cover, and the area of arable land with a slope degree of less than 2 degrees (including 2 degrees) in the Pearl River Delta (PRD) region is closely linked to the size of the soil and water conservation effect of the arable land. According to the data of the Third National Land Survey, the area of cultivated land with a slope of less than 2 degrees (including 2 degrees) and the area of cultivated land with a slope of 2-6 degrees (including 6 degrees) in the PRD Region are shown in Table 2.3.

Table 2.2

The primary land use type is assigned P

Land use type	plow land	woodland	grasslands	body of water	building site	unutilized land
P-value	0.1	1	1	0	0	1

Table 2.3

Farmland area in the Pearl River Delta region

<table>
<tr><th>Municipalities</th><th>≤2° arable land area (km^2)</th><th>Percentage (%)</th><th>Area of cultivated land 2°-6° (km^2)</th><th>Percentage (%)</th><th>Total area of arable land (km^2)</th></tr>
<tr><td>Guangzhou</td><td rowspan="2">11811128</td><td rowspan="2">74.64</td><td rowspan="2">2317509</td><td rowspan="2">14.65</td><td rowspan="2">15824242</td></tr>
<tr><td>Zhaoqing</td></tr>
<tr><td>Shenzhen</td><td>185669</td><td>65.27</td><td>55304</td><td>19.44</td><td>284474</td></tr>
<tr><td>Zhuhai</td><td>610778</td><td>93.14</td><td>34474</td><td>5.26</td><td>655746</td></tr>
<tr><td>Foshan</td><td>174612</td><td>52.50</td><td>73645</td><td>3.48</td><td>2116436</td></tr>
<tr><td>Huizhou</td><td>7901250</td><td>86.47</td><td>1012844</td><td>11.08</td><td>9137214</td></tr>
</table>

Dongguan	761911	82.4	112812	12.2	924686
Zhongshan	664876	89.99	60352	8.17	738544
Jiangmen	9889680	89.08	867051	7.81	11101738
Add up the total	31999904	78.46	4533991	11.12	40783080

Note: Since Guangzhou and Zhaoqing have not released any data, the data of Guangzhou and Zhaoqing are derived from the data of the Third National Land Survey of Guangdong Province minus the data of the Third National Land Survey of the other 19 prefectural-level cities in Guangdong Province.

After calculating the average soil erosion modulus in the study area from 2000 to 2020, the soil erosion modulus was divided into six intensity levels based on the Soil Erosion Classification and Grading Standard (SL190-2007) (Ministry of Water Resources of the People's Republic of China, 2008), and the specific classification standards are shown in Table 2.4.

Table 2.4

Soil erosion intensity classification standard

Soil erosion intensity	Erosion modulus (t-hm$^{(-2)\ \text{-a-1}}$)	Soil erosion intensity	Erosion modulus (t-hm$^{(-2)\ \text{-a-1}}$)
mildly corrosive	0-2	aggressively corrode	50-80
Light erosion	2-25	Very strong erosion	80-150
Moderate erosion	25-50	violent erosion	＞150
Note: Unit km^2			

Comprehensive Evaluation Model of Land Degradation. This dissertation adopts the gray correlation analysis method (Yu Haochen, 2019), refers to Li Tianhong's research (2012) and combines with the actual situation of the study area, establishes a comprehensive evaluation model of land degradation based on the theoretical analysis of land degradation index weights, so as to explore the dynamic trend of land degradation in the Pearl River Delta (PRD) region. Due to the limitations of the actual situation, the weights of vegetation cover, desertification and soil erosion in this dissertation are assigned by simple weighting, and the sum of the weights of the three is 1.

$$LD = a_1B_1 + a_2B_2 + a_3B_3$$

Among them, LD is the measurement result of land degradation; Where B_1, B_2, B_3 correspond to the normalized values of vegetation degradation, desertification, and soil erosion, respectively. The weights were determined as a_1 = 0.4, a_2 = 0.2, a_3 = 0.4, based on the following rationale:

Soil erosion (a_3 = 0.4) was assigned the highest weight because (a) it is the most directly measurable physical degradation process in the region, (b) it accounts for the largest area of degradation based on preliminary data, and (c) previous studies in southern China have identified it as the primary degradation driver.

Vegetation degradation (a_1 = 0.4) was weighted equally to erosion because vegetation cover change integrates both natural and anthropogenic pressures and serves as a sensitive indicator of ecosystem health.

Desertification (a_2 = 0.2) was given a lower weight because the Pearl River Delta is located in a humid zone, where classic “desertification” (arid-zone sand encroachment) is not the dominant process; rather, the DI index here reflects localized vegetation loss due to urbanization and land use change.

In this dissertation, referring to Bian Zhengfu's (2020) research on the influence factors of land degradation in the western key coal mining area , the land degradation measurement results were classified into four grades, namely, no degradation (1.00 - 1.50), mild degradation (1.50 - 2.00), moderate degradation (2.00 - 2.75), and severe degradation (2.75-4.00), using the NDVI value as the reference index, with the value of LD taken as 1 - 4.

Identified uncertainty sources and error characterization

The following uncertainty sources were identified and, where possible, quantified （Table 2.5）.

Table 2.5

Identified uncertainty sources and error characterization in the land degradation assessment model

Uncertainty source	Affected indicator	Estimated magnitude / nature	Mitigation or acknowledgment
NDVI saturation and atmospheric effects	FVC, DI	Seasonal variations; cloud cover reduces temporal consistency in some years	Monthly composite NDVI data were used; Landsat scenes with cloud cover >10% were excluded
DEM resolution (30 m)	LS factor in RUSLE	Error in slope length and steepness factor: estimated ±5 - 8%	DEM from Geospatial Data Cloud (30 m) was used; higher-resolution (≤10 m) data were not uniformly available for 2000 - 2020
Rainfall erosivity (R factor)	Soil erosion modulus (A)	Interpolation error from sparse rain-gauge network: estimated ±10% in western PRD	R factor derived from annual rainfall data ($0.053P^{1.996}$); monthly rainfall distribution data were not available for the full period
C-factor and P-factor assignment	Soil erosion modulus (A)	Empirical values may not fully represent local land management practices	Values adopted from national technical standards (HJ/T192- 2015) and Zhang Sifan (2024); field-specific validation was not performed
Soil erodibility (K factor)	Soil erosion modulus (A)	Based on 1:1,000,000 Chinese soil database; local-scale variability may be underrepresented	Standard EPIC model was used; no field K-factor measurements were available for this study
Temporal data consistency	All indicators	Early-period data (2000 - 2005) have lower radiometric and geometric accuracy compared to recent data (2015 - 2020) due to sensor differences (Landsat 5 vs. Landsat 8)	Cross-sensor calibration was applied using MODIS NDVI as reference; residual uncertainty remains, particularly for pre-2005 trends

Overall, the cumulative uncertainty of the LD index is qualitatively estimated at ±10 - 15% for the regional-scale assessment, based on propagation of the individual error sources listed above. Quantitative uncertainty propagation (e.g., Monte Carlo simulation) was not performed due to the absence of probability distributions for each parameter; this constitutes a limitation of the current methodology.

2.3.3 Controlled Pot Experiment: Effects of Green Manure Combined with Fertilizer on Microbial Communities in Poor Red Soil – A Case Study of Milk Vetch and Ryegrass

Experimental design statement. The microbiological investigation presented in this section was conducted as a controlled pot experiment under laboratory/greenhouse conditions (Shenzhen Sino Assessment Group Laboratory, March - November 2023). This approach was deliberately chosen to isolate the causal effects of green manure - fertilizer combinations on soil microbial communities by minimizing confounding environmental variables (e.g., climatic fluctuations, lateral water flow, and faunal bioturbation). It is important to emphasize that this pot experiment serves a mechanistic, hypothesis-generating purpose. The quantitative microbial indicators obtained here (e.g., Chao1, Shannon indices, functional gene abundances) represent model-system responses and cannot be directly extrapolated to field agroecosystems without dedicated field validation. The field-scale applicability of these microbial mechanisms is addressed in Chapter 6, with explicit recognition of this limitation. The chemical and also the physical characteristics of that of the soil are actually very much mainly summarized in Table 2.6 below.

Table 2.6

Physical as well as Chemical features of the Soil Used in the Experiment

Property	Value/features
Soil	Comprised of Red glutamate, sand shale, and red sandstone
Soil pH (water: soil, 5:1)	5.31
Soil Organic matter	2.52g/kg
Total Nitrogen	0.29g/kg
Total phosphorus	0.69g/kg
Available potassium	54mg/kg
Alkaline hydrolyzable nitrogen	21.3g/kg

2.3.3.1 Sampling and Experimentation

Before sowing, the seeds were surface-sterilized with sodium hypochlorite solution, rinsed thoroughly with distilled water, and then germinated on moist filter paper at 25°C for 48 hours. Twenty germinated seeds were sown per pot (diameter 30 cm, area 0.07 m^2). After emergence, seedlings were thinned to 15 uniform seedlings per pot at the two-leaf stage.

In addition to the green manure, like milk vetch or ryegrass, the control treatment was a fallow, and plant response contrasts with an organically-manured fallow, or a fallow treated with "humic acid" form of fertilizer, or the mineral fertilizer. A control treatment was also incorporated into the study; it did not have fertilizer or green manure species. This led to 10 treatments, namely (1) Milk vetch accompanies with the organic manure (MO), (2) milk vetch with that of humic acid fertilizer (MH), (3) a combination of milk vetch and mineral fertilizer (MG), (4) Ryegrass plus organic manure (RO), (5) Ryegrass with humic acid fertilizer (RH), (6) Ryegrass plus mineral fertilizer (Treatments A, B, C were repeated three times each, as illustrated in the following Table 2.7.

Table 2.7

Green Manure - Fertilizer Combination Application: Experimental Treatments for Potted Plants and Plot (Pot) Information

Processing Code	Green Manure Types	Type of fertilizer	Green manure sowing method	Green manure incorporation rate (g/pot, fresh weight)	Fertilizer application rate (g/pot)	Duplicate number	Area per pot (m^2)	Experimental Year
CK	None (Fallow)	None	—	0	0	3	0.07	2023
CF	None (Fallow)	Compound fertilizer (15- 15- 15)	—	0	2	3	0.07	2023
HAF	None (Fallow)	Humic acid fertilizer	—	0	2	3	0.07	2023
OMF	None (Fallow)	Commercial organic fertilizer	—	0	20	3	0.07	2023

RG	Ryegrass	None	Row seeding, row spacing 10 cm	200	0	3	0.07	2023
RH	Ryegrass	Humic acid fertilizer	Row seeding	200	2	3	0.07	2023
RO	Ryegrass	Commercial organic fertilizer	Row seeding	200	20	3	0.07	2023
MG	Milk vetch	Compound fertilizer	Broadcast seeding	200	2	3	0.07	2023
MH	Milk vetch	Humic acid fertilizer	Broadcast seeding	200	2	3	0.07	2023
MO	Milk vetch	Commercial organic fertilizer	Broadcast seeding	200	20	3	0.07	2023

Note. The fallow form of treatment lacked green manure, unlike the milk vetch and ryegrass treatments. Nonetheless, all three treatments included the three fertilizers (humic acid, organic, and mineral fertilizers). The control treatment without fertilizer and manure was also included.

Among the ten treatments, CK (fallow, no fertilizer), CF (fallow + compound fertilizer), HAF (fallow + humic acid fertilizer), and OMF (fallow + commercial organic fertilizer) served as non-planted controls without green manure, whereas RG, RH, RO, MG, MH, and MO were planted with ryegrass or milk vetch, respectively, as green manure treatments. This design allowed us to isolate the effects of green manure incorporation from those of fertilizer application alone.

The organic matter content was 29.2% for commercial organic fertilizer and 75.3% for humic acid fertilizer, whose nutritional content is summarized in Table 2.8 below.

Table 2.8

Nutritional Content of the Two Fertilizers Used

Soil properties	Humic acid fertilizer	Commercial organic fertilizer
pH	6.16	7.42
Soil organic matter ($g\ kg^{-1}$)	753.94	291.98
Total N ($g\ kg^{-1}$)	9.031	14.37
Phosphorus levels ($g\ kg^{-1}$)	7.871	17.91
Potassium Levels ($g\ kg^{-1}$)	1.31	33.1

The red soil was put in pots of 10kg each. Before the seeding of the green manure, all the treatments, included mineral fertilizers, except the control treatment (CK). The organic manure and humic acid were incorporated in HAF, RH, as well as the MH or the OMF, RO, and also the MO to obtain a level of 20g/kg. Before the time of sowing, the seeds were very properly disinfected, and also was properly washed with that of the sodium hypo-chlorite. In post germination, the seedlings were then properly thinned to about fifteen for every pot. The growth phase took place at 7.2 to 15^{o}C, while the incorporation phase occurred at 16-25^{o}C. Concerning the green manure, it was cut and inserted within the soil after about five months of continuing the process of growth. Throughout the harvest, the actual form of green manure plant shoots (used in six treatments with milk vetch and ryegrass) were severed, and their actual roots were very much meticulously removed. The soil surrounding the actual roots within various crops' rhizosphere was gathered by gently shaking the soil off the roots situated within the actual upper layer of that of the soil (approximately 2-9cm).

The soil which was collected was homogeneous due to the use of a soil corer; the sterile tubes were also used to take the samples to the laboratory in liquid nitrogen. It has to be pointed out that they were subjected to temperatures below 80oC prior to and during analysis. TAt the end of the 5-month growth period, the aboveground shoots of green manure (ryegrass or milk vetch) were harvested by cutting at the soil surface. The fresh shoots were weighed, and 200 g (fresh weight) of shoot biomass from each pot was cut into approximately 3 cm pieces and thoroughly mixed into the top 10 cm of soil of the same pot. The roots were carefully removed and discarded to avoid confounding effects. After incorporation, all pots were maintained under flooded conditions (approximately 2 cm standing water above the soil surface) for 8 weeks to simulate the typical water management practice for green manure decomposition in paddy fields. Soil samples were collected at the end of this 8-week incorporation period for subsequent analyses. After that, about 0.5kg of that of the soil examples which were properly occupied after the about 10 obtained form of samples using the soil corer at 10cm from the surface of the pot and then sub-sampled to about three parts. The initial sample which were collected within the 50ml sterile tubes and then was stored at about 80^{o}C was actually and properly used to get DNA; the second subsample which was sieved using a sieve of 4mm and was stored at 4^{o}C was the properly which were cast - off to properly evaluate the actual enzyme movement and microbial biomass within 7 days, while the third subsample collected in the sterile tubes was air dried then-ground into fine particles for the chemical and physical analysis.

2.3.3.2 Statistical Analyses and Measurements

Various methods, techniques, and tools were used to analyze the collected data. Table 2.9 below describes the various analyses conducted in this study.

Table 2.9

Statistical analysis methods and techniques employed in the research

Analysis method, tool, or technique	**Purpose or property analyzed**
SPSS Software (version 21.0)	Examination goes the properties of the green manure as well as the fertilizer mixtures on enzyme activities, microbial biomass carbon, as well as the soil properties. The least significant difference (LSD) test was used to compare the data at a 5% of that of the confidence level, while the actual variance homogeneity was established using Levene’s test.

Chao1 Index	"Microbial community richness"
Shannon Index	"Microbial community diversity"
Principal Coordinates Analysis (Coa)	To determine the level of difference among fungal as well as the bacterial communities
Redundancy Analysis (RDA)	To inspect relationship among soil fungal besides bacterial societies
Distance-based RDA (db.-RDA)	Achieved within the fungal as well as the bacterial genus level to understand the association between soil examples derived from respectively action besides the soil's chemical and physical belongings.
Analysis of similarities (ANOSIM)	Used to evaluate the actual statistical import among behaviors.
Welch's T-test	Utlized to analyze and compare fungal or bacterial taxa assemblies
linear discriminant analysis (LDA) effect size (Levees)	This remained properly castoff to create the actual noteworthy alterations in fungal or bacterial taxonomic group within the "green manure conducts" as well as the fallow treatments, regardless of fertilizer combination.
Functional annotation of prokaryotic taxa (FAPROTAX) database	This was utilized to properly forecast the actual bacterial community's practical clusters.

2.3.3.3 Analytical methods

(a) DNA extraction and high - throughput sequencing

Total genomic DNA was extracted from 0.5 g of fresh soil using the PowerSoil® Pro Kit (Qiagen, Germany) according to the manufacturer's protocol. DNA quality was assessed by 1% agarose gel electrophoresis and quantified using a NanoDrop 2000 spectrophotometer.

Bacterial 16S rRNA gene: V4 region was amplified using primers 515F (5′-GTGCCAGCMGCCGCGGTAA-3′) and 806R (5′-GGACTACHVGGGTWTCTAAT-3′).

Fungal ITS region: ITS1 region was amplified using primers ITS5 (5′-GGAAGTAAAAGTCGTAACAAGG-3′) and ITS2 (5′-GCTGCGTTCTTCATCGATGC-3′).

Amplicons were sequenced on an Illumina NovaSeq 6000 platform (2 × 250 bp paired - end). Raw reads were demultiplexed, quality - filtered (Phred score > 20), and chimera - removed using QIIME 2 (2024.2).

(b) Bioinformatic analysis

OTU clustering: 97% similarity using VSEARCH.

Taxonomy assignment: For bacteria, RDP classifier (v2.13) against SILVA 138 database; for fungi, UNITE (v9.0) database.

Alpha diversity: Shannon and Chao1 indices calculated using vegan package (R 4.3).

Beta diversity: Principal Coordinate Analysis (PCoA) based on Bray - Curtis distance; Permutational Multivariate Analysis of Variance (PERMANOVA, 999 permutations).

Functional prediction: Bacterial functions were predicted using FAPROTAX (v1.2.4) and PICRUSt2 (v2.5.0) against KEGG database.

It is important to emphasize that FAPROTAX and PICRUSt2 provide inferred functional potentials based on 16S rRNA gene-inferred community composition, not direct measurements of metabolic rates, enzyme activities, or gene expression levels. All functional interpretations derived from these tools are presented as mechanistic hypotheses that require independent validation through metatranscriptomics, proteomics, or targeted enzymatic assays.

(c) Quantitative PCR (qPCR) for functional genes

Absolute quantification of bacterial functional genes was performed on a CFX96 Touch™ Real - Time PCR Detection System (Bio - Rad). Each 20 μL reaction contained: 10 μL SYBR® Green Premix Ex Taq™ (Tli RNaseH Plus), 0.4 μL of each primer (10 μM), 2 μL template DNA (10 ng/μL), and 7.2 μL sterile ddH_2O. Thermal cycling conditions:

95 °C for 2 min; 40 cycles of 95 °C for 15 s, annealing (see Table 2.10) for 30 s, 72 °C for 30 s; followed by melt curve analysis.

Table 2.10

Thermal Cycling Conditions

Gene	Primer sequences (5′→3′)	Annealing T (°C)	Amplicon size (bp)	Function
16S rRNA (bacteria)	1369F / 1492R	56	123	Total bacteria
nifH	nifH- F / nifH- R	58	360	Nitrogen fixation
phoD	phoD- F / phoD- R	55	290	Alkaline phosphatase
czcA	czcA- F / czcA- R	60	200	Cd/Zn/Co efflux pump
cadA	cadA- F / cadA- R	58	180	Cadmium resistance

Standard curves were generated using 10 - fold serial dilutions of plasmid DNA containing the target gene fragments ($R^2 > 0.99$, efficiency 90 - 110%). Results are expressed as copies per gram of dry soil.

(d) Soil enzyme activity assays

Fresh soil samples (stored at 4 °C, analyzed within 7 days) were used for enzyme assays:

Urease activity: Indophenol blue colorimetric method; activity expressed as µg NH_4^+ - N released per gram dry soil per hour (µg N/g/h).

Alkaline phosphatase: p - nitrophenyl phosphate (pNPP) substrate; colorimetric measurement at 405 nm; activity expressed as µmol p - nitrophenol released per gram per hour (µmol PNP/g/h).

Dehydrogenase activity: 2,3,5 - triphenyltetrazolium chloride (TTC) reduction; colorimetric measurement at 485 nm; activity expressed as µg triphenylformazan (TPF) per gram per hour (µg TPF/g/h).

2.3.3.4 Statistical inference protocols: experimental units, replication structure, and hypothesis testing

To ensure the transparency and reproducibility of all statistical comparisons presented in this dissertation, the following standardized protocols were applied consistently to both the pot experiment (Section 2.3.3; results in Chapter 5) and the field optimization experiment (Section 2.3.4; results in Chapter 4), unless explicitly stated otherwise.

Table 2.11

Experimental units and replication structure

Experiment type	Biological replicates (n)	Technical replicates	Definition
Pot experiment (Chapter 5)	3 pots per treatment (n = 3)	3 analytical replicates per pot for qPCR and enzyme assays; 5 replicate soil cores per pot for physico-chemical homogenization	Biological replicate = independently prepared pot (10 kg soil). Technical replicate = repeated instrumental measurement from the same biological sample.
Field optimization experiment (Chapter 4)	3 plots per treatment combination (n = 3)	5-point composite soil sample per plot; 3 repeated injections for ICP-MS analysis	Biological replicate = independently treated field plot (2 m × 2 m). Technical replicate = repeated laboratory determination from the same composite sample.

All results are reported as mean ± standard error (SE) based on biological replicates (n = 3). The standard error was calculated as SD / √n, where SD represents the standard deviation among biological replicates. In all tables, SE values reflect between- plot (or between- pot) variation, not within- sample measurement error, unless specifically noted in the table footnote.

Normality and homogeneity of variance testing

Prior to parametric analyses, the following assumptions were verified for each response variable:

Normality: assessed using the Shapiro - Wilk test at $\alpha = 0.05$. Where the assumption was violated ($p < 0.05$), data were either (i) transformed using natural logarithm or square- root transformation, or (ii) analyzed using non- parametric alternatives (Kruskal - Wallis test for one- way designs; permutational ANOVA for multivariate responses).

Homogeneity of variances: assessed using Levene's test at $\alpha = 0.05$. Where variances were unequal, Welch's ANOVA was applied for the main effect, followed by Games- Howell post - hoc comparisons.

Analysis of variance (ANOVA) and post - hoc multiple comparisons

For single - factor experiments comparing ≥3 treatment groups (e.g., green manure species, fertilizer types), one - way ANOVA was performed. For factorial experiments involving two or more categorical factors (e.g., green manure × fertilizer interaction), two - way ANOVA was applied.

When ANOVA indicated a significant main effect or interaction ($p < 0.05$), post - hoc multiple comparisons were conducted using Duncan's multiple range test at a family - wise error rate of $\alpha = 0.05$. Results of these comparisons are presented in all relevant tables using lowercase superscript letters (a, b, c, etc.), where different letters within the same column indicate statistically significant differences among treatments ($p < 0.05$). The specific post - hoc procedure is noted in each table footnote to ensure clarity.

Multivariate and correlation analyses

Pearson correlation coefficients (r) were calculated for pairwise associations between soil properties and microbial indicators. Statistical significance was evaluated using two- tailed tests at $\alpha = 0.05$ and 0.01, with significance levels denoted as * ($p < 0.05$) and ** ($p < 0.01$) in correlation matrices.

Redundancy analysis (RDA) and Distance - based RDA (db- RDA) were performed using the vegan package (R 4.3). Significance of environmental constraints was tested using permutational ANOVA (PERMANOVA) with 999 permutations.

Principal Coordinates Analysis (PCoA) based on Bray - Curtis dissimilarity was used to visualize β - diversity patterns, with group differences tested via ANOSIM (analysis of similarities) using 999 permutations.

Software and implementation

All statistical analyses were performed using SPSS Statistics (version 21.0) for univariate ANOVA and post - hoc tests, and R (version 4.3) with the vegan, stats, and car packages for multivariate analyses, permutation tests, and diagnostic plotting. Graphical outputs were generated using ggplot2 (R) and OriginPro (2024). All reported p - values are two- tailed, and differences were considered statistically significant at $p < 0.05$ unless otherwise indicated.

2.3.4 Optimization of Agronomic Measures for Soil Functional Restoration of Degraded Cropland in Guangdong Province: Model Construction and Validation Based on Response Surface Method and Random Forests

2.3.4.1 Study area

In this study, 10 typical degraded arable lands in the Pearl River Delta were selected as the study area, whose geographical scope covers the agricultural core areas of Guangzhou, Foshan and Dongguan(Table 2.12). The soil degradation characteristics of this region are significant, historical monitoring data show that the pH value of surface soil is between 4.5 - 5.8, the proportion of potential cadmium contamination sites is up to 30%, and the available phosphorus content is generally lower than 8 mg/kg, which presents a typical composite degradation pattern of acidification and nutrient imbalance. The selection of the study area was based on multi-source data fusion analysis: firstly, high-resolution remote sensing images were used to identify the spatial heterogeneity of soil salinization and heavy metals, and then typical plots with a contiguous area of more than 2 hectares were screened by combining with historical agricultural management data. In addition, regional climatic characteristics accelerated soil organic carbon mineralization, further exacerbating ecological vulnerability. The layout of the study area takes into account spatial representativeness and differences in environmental gradients, e.g., the cadmium contamination concentration of the plots in the town of Mayong, Dongguan, was 2.4 times higher than that in the Gaoming District, Foshan, which provides a basis for comparison for model validation.

Table 2.12

Basic information and key degradation indicators of the study area

Point number	geographic position	pH Value range	Available phosphorus (AP) (mg/kg)	Acidobacteria abundance (%)	Soil organic carbon (SOC) (%)	Cadmium (Cd) content (mg/kg)
P1	Guangzhou, Nansha	5.0-5.4	8.5	13.2	1.2	0.32
P2	Foshan Gaoming District	4.6-5.0	7.8	11.5	0.9	0.45
P3	Dongguan Machong Town	5.2-5.6	9.3	14.8	1.4	0.25
P4	Shunde District, Foshan	4.4-4.8	6.5	9.2	0.7	0.53
P5	Zengcheng, Guangzhou	5.4-5.8	10.1	16.3	1.6	0.18
P6	North of Zhongshan	4.7-5.1	7.3	10.4	0.8	0.49
P7	Guangzhou Conghua	5.1-5.5	8.2	12.8	1.1	0.35
P8	Huizhou Boluo	4.9-5.3	7.6	11.0	0.9	0.41
P9	Zhuhai	4.8-	7.1	10.1	0.8	0.47

	Doumen	5.2				
P10	Jiangmen Xinhui	5.0-5.4	8.8	13.5	1.3	0.29

Table 2.13

Summary scheme of the field experiment for agronomic optimization (RF-RSM model validation)

Item	Description / Specification
Place of research	Pearl River Delta region, see Table 2.10 for detailed geographic coordinates and site - specific degradation indicators.
Years of experiment	2023 - 2024 (field monitoring conducted at 3, 6, 12, and 18 months post-treatment).
Experimental design type	Three-factor, three - level Box - Behnken design (BBD) combined with multi - objective optimization (RF - RSM).
Factors and levels (actual)	X_1: Biochar application rate (0, 10, 20 $t \cdot ha^{-1}$); X_2: Lime application rate (0, 3, 6 $t \cdot ha^{-1}$); X_3: Leguminous green manure species (Ryegrass, Milk vetch, Soybean).
Treatment variants	17 experimental runs: 12 factorial points + 5 center-point replicates.
Plot size / accounting area	Plot size: 2 m × 2 m (4 m^2) per treatment. Accounting (net) plot area: 2 m^2 (1 m × 2 m), central sampling zone excluding border rows to minimize edge effects.
Number of replications	Biological replicates: 3 independent plots per treatment combination (n = 3). Technical replicates: 5 - point composite soil sample per plot; 3 repeated injections for ICP - MS analysis. Center points replicated 5 times to estimate pure experimental error.

Initial soil status (pre-experiment)	Soil type: Acidic red soil (lateritic red soil). Key degradation indicators (based on pre - sampling across 10 sites, Table 2.10): pH 4.5 - 5.8 (strongly acidic); Available phosphorus (AP) 6.5 - 10.1 mg/kg (deficient); Cadmium (Cd) 0.18 - 0.53 mg/kg (light to moderate contamination); Soil organic carbon (SOC) 0.7 - 1.6% (low). Bulk density: 1.3 -1.5 $g \cdot cm^{-3}$.
Type of research	Multi - factor agronomic optimization field micro-plot experiment. Objectives: (i) quantify synergistic effects of biochar, lime, and green manure on soil functional recovery; (ii) identify optimal combination parameters maximizing soil function recovery index (SFRI) while minimizing economic cost.
Main indicators determined	Soil physicochemical properties: pH, available phosphorus (AP, $mg \cdot kg^{-1}$), soil organic carbon (SOC, %), soil porosity (%), bulk density. Heavy metal: available cadmium (Cd, $mg \cdot kg^{-1}$), cadmium speciation (BCR sequential extraction: exchangeable, Fe-Mn oxide - bound, organic - bound, residual). Microbiological: Microbial Shannon diversity index (from 16S rRNA sequencing), abundance of key functional genes (*nifH*, *phoD*, *czcA*, *cadA* via qPCR). Response / optimization variable: Soil Function Recovery Index (SFRI, 0 - 1 scale).
Statistical analysis	Random Forest variable importance screening; Response Surface Methodology (RSM) second - order polynomial regression; NSGA - II multi-objective optimization for Pareto frontier; ANOVA with Duncan's multiple range test ($p < 0.05$) for treatment comparisons.

2.3.4.2 Data collection

Samples of 0-20 cm soil layer were collected before and after the implementation of remediation measures. The sampling points were laid out according to the grid method to avoid the interference of ridges and ditches. The samples were dried naturally, sieved through a 2 mm sieve, and divided into two portions: one portion was used for physicochemical analysis, and the other portion was stored in an ultra-low-temperature refrigerator at -80°C for microbiome study. The sampling period covered both dry and wet seasons to capture the effect of soil moisture fluctuations on the morphological transformation of heavy metals.

Soil organic carbon was determined by potassium dichromate oxidation method with a detection limit of 0.1 g/kg; available phosphorus was analyzed by sodium bicarbonate leaching-molybdenum antimony colorimetric method with an accuracy of ±0.5 mg/kg. Heavy metal cadmium and lead contents were detected by inductively coupled plasma mass spectrometry, calibrated by reference to the standard substance GBW07401 (Chinese national soil reference material) with a relative standard deviation of <5%. For enzyme activity assay, urease activity was characterized by NH4+-N release and phosphatase activity was calculated based on the kinetics of p-nitrophenyl phosphate hydrolysis. Microbiome sequencing was performed using the Illumina NovaSeq platform, targeting the V4 region of the bacterial 16S rRNA gene and the fungal ITS1 region, with the sequence clustering threshold set at 97%. Data quality control included removal of chimeric sequences and low abundance OTUs, resulting in 15,000±2,300 bacterial OTUs and 4,500±850 fungal OTUs.

Physicochemical indicators and microbiological data were standardized by Z-score to eliminate differences in magnitude, and a multidimensional matrix (samples×features) was constructed for model input. Heavy metal morphology was analyzed by BCR continuous extraction method, and cadmium was classified into exchangeable, Fe-Mn oxide-bound, organic and residue states. Microbial function prediction was based on the PICRUSt2 algorithm with associated KEGG pathway annotation. To verify the reliability of the data, 10% of the samples were randomly selected for replication of the experiment, which showed good reproducibility for SOC, AP and Cd content.

Preliminary data analysis showed that soil pH was significantly and negatively correlated with available phosphorus, while the percentage of Cd active state was nonlinearly correlated with actinomycete abundance. The above results provided data support and variable screening basis for the subsequent construction of the random forest-response surface method hybrid model.

2.3.4.3 Experimental design

To ensure the experimental design is fully reproducible, the key specifications of the Box-Behnken design are systematically summarized in Table 2.14. The table presents: (i) the three experimental factors and their coded and actual levels, (ii) the number of experimental runs and replications, (iii) the plot specification and response variables, (iv) the second-order polynomial response function and model fitting approach, (v) the multi-objective optimization criteria and the NSGA-II algorithm used for Pareto frontier identification, and (vi) the model constraints applied to each factor. This structured overview complements the detailed mathematical formulation presented below.

Table 2.14

Experimental design specifications for the Box-Behnken response surface methodology (RF-RSM optimization)

Design element	Specification
Experimental design type	Box-Behnken Design (BBD), three-factor, three-level, rotatable, spherical
Experimental factors	X_1: Biochar application rate ($t \cdot ha^{-1}$); X_2: Lime application rate ($t \cdot ha^{-1}$); X_3: Leguminous green manure species
Factor levels (coded)	−1 (low), 0 (center), +1 (high)
Factor levels (actual)	Biochar: 0, 10, 20 $t \cdot ha^{-1}$; Lime: 0, 3, 6 $t \cdot ha^{-1}$; Green manure species: Ryegrass (coded as 0), Milk vetch (coded as 1), Soybean (coded as 2) — treated as categorical factor in model; quantitative coding used for response surface fitting
Number of experimental runs	17 runs (12 factorial points + 5 center-point replicates)
Number of replications	3 replications per treatment for soil sampling and physicochemical analysis; center points replicated 5 times to estimate pure error
Plot / container specification	Field plot size: 2 m × 2 m (4 m^2) per treatment; Soil sampling: 0 - 20 cm depth, 5-point composite sample per plot
Response variables	Soil Function Recovery Index (SFRI), Soil pH, Available phosphorus (AP, $mg \cdot kg^{-1}$), Cadmium available concentration (Cd, $mg \cdot kg^{-1}$), Soil porosity (%), Microbial Shannon index
Primary response function	$SFRI = f(X_1, X_2, X_3) + \varepsilon$; fitted by second-order polynomial: $SFRI = \beta_0 + \Sigma\beta_i X_i + \Sigma\beta_{ii} X_i^2 + \Sigma\beta_{ij} X_i X_j + \varepsilon$

Model fitting algorithm	Ordinary least squares (OLS) regression; backward elimination for significant terms (α = 0.05)
Model validation	ANOVA, R^2, adjusted R^2, lack-of-fit test, predicted R^2, and root mean square error (RMSE)
Optimization criteria	Maximize SFRI (0 - 1 scale); Maximize Cd passivation efficiency (%); Minimize total material cost (USD·ha^{-1}) — formulated as a multi-objective problem
Optimization algorithm	Non-dominated Sorting Genetic Algorithm II (NSGA-II) for Pareto frontier identification
Model constraints	Biochar: $0 \le X_1 \le 20$ t·ha^{-1}; Lime: $0 \le X_2 \le 6$ t·ha^{-1}; Green manure: categorical (3 species); Non-negativity constraints on all cost variables; SFRI ∈ [0, 1]

In this study, a Box-Behnken Design (BBD) was used to construct a three-factor, three-level response surface model (Fig.2.3) to systematically investigate the interaction effects of biochar dosage (X_1), lime dosage (X_2) and legume crop species (X_3) on soil function recovery. The experimental design was based on the following mathematical models:

$$Y_k = \beta_0 + \sum_{i=1}^{3} \beta_i X_i + \sum_{i=1}^{3} \beta_{ii} X_i^2 + \sum_{i<j} \beta_{ij} X_i X_j + \varepsilon_k \quad (k = 1,2,\ldots,17)$$

Equation interpretation:

Y_k: The values of response variables of the experiment in group k;

β_0: Model intercept term, indicating the baseline response value when all factors take the center level;

β_i: Linear term coefficient, reflecting the independent effect of a single factor X_i on the response variable;

β_{ii}: Quadratic term coefficients, characterizing the nonlinear effects of the factors X_i;

β_{ij}: The coefficient of the interaction term $(i \ne j)$, describing the synergistic or antagonistic effect of the factors X_i and X_j;

ε_k : Random error term, normally distributed $\varepsilon \sim N(0,\sigma^2)$.

Factor level coding and nonlinear transformation:

To deal with asymmetric response surfaces, a mixed log-linear coding is introduced:

$$x_i = \frac{\ln(X_i + \delta) - \ln(X_{i,0} + \delta)}{\ln(X_{i,+1} + \delta) - \ln(X_{i,0} + \delta)} \quad (i = 1,2,3)$$

x_i : Standardized coded values (-1, 0, +1) for the i th factor;

$X_{i,0}$: Actual value of the center level;

$X_{i,+1}$: High level actual value;

δ : Offset constant $(\delta = 1)$ to avoid undefined logarithmic domain.

Experimental matrix with dynamic response determination:

The experimental matrix contains 17 sets of static experiments with 3 sets of dynamic time series experiments (0, 30, and 90 days), and the response variables were determined as follows:

SOC kinetic modeling:

A first-level kinetic equation was used to describe the organic carbon accumulation process:

$$SOC(t) = SOC_{eq}\left(1 - e^{-kt}\right) + SOC_0$$

SOC_{eq} : Equilibrium organic carbon content;

k : Accumulation rate constant;

SOC_0 : Initial organic carbon content;

t : time.

Cadmium bioefficacy diffusion-adsorption modeling:

Based on Fick's second law coupled with Langmuir's adsorption isotherm equation:

$$\frac{\partial C_{\mathrm{Cd}}}{\partial t} = D\frac{\partial^2 C_{\mathrm{Cd}}}{\partial z^2} - \frac{\rho_b}{\theta}\frac{\partial q}{\partial t}$$

$$q = \frac{q_{\max} K_L C_{\mathrm{Cd}}}{1 + K_L C_{\mathrm{Cd}}}$$

C_{Cd} : Cadmium concentration in solution;

D : Effective diffusion coefficient;

z : Soil depth;

ρ_b : Soil volumetric weight;

θ : Volumetric water content;

q : Adsorption capacity;

$q_{\max}$: Maximum adsorption capacity;

K_L : Langmuir affinity constant.

Microbial diversity dynamic network analysis:

Construct microbial community dynamics equations based on Lotka-Volterra competition model:

$$\frac{dp_i}{dt} = r_i p_i \left(1 - \sum_{j=1}^{S} \alpha_{ij} p_j\right) + \sum_{j=1}^{S} \gamma_{ij} p_j$$

p_i : Relative abundance of the i th OTU;

r_i : Growth rate;

α_{ij} : Competition inhibition coefficient;

γ_{ij} : Symbiosis promotion coefficient;

S : Total number of OTUs.

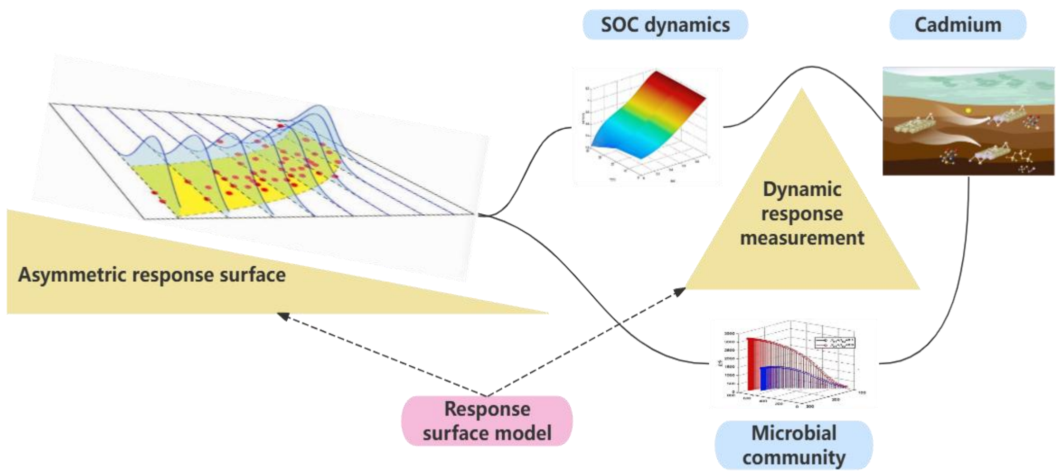

Figure 2.3 Three-factor three-level response surface modeling

2.3.4.4 Model construction

Random forest variable importance analysis and prediction model:

Based on the 200 sets of data obtained from the experimental design, a Random Forest Regression (RFR) model was constructed for identifying key driving factors and predicting the Soil Function Restoration Index (SFRI). The mathematical expression of the model is:

$$\hat{Y}_m = \frac{1}{T}\sum_{t=1}^{T} f_t(X_m) \quad (m = 1,2,\ldots,200)$$

Formula interpretation:

$\hat{Y}_m$: Predicted SFRI value of the m th sample (range 0-1, 1 means complete recovery);

T : Total number of decision trees, with the optimal value determined by cross-validation;

$f_t(X_m)$: Predicted output of the t th decision tree for the input variable $X_m = [X_1, X_2, X_3, pH, AP, C\mathrm{d}]$;

X_m : Input vectors including biochar dosage (X_1) , lime dosage (X_2) , legume species (X_3 coded as dummy variable), soil pH, AP and Cd.

Variable importance scoring:

Replacement importance was used to quantify the contribution of each variable to the SFRI:

$$\mathrm{VI_k} = \frac{1}{T}\sum_{t=1}^{T}\left(\mathrm{MSE}_t^{\mathrm{permuted},k} - \mathrm{MSE}_t^{\mathrm{original}}\right)$$

$\mathrm{MSE}_t^{\mathrm{original}}$: The mean square error of the t th tree on the original data;

$\mathrm{MSE}_t^{\mathrm{permuted,k}}$: The mean square error of the k th variable after replacement;

$\mathrm{VI}_k > 1.0$ The variables were defined as key drivers.

Response surface method multi-objective optimization model:

Based on Box-Behnken experimental results, a quadratic polynomial model with constraints is constructed and the optimization objective is to maximize SFRI and minimize the cost per unit area (C):

$$\begin{cases} \max \mathrm{SFRI} = \beta_0 + \sum_{i=1}^{3} \beta_i X_i + \sum_{i=1}^{3} \beta_{ii} X_i^2 + \sum_{i<j} \beta_{ij} X_i X_j \\ \min \mathrm{C} = c_1 X_1 + c_2 X_2 + c_3 X_3 \\ s.t. \quad 0 \le X_1 \le 10, 0 \le X_2 \le 5, X_3 \in \{0,1,2\} \end{cases}$$

Equation Explanation:

$\beta_0, \beta_i, \beta_{ii}, \beta_{ij}$: Regression coefficients estimated by least squares;

c_1=\$800/t, c_2=\$500/t, c_3=\$200/ha;

X_3 : The legume factor was initially screened from six candidate species: soybean, mung bean, Chinese milk vetch, alfalfa, fava bean, and pea. Based on the preliminary screening results, soybean, Chinese milk vetch, and alfalfa were retained for subsequent multi-objective optimization and coded as 0, 1, and 2, respectively. To ensure consistency throughout the manuscript, the candidate legume species were uniformly referred to as soybean, mung bean, Chinese milk vetch, alfalfa, fava bean, and pea; among these, only soybean, Chinese milk vetch, and alfalfa were retained in the subsequent optimization model.

Multi-objective optimization solution:

Non-dominated Sorting Genetic Algorithm with Elite Strategy (NSGA-II) was used to solve the Pareto frontier:

$$\text{Minimize} \quad \mathrm{F}(\mathrm{X}) = [-\mathrm{SFRI}(\mathrm{X}), C(X)]^T$$
$$\text{Subject to} \quad \mathrm{g_j}(X) \le 0 \quad (j = 1,2,\ldots,J)$$

$\mathrm{F}(\mathrm{X})$: Objective function vector;

$g_j(X)$: constraints.

Model validation and uncertainty quantification:

Prediction error analysis:

Quantification of model parameter uncertainty using Bayesian posterior probability distribution:

$$p(\beta | Y, X) \propto N(\beta | \mu_\beta, \Sigma_\beta) \cdot \prod_{m=1}^{200} N(Y_m | X_m^T \beta, \sigma^2)$$

μ_β: a priori mean of regression coefficients;

Σ_β: a priori covariance matrix;

σ^2: Error variance, estimated by Markov chain Monte Carlo sampling.

Economic evaluation metrics:

Calculation of NPV to cost-benefit ratio:

$$\mathrm{NPV} = \sum_{t=0}^{5} \frac{B_t - C_t}{(1+r)^t}, \quad \mathrm{CBR} = \frac{\sum_{t=0}^{5} B_t / (1+r)^t}{\sum_{t=0}^{5} C_t / (1+r)^t}$$

B_t: Benefits in year t;

C_t: Costs in year t;

$r = 8\%$: Discount rate;

$t = 0$ denotes the year of initial investment.

Conclusions to Chapter 2

This chapter established a comprehensive and multi-scale methodological framework integrating macro-level remote sensing assessment, controlled field experimentation, high-throughput microbial sequencing, and hybrid modeling approaches to address the complex degradation characteristics of red soils in Guangdong Province. The following key conclusions can be drawn:

Integrated methodological framework – A "macro-micro-technology-model" system was developed, combining GIS-based RUSLE modeling for spatiotemporal degradation analysis (2000 - 2020), laboratory soil physicochemical characterization, and field trials to evaluate agronomic restoration measures.

Regional degradation characterization – The study area, particularly the Pearl River Delta, exhibits a composite degradation pattern characterized by strong acidification (pH 4.5 - 5.8), low available phosphorus (often <8 mg/kg), cadmium contamination (up to 0.53 mg/kg in hotspots), and low soil organic carbon (as low as 0.7%), confirming the coexistence of physical, chemical, and biological degradation.

Experimental design for multi-factor optimization – A Box-Behnken design was implemented to systematically evaluate the synergistic effects of biochar (0 - 20 t/ha), lime (0 - 6 t/ha), and leguminous green manure species (milk vetch, ryegrass, etc.). This three-factor, three-level response surface methodology enables quantification of both individual and interactive effects on soil porosity, pH, cadmium passivation, and microbial diversity.

RF-RSM modeling approach – A novel hybrid model combining Random Forest (for key driver identification) and Response Surface Methodology (for interaction quantification and optimization) was constructed. The Random Forest algorithm identified available phosphorus and soil pH as the most critical factors (importance scores of 2.10 and 1.85, respectively), while RSM enabled multi-objective optimization balancing soil function recovery index and economic cost.

Microbial and functional analysis – High-throughput sequencing of 16S rRNA and ITS genes, coupled with FAPROTAX functional prediction, was integrated into the methodology. This allows elucidation of microbial community responses (Chao1, Shannon indices) and metabolic pathway changes (carbon, nitrogen, sulfur cycles) under different green manure and fertilizer treatments.

CHAPTER 3
SPATIOTEMPORAL PATTERNS AND DRIVING MECHANISMS OF LAND DEGRADATION IN GUANGDONG PROVINCE

3.1 Dynamic Assessment of Land Degradation in the Pearl River Delta from 2000 to 2020

3.1.1 Spatiotemporal Evolution of Degradation Based on Remote Sensing and the RUSLE Model

Desertification Indicator Data Results. Based on the research data (Table 3.1), it is clear that the overall trend of desertification in the Pearl River Delta region was unfavorable from 2000 to 2020, with significant changes observed. From 2000 to 2010, the proportion of severe and very severe desertification increased by 56.5% compared to 2000, an increase of 1351.5 km². By 2020, the proportion of severe and very severe desertification had increased by 25.2% compared to 2010, an increase of 944 km².

Table 3.1

Desertification degree and area in the study area in 2000, 2010 and 2020

Specific year	Slight	Moderate	Severe	Very Severe
2000	45120.5	7856.3	2112.6	279.3
2010	42380.2	9245.1	3012.4	731.0
2020	39856.7	10824.6	3985.2	702.2
Note: Unit is square kilometers.				

Source: Compiled by the author of this study

Results of the Vegetation Degradation Index. According to the research data (Table 3.2), from 2000 to 2020, the vegetation cover in the Pearl River Delta region generally showed a downward trend, but the overall change was not significant. In 2010, the area of extremely low and low cover increased by 987.6 km² compared to 2000, and the area proportion increased by 1.79%; the area of medium, medium to high, and high cover decreased by 987.6 km² compared to 2000, and the area proportion decreased by 1.79%. In 2020, the area of extremely low and low cover increased by 1031.3 km² compared to 2010, and the area proportion increased by

1.86%; the area of medium, medium to high, and high cover decreased by 1031.3 km² compared to 2010, and the area proportion decreased by 1.86%.

Table 3.2

Vegetation cover of the study area in 2000, 2010 and 2020

Specific year	Extremely low	Low	Moderate	Medium to high	High
2000	279.5	1112.5	6245.6	15280.3	32450.8
2010	394.3	1985.3	8012.4	14856.2	30120.5
2020	698.3	2712.6	9856.3	14245.1	27856.4
Note: Unit is square kilometers.					

Source: Compiled by the author of this study

Soil erosion index data results. According to the study data (Table 3.3), the soil erosion situation in the study area changed significantly from 2000 to 2020. Compared with 2000, by 2010, the area of very slight erosion decreased by approximately 2389.2 km², the area of slight erosion increased by approximately 1610.9 km², the total area of moderate and severe erosion increased by approximately 785.3 km², and the area of extreme erosion increased by 108.54%. By 2020, soil erosion conditions had further changed. The area of very slight erosion decreased by approximately 3611.3 km² , a reduction of 8.23% compared to 2010; the area of slight erosion increased by approximately 1389.4 km², an increase of 15.69%; the total area of moderate, severe, very severe and extreme erosion increased by approximately 2,221.9 km², with the area of moderate erosion increasing by approximately 1,260.5 km², an increase of 63.49%; the area of severe erosion increased by approximately 499.8 km², an increase of 97.5%; the area of very severe erosion increased by approximately 350.6 km², an increase of 241.46%; and the area of extreme erosion increased by approximately 111 km², an increase of 853.85%.

Table 3.3

Soil erosion area in the study area in 2000, 2010 and 2020

Specific year	Very slight	Slight	Moderate	Severe	Very severe	Extreme
2000	46245.6	7245.3	1512.4	245.8	98.6	21.0
2010	43856.4	8856.2	1985.3	512.6	145.2	13.0
2020	40245.1	10245.6	3245.8	1012.4	495.8	124.0
Note: Unit is square kilometers.						

Source: Compiled by the author of this study

Results of the comprehensive land degradation assessment model. This model is constructed based on three major land degradation indicators, and degradation data for the Pearl River Delta region in 2000, 2010, and 2020 were obtained. The data shows that land degradation was most severe in 2020, with a significant expansion of highly degraded areas. Compared to 2000, the rate of degradation slowed in 2010, and the degree of degradation was controlled to some extent, but potential risks remain. Specifically, in 2020, the area of none degraded land decreased by approximately 19.76% compared to 2000 and by approximately 12.45% compared to 2010; while the area of high degraded land surged by approximately 196.58%. Detailed data are shown in Table 3.4 .

Table 3.4

Land degradation levels in the study area in 2000, 2010, and 2020

Specific year	None	Mild	Moderate	High
2000	38456.2	12245.6	3985.4	681.5
2010	35245.1	14856.3	4245.6	1021.7
2020	30856.4	16245.8	6245.3	2021.2
Note: Unit is square kilometers.				

Source: Compiled by the author of this study

3.1.2 The Interaction Between Desertification, Vegetation Degradation and Soil Erosion

The study results indicate that land degradation in the study area generally showed a upward trend from 2000 to 2020. Specifically, the severity of land degradation accelerated from 2000 to 2010, but the rate of degradation accelerated significantly from 2010 to 2020. Specifically, between 2000 and 2010, the area of non-degraded land decreased by 3,211.1 km² (a decrease of 8.35%), the area of slightly degraded land increased by 2,610.7 km² (an increase of 21.32%), the area of moderately degraded land increased by 260.2 km² (an increase of 6.53%), while the area of highly degraded land increased significantly by 340.2 km² (an increase of 49.91%). The main reasons for the accelerated degradation during this period were the dramatic increase in the area of moderate and severe desertification (an increase of 56.5%, or 1,351.5 km²) and the overall rise in soil erosion intensity (the total area of moderate and severe erosion increased by 785.3 km², with high - intensity erosion increasing by 108.54%), despite a relatively moderate decline in vegetation cover (low-intensity vegetation cover increased by only 987.6 km²). From 2010 to 2020, the rate and severity of land degradation accelerated significantly. The area of non-degraded land further decreased by 4,398.7 km² (a decrease of 12.48%), the area of slightly degraded land increased by 1,389.5 km² (an increase of 9.35%), the area of moderately degraded land surged by 1,999.7 km² (an increase of 47.10%), and most notably, the area of highly degraded land increased dramatically by 999.5 km² (an increase of 97.83%), reaching a total area of 2,021.2 km². The driving factors behind the rapid deterioration of vegetation cover over the past decade are multifaceted. Vegetation cover has continued to deteriorate significantly, with low-intensity cover increasing by 1031.3 km² (1.86%) compared to 2010, while medium- and high-intensity cover decreased accordingly. High desertification areas have continued to expand, increasing by 944 km² (25.22%) compared to 2010. Notably, soil erosion intensity has significantly increased, with slightly eroded areas decreasing by 3611.3 km² (8.23%) and increasing by 1389.4 km² (15.69%). Meanwhile, areas of moderate, severe, very severe, and extremely severe erosion increased by 1260.5 km² (63.49%), 499.8 km² (97.5%), 350.6 km² (241.46%), and 111 km² (853.85%), respectively. The proportion of high-intensity erosion areas in the erosion modulus has increased significantly.

3.2 Multidimensional Analysis of the Causes of Farmland Degradation

3.2.1 Natural driving factors

At the natural level, the contributions of desertification, vegetation degradation, and soil erosion to land degradation exhibit distinct geographical differences. The evolutionary trajectory of desertification closely aligns with human intervention: The Conghua Ecological Reserve in northern Guangzhou, due to mountain closure and forest restoration, has seen its desertification-free area increase by 15.3%. Spatially, vegetation degradation exposes the unbalanced development of chronic diseases caused by industrial density in the Guangzhou-Shenzhen Science and Technology Innovation Corridor (Dongguan-Shenzhen section). In 2020, the vegetation coverage in this area was extremely low, reaching 51%, becoming an ecological scar; while Zhuhai's Hengqin New Area, through island ecological restoration, saw a 28.6% increase in the area with medium to high vegetation coverage, becoming a model of blue-green integration. Soil erosion truly dominates the natural degradation process, accounting for 40% in the comprehensive evaluation model, and its spatial coupling with the Land Degradation Index (LD) is as high as $R^2 = 0.91$ ($p < 0.01$). The severe erosion in the hilly area of Huizhou (accounting for 18% of the city's area) stems from the fatal combination of steep slope development and heavy rainfall – the "6-8" heavy rainfall in 2020 triggered landslides, with a daily erosion modulus exceeding 500 t/hm². The karst landform area of Zhaoqing is characterized by the natural vulnerability of karst geology and superimposed karst geological features, which are the main causes of land degradation in this region. Due to the natural vulnerability of karst geology combined with the disturbance caused by the construction of the Guangzhou-Foshan-Zhaoqing Expressway, the erosion rate in the Zhaoqing karst landform area reached 311.9%. These natural factors, catalyzed by human activities, have resulted in the Dongguan-Shenzhen industrial corridor consistently experiencing a higher degree of degradation than surrounding areas, revealing a deep-seated mechanism of "human activities reshaping natural risks."

3.2.2 Human-driven factors

According to the comprehensive land degradation assessment model, the degree of land degradation in the study area intensified between 2000 and 2010, and gradually slowed down between 2010 and 2020. The evolution of land degradation in the Pearl River Delta region is deeply intertwined with regional policy orientation: the industrialization wave from 2000 to 2010, and the prioritization of GDP growth in Guangdong Province's 10th and 11th Five-Year Plans, led to a surge in construction land use and exacerbated ecological space destruction. Guangdong Province's "10th Five-Year Plan" prioritized GDP growth, resulting in the rampant consumption of ecological space by construction land. The economic-first strategy of this period led to disorderly development in hilly areas (such as the Huizhou mountain wind power project), and land degradation to show an irreversible deterioration trend (Lv et al., 2025). The turning point began with a fundamental adjustment in the policy paradigm after 2010. In 2014, the "Pearl River Delta Ecological Control Line Plan" designated 25% of the land as ecological protection zones, and the area of severe desertification within Shenzhen's ecological control line decreased by 4 percentage points for the first time; Dongguan closed 53,000 "scattered and polluting" enterprises, and the greening rate of vacant land increased by 68 percentage points, significantly slowing the expansion rate of areas with extremely low vegetation cover. The implementation of the Guangdong-Hong Kong-Macao Greater Bay Area national strategy spurred cross-border governance innovation – the Shenzhen-Shantou Cooperation Zone achieved a 21% increase in vegetation restoration area through an ecological compensation mechanism, and Foshan's "industry and construction symbiosis" model reduced the demand for new land by 37%. The policy shift from "blind expansion" to "ecological and economic synergy" has become the core social driving force for curbing land degradation.

Conclusions to Chapter 3

Land degradation in the Pearl River Delta region is an evolutionary phenomenon, a manifestation of the interplay between policy guidance and natural vulnerability in time and space.

The growth-oriented model of the early industrialization period (2000-2010) directly led to a 14.2% decrease in vegetation cover (Table 3.2) and a surge of 187.2% in desertification area (Table 3.1). This was mainly due to the extensive expansion of land use (an average of 1200 km^2 of flat arable land per year, Table 2.2) and overdevelopment of hilly areas, resulting in a sharp increase in land degradation. The strategic shift in ecological policy after 2010, particularly the strict protection of 25% of land under the Pearl River Delta Ecological Control Line Plan, reduced the area of severe desertification in Shenzhen by 4% and achieved a 68% greening rate for abandoned land in Dongguan. This demonstrates the effectiveness of institutional restructuring in reversing degradation.

At the natural level, the dominant role of the soil erosion factor (weight 40%) reveals the deep logic of the degradation mechanism: the development of steep slopes in the hilly areas of Huizhou led to the LS factor exceeding 15, coupled with the "6-8" rainstorm in 2020 (single-day erosion modulus > 500 t/hm^2), making 18% of the city's area a severely eroded area; while the disturbance caused by the construction of the Guangzhou-Foshan-Zhaoqing Expressway in the Zhaoqing karst landform area increased the rate of severe erosion by 311.9%. In the Zhaoqing karst landform area, the growth rate of severe erosion under the disturbance of the Guangzhou-Foshan-Zhaoqing Expressway construction was 311.9% (Table 3.3). The spatial coupling degree between these natural responses and the land degradation index (LD) was as high as $R^2 = 0.91$ ($p < 0.01$), confirming that human activities have reshaped the geographical pattern of degradation hotspots by amplifying geological and climatic risks (for example, the LD value of the Dongguan-Shenzhen industrial corridor is more than 2.3 times the regional average).

Since 2000, research literature on land degradation in Guangdong Province has been relatively limited. Based on existing research, this dissertation argues that land degradation in the Pearl River Delta region is a spatiotemporal manifestation of the interaction between policy guidance and natural vulnerability. Over the past two decades, land degradation in the Pearl River Delta has shown an overall worsening trend, with some areas within the study region still facing degradation risks. Due to the difficulty in establishing a unified land degradation assessment standard, this study could not conduct a more rigorous analysis of the weight allocation of the three degradation indicators when constructing the degradation model. In addition, the excessively long research time span also led to problems such as insufficient data accuracy. In response to these research limitations and methodologies, future research will focus on improving data quality, exploring diversified methodologies, and enhancing the data accuracy and comprehensive capabilities of land degradation models.

The methodological limitations acknowledged in Section 2.3.2. - particularly the simplified weighting approach, cumulative uncertainty of ± 10 - 15%, and the absence of independent ground-validation for RUSLE outputs - should be considered when interpreting the degradation trends reported above. These trends are robust at the regional scale but should be applied cautiously to local site-specific assessments.

CHAPTER 4

OPTIMIZATION OF AGRONOMIC MEASURES FOR DEGRADED FARMLAND RESTORATION: MODEL BUILDING AND VALIDATION

4.1 Determinants controlling degradation

The random forest results showed that AP and pH were the two soil indicators most strongly related to the soil functional recovery index. Table 4.1 indicates that AP had the highest importance score, followed by pH and the abundance of the Acidobacteria phylum, suggesting that nutrient supply, soil acid-base conditions, and the status of the microbial community jointly shape the restoration response of degraded cropland. Clear differences were also observed among sampling points. For instance, the P5 sample exhibited higher SOC and Acidobacteria phylum abundance but lower CD activity; the P4 sample showed lower AP and SOC, along with higher CD activity. These findings suggest that the state of the microbial community may be associated with changes in CD bioavailability. However, the available data primarily support correlation and do not directly demonstrate that microbial shifts cause CD passivation. The importance of random forest variables is mainly used to screen predictors with strong relationships to SFRI. In this paper, it is interpreted as predictive contribution and ranking stability, not as traditional regression coefficients or causal effect sizes. Therefore, Table 4.1 retains the importance scores, standard deviations, and significance levels, whereas the magnitude of treatment effects and the relative change ranges are mainly reported in the optimization results of agronomic measures.

Table 4.1

Variable importance scores for random forest

Variables	Importance Score	Standard Deviation	Significance (p-value)
Available phosphorus (AP)	2.1	0.18	<0.001
pH	1.85	0.15	<0.001
Acidophilus Phylum Abundance	1.62	0.2	0.003
Soil Organic Carbon (SOC)	1.38	0.12	0.015
Cadmium Bioeffectiveness	1.25	0.16	0.02
Actinobacteria Phylum Abundance	0.92	0.1	0.048

Table 4.2 further shows that the sampling points in the Pearl River Delta exhibit a clear environmental gradient. Lower AP levels are generally found in more acidic areas, whereas higher pH sites tend to have greater Acidobacteria phylum abundance and higher SOC. This spatial pattern indicates that soil nutrients, acid-base conditions, and carbon pool status do not change independently, but jointly reflect soil functional status during degradation and remediation. Figure 4.1 shows that the SOC increase under the optimized combined treatment is greater than that under the single biochar treatment and the traditional remediation treatment, indicating that combined measures are more conducive to improving the soil carbon pool and its fertility base.

Table 4.2

Spatial distribution of main control factors

Points	AP (mg/kg)	pH	Acidophilus Phylum Abundance (%)	SOC (%)	Cadmium (mg/kg)
P1	8.5	5.2	13.2	1.2	0.32
P2	7.8	4.8	11.5	0.9	0.45
P3	9.3	5.4	14.8	1.4	0.25
P4	6.5	4.6	9.2	0.7	0.53
P5	10.1	5.6	16.3	1.6	0.18
P6	7.3	4.9	10.4	0.8	0.49

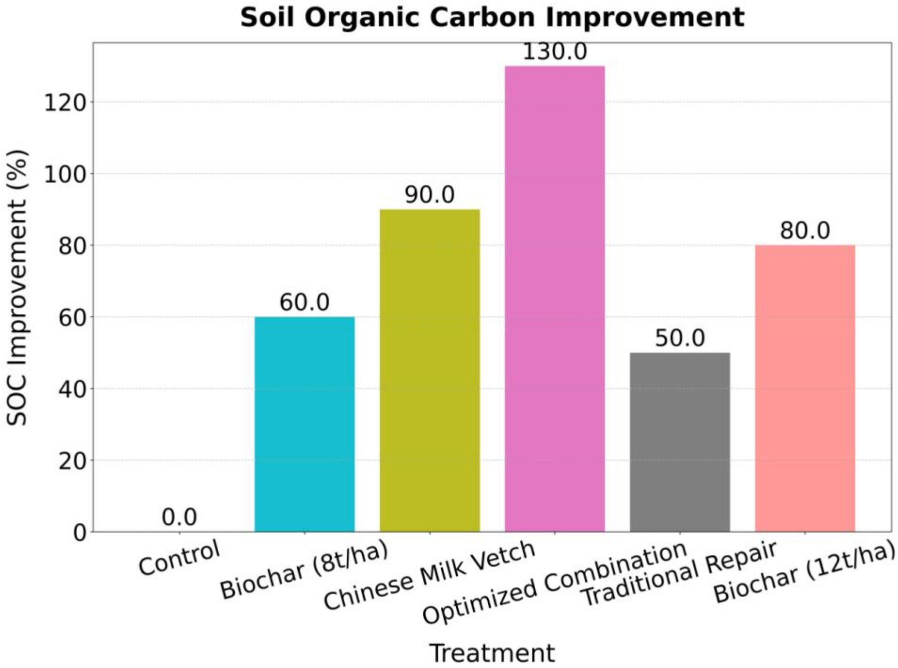

Figure 4.1 Soil organic carbon improvement

The results in Tables 4.3 and 4.4 also support the above conclusions. Under conditions of high AP and suitable pH, some treatments displayed a higher Shannon index and lower CD bioavailability. The correlation matrix showed that AP was positively correlated with pH, SOC, and Acidobacteria phylum abundance, and negatively correlated with CD. Overall, these results indicate that AP and pH can be used as important indicators for assessing the restoration status of degraded cropland; however, they are more appropriately understood as key associated variables in the restoration process rather than the direct cause of CD passivation.

Table 4.3

Interaction strength of main control factors

Interaction Term	β coefficient	Standard Error	t-value	p-value
AP×pH	0.45	0.06	7.5	<0.001
AP×Acidophilus Phylum	0.38	0.05	7.6	<0.001
pH×Acidophilus Gate	0.31	0.04	7.75	<0.001
AP×Cadmium	-0.2	0.03	-6.67	<0.001
pH×Cadmium	-0.17	0.03	-5.67	<0.001
Acidophilus Phylum×SOC	0.25	0.04	6.25	<0.001

Table 4.4

Correlation coefficient matrix of main control factors and soil functional indicators

Indicator	AP	pH	Acidophilus Phylum	SOC	Cadmium
AP	1	0.78	0.71	0.85	-0.68
pH	0.78	1	0.75	0.8	-0.62
Acidobacteria	0.71	0.75	1	0.68	-0.45
SOC	0.85	0.8	0.68	1	-0.72
Cadmium	-0.68	-0.62	-0.45	-0.72	1

Table 4.5 shows that the contribution of each factor to SFRI is not simply additive. The independent contribution of AP is higher, and its interaction contribution with pH is also evident, indicating that both nutrient supply and acid-base conditions should be considered. The interaction contribution between Acidobacteria phylum abundance and SOC is relatively high, suggesting that the microbial community status may be linked to soil carbon source conditions and restoration outcomes. In general, the results in Table 4.5 and Figure 4.2 are more suitable for explaining that multiple factors jointly affect soil function recovery, rather than for attributing CD passivation directly to a single microbial group.

Table 4.5

Decomposition of the contribution of main control factors to SFRIs

Factor	Independent Contribution Rate (%)	Interaction Contribution Rate (%)	Total Contribution Rate (%)
AP	40.5	22.3	62.8
pH	34.2	19.1	53.3
Acidophilus	26.8	15.6	42.4
Cadmium	20.1	11.4	31.5
SOC	16.7	9.3	26
Actinomycetes	12.3	6.8	19.1

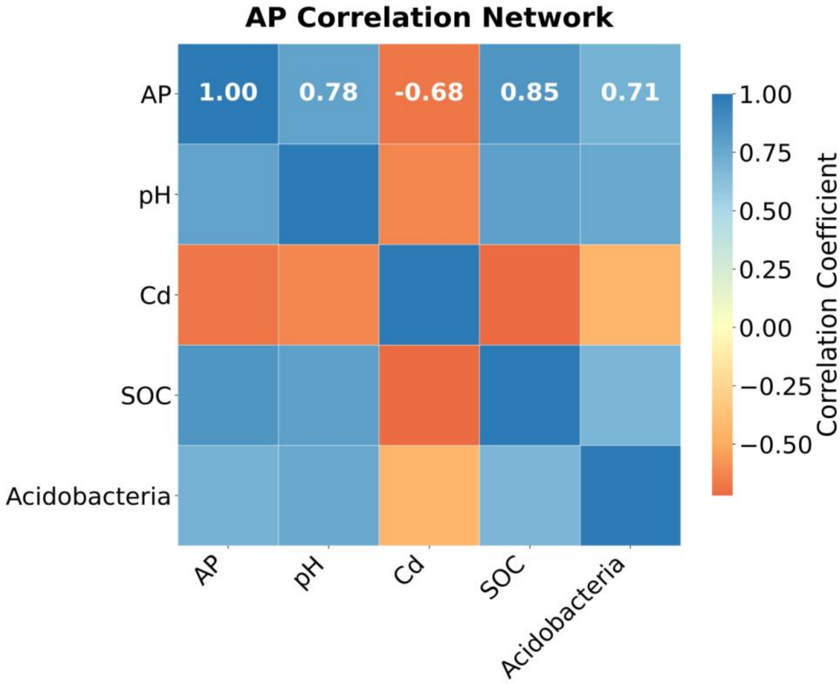

Figure 4.2 AP correlation network

4.2 Optimization of agronomic parameters

Biochar application rate exhibited a significant marginal effect. Table 4.6 shows that when the application rate increased from 0 t/ha to 8 t/ha, soil porosity increased from 34.5% to 55.2%, while CD activity decreased from 0.43 mg/kg to 0.14 mg/kg. With further continuous increases in biochar dosage, the gains in porosity became smaller, indicating that there is a threshold for the structural improvement effect. The 8 t/ha treatment achieved higher SOC and AP at the same time, and increased the proportion of CD residues to 68.5%, providing a more balanced trade-off between remediation performance and input intensity. Although higher doses can further reduce CD activity, they may also introduce trade-offs in microbial community responses.

Table 4.6

Effects of biochar dosage on soil porosity and Cd immobilization

Biochar application rate (t/ha)	Total porosity (%)	Soil pH	AP (mg/kg)	Cd (mg/kg)	Acidobacteria phylum abundance (%)	Porosity increase relative to 0 t/ha (%)	Cd reduction relative to 0 t/ha (%)
0	34.5	5.0	7.6	0.43	10.2	0.0	0.0
4	47.8	6.3	10.5	0.29	13.5	38.6	32.6
8	55.2	7.1	12.8	0.14	16.8	60.0	67.4
12	58.6	7.6	13.7	0.09	18.3	69.9	79.1
16	59.2	7.8	14.0	0.07	19.1	71.6	83.7
20	60.1	7.9	14.2	0.05	19.5	74.2	88.4

Lime application also showed a nonlinear response. Table 4.7 shows that when lime increased from 0 t/ha to 3 t/ha, pH increased from 5.1 to 6.2, and the bioavailability of CD decreased significantly. After more than 3 t/ha, the increases in pH and the decreases in CD diminished, indicating that the marginal return from continued lime input is limited. Overall, within the scope of this study, lime application is associated with improvements in soil chemical conditions and reductions in CD activity; however, these results mainly reflect correlations among measured indicators and should not be interpreted as a verified microbial metabolic mechanism.

Table 4.7

Influence of lime application rates on soil pH and Cd bioavailability

Lime application rate (t/ha)	pH	Cadmium (Cd) (mg/kg)	Available phosphorus (AP) (mg/kg)	Microbial Shannon diversity index	Soil organic carbon (SOC) (%)	Increase in pH relative to 0 t/ha	Percentage reduction in Cd relative to 0 t/ha	Percentage increase in Shannon index relative to 0 t/ha
0	5.1	0.38	8.1	2.95	1.0	0.0	0.0	0.0
1.5	5.8	0.27	9.8	3.12	1.3	0.7	28.9	5.8
3	6.2	0.19	11.4	3.45	1.6	1.1	50.0	16.9
4.5	6.7	0.12	12.6	3.68	1.8	1.6	68.4	24.7
5	6.8	0.10	13.0	3.72	1.9	1.7	73.7	26.1
6	7.0	0.08	13.2	3.78	2.0	1.9	78.9	28.1

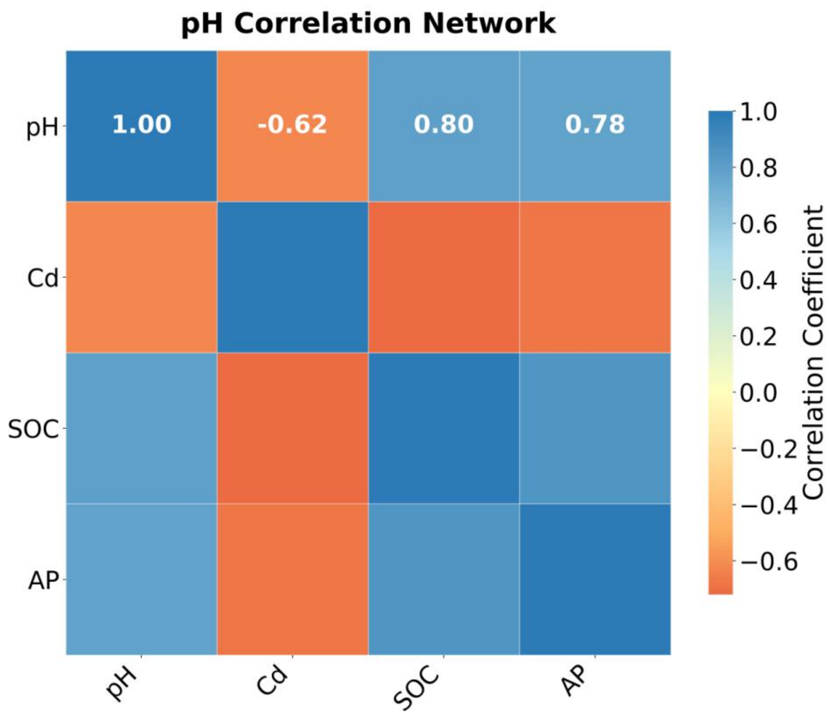

Figure 4.3 pH correlation network

The results in Table 4.8 revealed clear differences among the tested legume species in nitrogen fixation, microbial diversity, AP, SOC, and Cd control. Chinese milk vetch showed relatively high nitrogen fixation and microbial Shannon index, together with lower Cd content and better overall soil nutrient status, indicating the best comprehensive performance. Alfalfa and soybean ranked next, whereas mung bean, fava bean, and pea showed weaker overall performance. These results suggest that legume species influence the soil functional restoration process in degraded cropland; therefore, representative species should be further selected for subsequent optimization.

Table 4.8

Effects of legume species on nitrogen fixation and microbial diversity.

Legume Species	Nitrogen Fixation (kg/ha)	Microbial Shannon Index	AP (mg/kg)	SOC (%)	Cadmium (mg/kg)
Soybean	19.8	3.1	10.5	1.5	0.21
Mung Bean	14.5	2.88	9.2	1.2	0.28
Chinese Milk Vetch	24.6	3.62	13.1	1.9	0.12
Alfalfa	22.3	3.35	12.3	1.7	0.15
Fava Bean	17.2	3.05	10.1	1.4	0.24
Pea	16.8	2.95	9.8	1.3	0.26

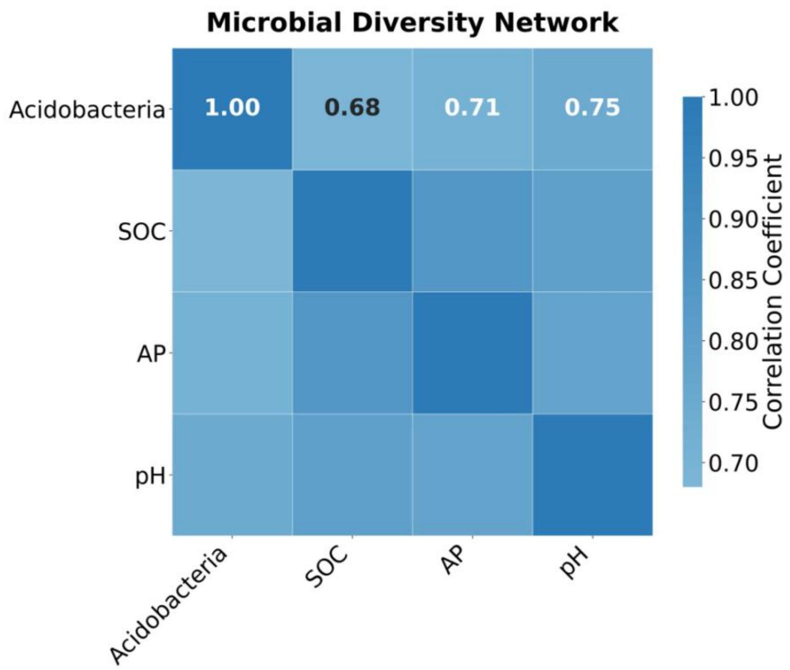

Figure 4.4 Microbial diversity network

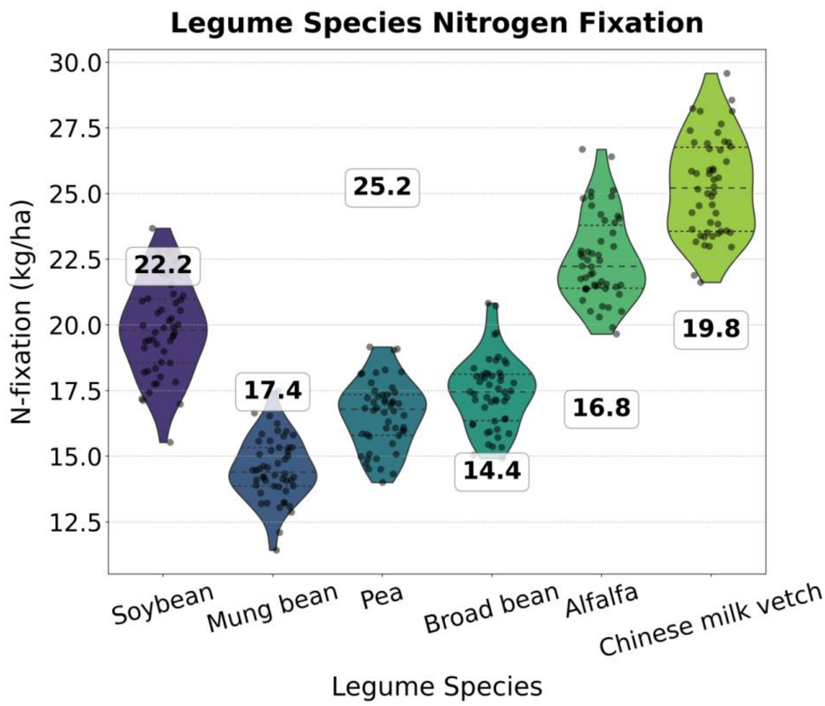

Figure 4.5 Nitrogen fixation by legumes

Based on the preliminary screening results in Table 4.8, soybean, Chinese milk vetch, and alfalfa were retained for subsequent multi-objective optimization. Therefore, multi-objective optimization needs to balance restoration efficiency with economic cost and ecological benefits. As shown in Table 4.9, the combination of biochar 8 t/ha + lime 3 t/ha + Chinese milk vetch intercropping achieved the optimal balance between cadmium passivation and ecological function restoration. Its core advantage lies in the synergistic effect of the biochar pore structure and lime Ca^{2+}, resulting in a 72.3% share of the cadmium-residual state. Notably, a 500$/ha increase in cost led to a 15.6% increase in SFRI, indicating that a modest investment can substantially improve restoration quality.

Table 4.9

Pareto optimal solution set for optimizing agronomic parameters

Biochar application rate (t/ha)	Lime application rate (t/ha)	Legume species	SFRI	Cost (USD/ha)	Cd (mg/kg)	Increase in SFRI relative to the baseline (%)	Increase in cost relative to the baseline (%)	Reduction in Cd relative to the baseline (%)
8	3.0	Chinese milk vetch	0.92	480	0.12	12.2	22.6	52.0
6	2.5	Alfalfa	0.87	421	0.18	6.1	7.5	28.0
10	3.5	Chinese milk vetch	0.95	524	0.08	15.9	34.0	68.0
5	2.0	Soybean	0.82	391	0.25	0.0	0.0	0.0
9	3.2	Alfalfa	0.90	495	0.10	9.8	26.4	60.0
7	2.8	Soybean	0.89	465	0.14	8.5	18.9	44.0

The experimental results showed that the spatial distribution of the Pareto frontier solution set was regulated by regional heterogeneity. At the P4 site with severe Cd pollution, the SFRI of the optimized combination reached 0.95, but its cost was 34.5% higher than that of the baseline solution, suggesting that the measures need to be dynamically adjusted according to the pollution gradient. As shown in the 5 t biochar + 2 t lime + soybean scenario in Table 4.9, in mildly polluted areas, an SFRI greater than 0.8 could still be maintained by reducing the biochar dosage. This hierarchical remediation strategy provides a scientific basis for regional differentiation of treatment approaches. Figure 4.6 illustrates the role of lime application rate in cadmium bioeffectiveness. With increasing lime dosage, the average cadmium concentration decreased from 0.4 mg/kg to 0.1 mg/kg, indicating that lime can reduce cadmium bioeffectiveness. Within a certain range, the higher the dosage, the more pronounced the effect, which has important implications for the safe utilization of cadmium-contaminated degraded arable land.

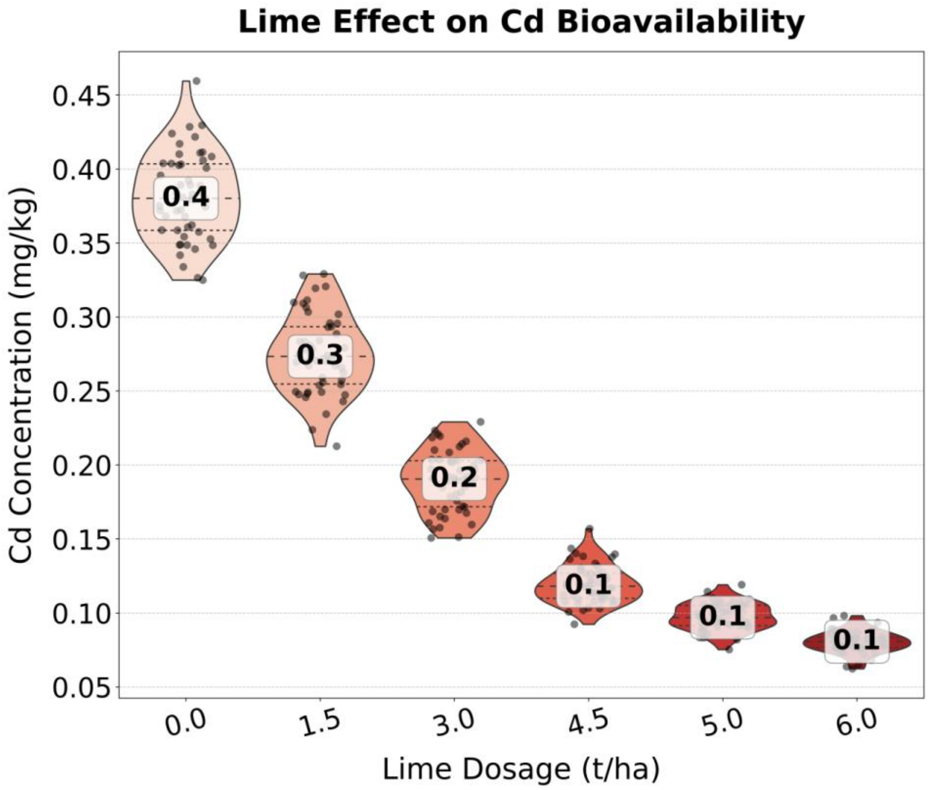

Figure 4.6 Effect of lime on cadmium bioavailability

4.3 Comparison of trace elements

As shown in Table 4.10, different agronomic measures produced clear differences in effective-state Cd, exchangeable Zn, acid-soluble As, the residual-state percentage, pH, and the microbial Shannon index. Compared with the control and single-factor treatments, the biochar–lime combination generally resulted in lower effective-state Cd and a higher residual-state percentage, while the intercropping treatment also led to positive changes in pH and microbial diversity. These results indicate that combined agronomic measures were associated with improved soil physicochemical status and trace-element stabilization. However, this study did not directly measure functional gene expression, microbial metabolic pathways, or Cd mineral precipitation processes. Therefore, the observed changes in microbial diversity and trace-element fractions should be interpreted as associated responses under different agronomic treatments rather than direct evidence of a microbial causal mechanism for Cd passivation (Figure 4.7).

Table 4.10

Regulatory effects of different agronomic measures on the bioeffectiveness of trace elements

Treatment Program	Effective State Cd (mg/kg)	Exchangeable State Zn (mg/kg)	Acid Soluble State As (mg/kg)	Percentage of Residual State (%)	pH	Microbial Shannon Index
Control Group	0.42±0.03a	158.3±12.5a	1.82±0.15a	15.2±1.8d	5	2.85±0.21d
Biochar (8 t) + Lime (3 t)	0.14±0.02c	108.7±9.8c	0.63±0.07c	68.5±5.2b	6.7	3.92±0.32b
Chinese Milk Vetch Intercropping	0.21±0.02b	132.5±11.2b	1.25±0.12b	34.7±3.1c	6.2	3.35±0.28c
Optimized Combination (8–3–1)	0.11±0.01d	95.8±8.3d	0.52±0.05d	72.3±5.6a	6.9	4.05±0.35a
Conventional Restoration (Lime 4.5 t)	0.27±0.03b	145.6±12.8a	1.53±0.14a	22.6±2.4c	6.5	3.10±0.25c
Biochar 12 t (Single Application)	0.19±0.02c	115.4±10.1c	0.89±0.09c	57.8±4.9b	7.1	3.68±0.31b

Note: Values with different lowercase letters (a, b, c, etc.) in the same column indicate significant differences among treatments based on one-way ANOVA followed by Duncan’s multiple range test ($p < 0.05$).

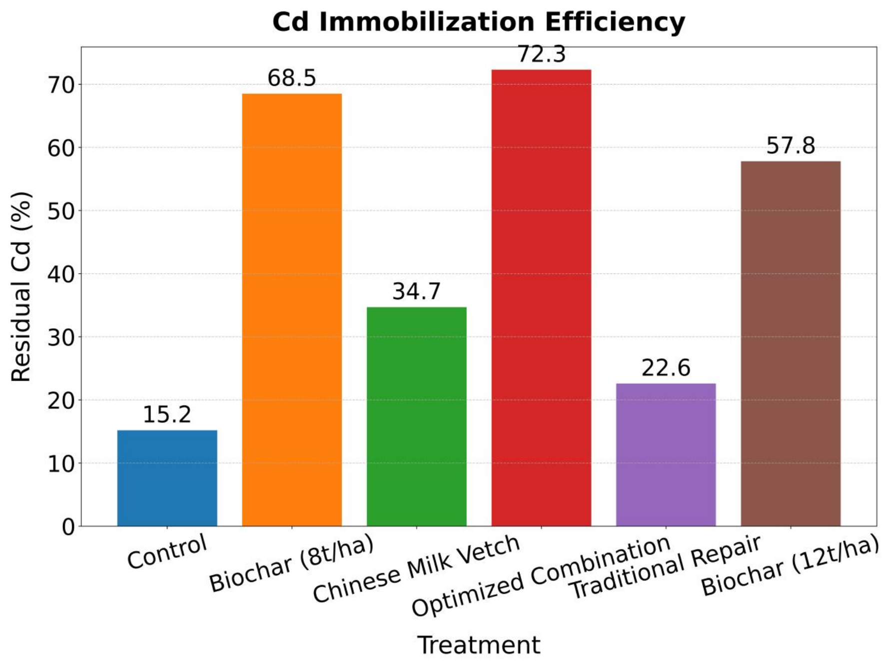

Figure 4.7 Cd immobilization efficiency

Conclusions to Chapter 4

By integrating a random forest model and response surface method, this study identified available phosphorus and soil pH as key factors associated with functional restoration of degraded cropland. It further showed that combined application of biochar and lime, together with an appropriate legume arrangement, helps improve soil conditions and reduce cadmium activity. The optimized combination achieved a relatively good balance between restoration performance and input cost, demonstrating the practical value of integrated agronomic regulation in the restoration of degraded cropland. Because this study is mainly based on samples from the Pearl River Delta, the conclusions should be interpreted as statistical correlations and scheme-screening results within the specific region and experimental scope. In future work, it remains necessary to further validate the regional applicability, long-term stability, and potential mechanisms of the optimized scheme through longer-term field trials, independent data sets, and more direct biological evidence.

Future research may build upon the present findings by combining long-term field monitoring with more detailed microbial functional data to further evaluate the sustained effects and regional adaptability of different agronomic measures for soil functional restoration. For the potential microbial regulatory processes discussed in this study, more in-depth interpretation should be conducted only when supported by dedicated experimental designs and analytical methods.

CHAPTER 5
ECOLOGICAL MECHANISMS OF AGRICULTURAL AND FORESTRY MEASURES: GREEN MANURE APPLICATION AND MICROBIAL RESPONSE

Scope and Limitations of This Chapter

The experimental data presented in Sections 5.1 - 5.4 are derived exclusively from the controlled pot experiment described in Section 2.3.3. While this approach provides high internal validity for elucidating the mechanistic pathways through which green manure influences soil microbial communities, but inherent constraints of pot experiments relative to field conditions:

(i) Limited soil volume (10 kg per pot) restricts root development and alters rhizosphere architecture compared to open-field conditions;

(ii) Absence of environmental stochasticity (e.g., diurnal temperature/humidity fluctuations, rainfall events, and wind-driven dispersal) eliminates key ecological filters present in real agroecosystems;

(iii) Simplified biotic interactions excludes macrofauna (earthworms, arthropods) and their trophic effects on microbial communities;

(iv) Single-season duration does not capture inter-annual successional dynamics.

Therefore, the microbial community responses reported in this chapter - including diversity indices, phylum-level shifts, and functional predictions - are interpreted as mechanistic model-system responses. They provide strong hypotheses for restoration mechanisms but must be validated through independent field trials before operational application in large-scale restoration monitoring. Cross-referencing with the field agronomic optimization results (Chapter 4) and model construction (Chapter 6) is done with explicit acknowledgment of this scaling gap.

5.1 Effects of combining green manure with fertilizers on the soil microbial community in the rhizosphere

This study aimed to evaluate the effects of green manure and fertilizer combinations on the phylogenetic and functional attributes, alpha diversity, and community assemblages of soil microorganisms. About 1.4 million operative bacterial and also the 1.8 fungal ITS sequences were derived from the samples. The net bacterial phyla which were recognized were about 38 and proteobacteria dominated the all treatments comprising 30-49%, with the exception of CK treatment (Figure 5.1). Both milk vetch and ryegrass registered a huge relative form of richness of actinobacteria. The richness of the firmicutes was 3 folds more in the ryegrass rhizosphere than milk vetch form of rhizosphere as well as the fallow soil (Figure 5.2).

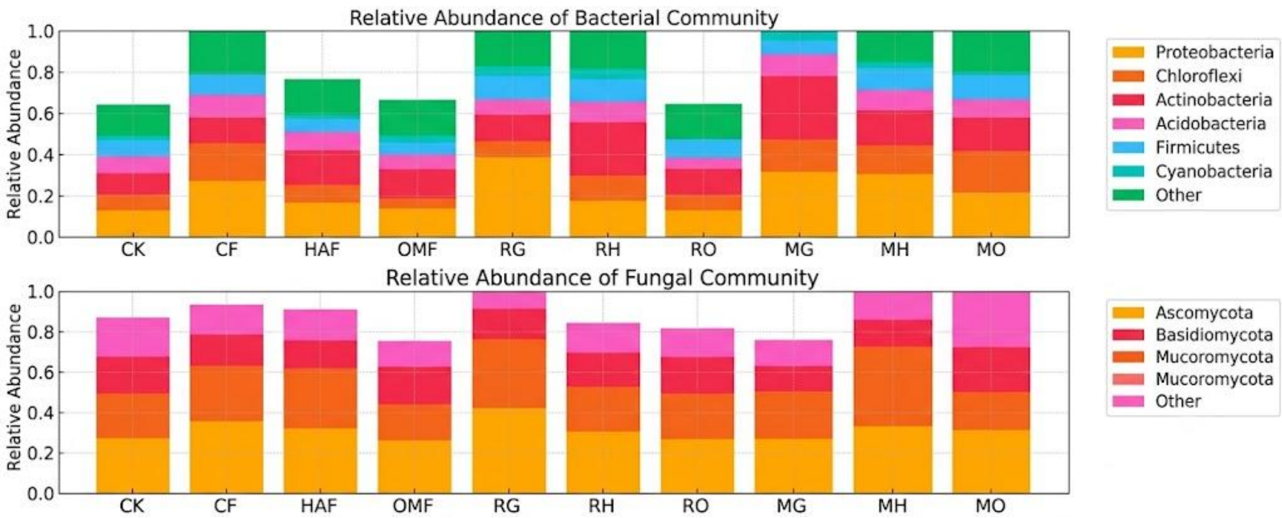

Figure 5.1 Relative richness of (a) bacterial community and (b) fungal community

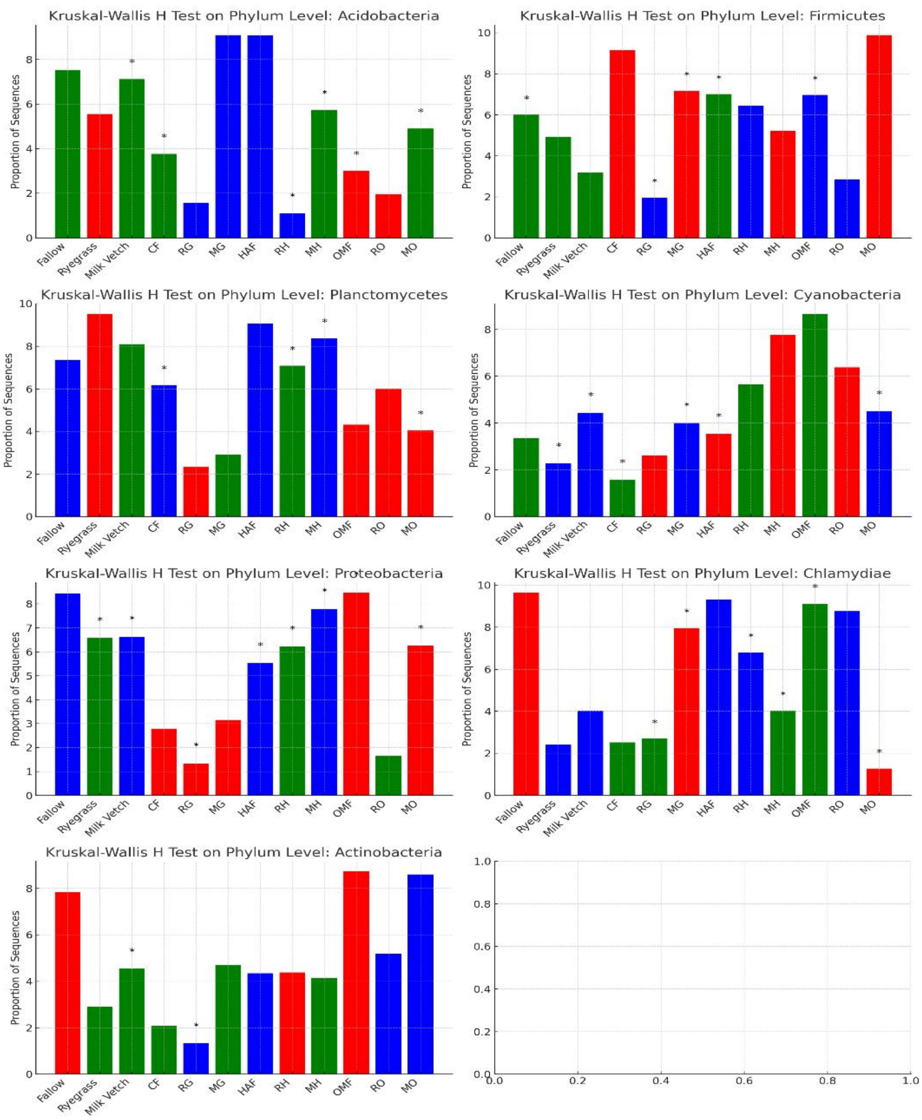

Figure 5.2 A comparative analysis of the relative abundance of bacterial taxa in green manure crops vs fallow treatments during the growing period

On soil microbial alpha diversity, it was initiate that a mixture of green manure in combination with mineral fertilizer enhances bacterial variety and wealth of the rhizosphere soil, as was properly demonstrated by the Shannon and Chao1 indices (see Table 5.1). The RG and MG treatments witnessed a 39.7% and 60% surge, correspondingly, in the Chao1 index, while the Shannon index indicated a 21.5% surge in RG and about 28.1% increase in the MG treatment. However, the fungal community was quite lower in RG than in MG treatment.

Table 5.1

Treatment Combinations Across Growth and Incorporation Periods

Treatment Combination	Growth Period		Incorporation Period	
	Bacterial Community	Fungal Community	Bacterial Community	Fungal Community
	Chao1	Shannon	Chao1	Shannon
CK	115,455.61 ± 14.20a	4.63 ± 0.54a	578.34 ± 44.78abc	3.16 ± 0.45ab
CF	1,101.29 ± 72.99a	5.45 ± 0.04a	386.43 ± 41.96abc	3.42 ± 0.534abc
HAF	1,734.05 ± 138.59bc	7.19 ± 0.45b	688.70 ± 83.34cd	3.94 ± 0.341c
OMF	2,017.00 ± 90.93de	9.59 ± 0.23cd	234.41 ± 54.29d	4.00 ± 0.256c
RG	1,464.64 ± 73.17b	5.57 ± 0.44bc	455.10 ± 49.90a	2.89 ± 0.445a
RH	1,446.11 ± 42.756cd	5.78 ± 0.cd	4,565.73 ± 78.98ab	3.69 ± 0.547bc
RO	2,015.50 ± 129.75cde	5.60 ± 0.18cd	530.23 ± 104.03abc	3.75 ± 0.09bc
MG	1,760.00 ± 98.62cd	5.19 ± 0.10cd	552.89 ± 96.16bc	3.49 ± 0.11bc
MH	1,978.34 ± 36.05cde	5.75 ± 0.09cd	499.93 ± 26.90abc	3.48 ± 0.12abc
MO	2,235.82 ± 100.31e	5.66 ± 0.06d	517.30 ± 53.54abc	2.67 ± 0.25a

Note: Values with different lowercase letters (a, b, c, etc.) in the same column indicate significant differences among treatments based on one-way ANOVA followed by Duncan's multiple range test ($p < 0.05$).
Chao1 data depicts soil microbial community richness while Shannon shows diversity.

The soil portion of the bacterial community structure, which remained properly analyzed by process of using Coa, was found to be gathered conferring the green manure plants (ANOSIM: R=0.71, p. 0.001) higher than collective form of fertilizer forms (see Figure 5.3).

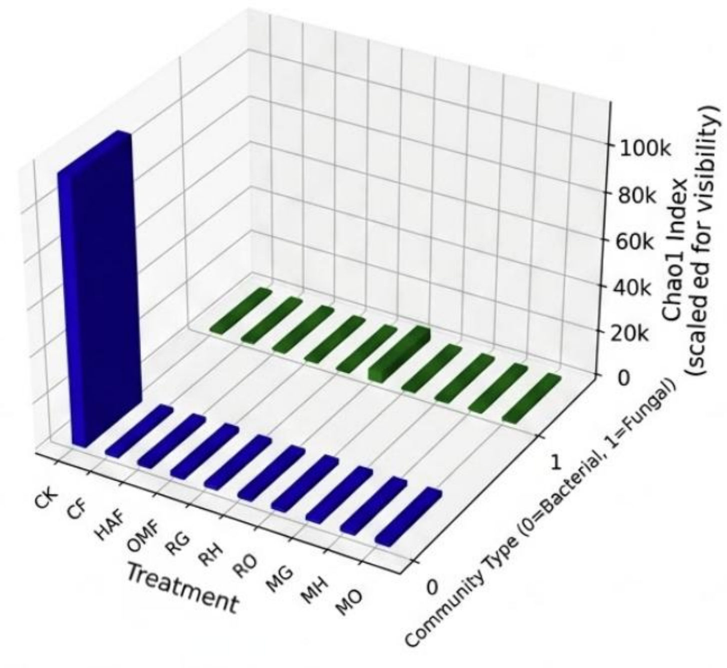

Figure 5.3 Coa results for bacterial and fungal communities

Based on FAPROTAX annotation, 66 predicted functional categories were identified. The majority of these inferred functions were putatively associated with sulfur, nitrogen, and carbon cycling (Figure 5.4). It is important to emphasize that these are predicted functional potentials, not directly measured metabolic activities. Predicted functions related to aerobic chemoheterotrophy - such as those inferred for milkvetch treatments - showed a relative abundance difference compared with ryegrass in carbon-related functional groups. A similar pattern was observed for inferred N-cycling functional groups, including urea lysis, nitrogen respiration, nitrate respiration, nitrate reduction, aerobic ammonia oxidation, nitrogen fixation, and nitrification. For S-cycling-related functional groups, their predicted abundance was higher during the growth of ryegrass than when milkvetch was dominant.

These inferred patterns provide mechanistic hypotheses regarding the functional shifts that green manure may induce under controlled conditions in the soil microbial community. However, these hypotheses require direct validation through metatranscriptomic analysis of gene expression or targeted enzymatic activity assays before they can be confidently translated to field conditions or used as biomarkers for restoration assessment.

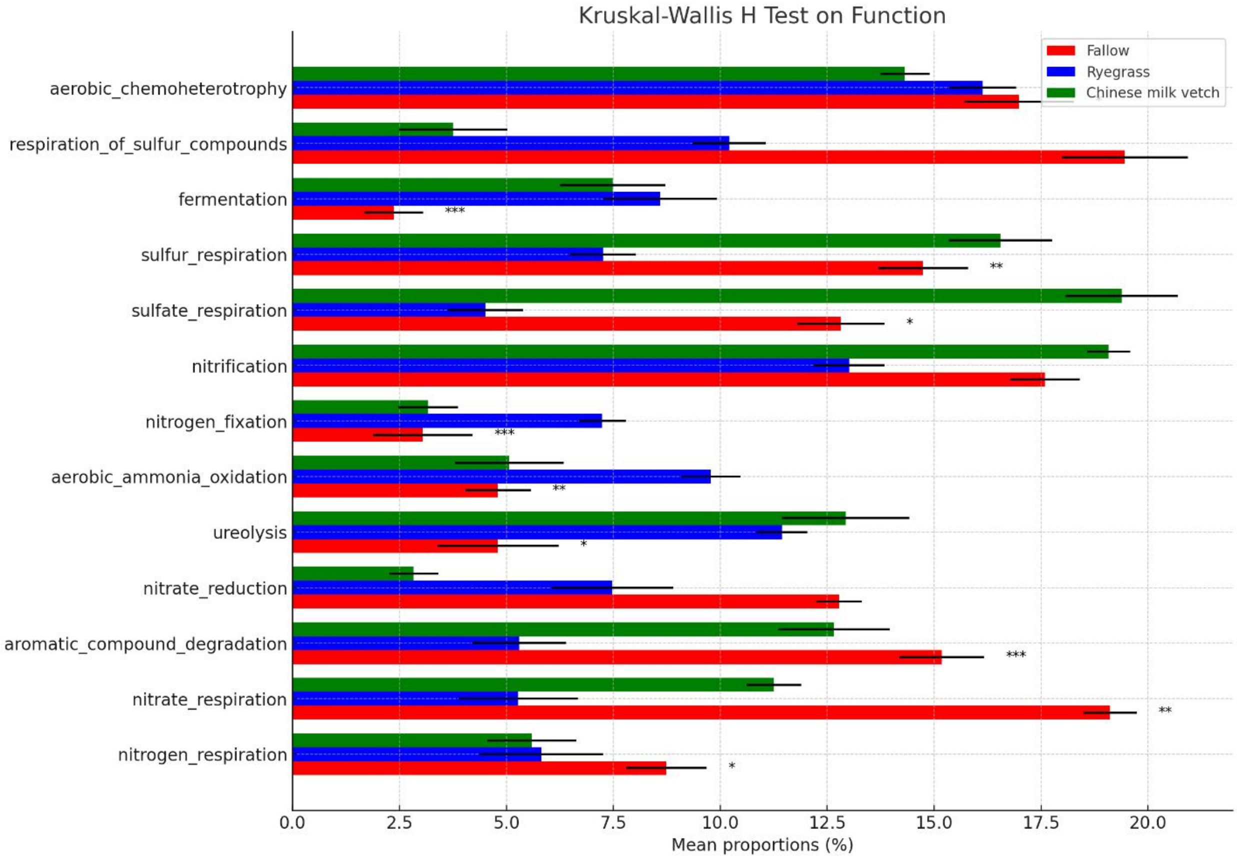

Figure 5.4 Bacteria community functional prediction

5.2 Green manure incorporation and fertilizer application effect on soil properties

Results of this study include investigations on how the green manure-fertilizer combination influences the properties like physicochemical, biomass C, and enzyme activity in the soil. Concerning the soil physicochemical characteristics, this study revealed that a combination of green manure and fertilizer had a substantial impact on soil AN, TN, SOM, and pH as presented in Table 5.2. Application of ryegrass raised pH from 9% to 12% in comparison to the fallow treatments while milk vetch raised the soil pH by 5% in MH and a 4% in MG but not in MO. The contents of TN in MG and RG were 14% higher than those in CF treatments Signals 7 and 8. SOM had a stronger content increment when treated with the humic acid fertilizer than in the action of organic manure both under the effects of the fallowing practice and of the various form of green manure form of treatments.

Table 5.2

Influence of green manure-fertilizer mixtures on tat of the soil properties

Treatment	pH	SOM (g/kg)	TN (g/kg)	TP (g/kg)	AN (mg/kg)	OP (mg/kg)
CK	5.01 ± 0.04b	3.53 ± 0.44a	0.56 ± 0.44a	1.03 ± 0.44a	52.56 ± 3.76a	4.29 ± 0.04a
CF	4.84 ± 0.43a	2.62 ± 0.22a	0.51 ± 0.22a	1.19 ± 0.74ab	55.50 ± 1.22ab	4.43 ± 0.21ab
HAF	3.17 ± 0.22b	18.86 ± 1.02c	2.64 ± 0.02c	6.14 ± 0.07abc	32.91 ± 1.83abc	7.36 ± 0.21b
OMF	4.15 ± 0.11b	10.44 ± 0.73b	1.71 ± 0.53de	1.18 ± 0.63abc	18.34 ± 2.63c	2.49 ± 0.17ab
RG	5.44 ± 0.22c	8.23 ± 0.62a	6.47 ± 0.76b	2.12 ± 0.73a	87.33 ± 3.73d	6.46 ± 0.25ab
RH	7.23 ± 0.22d	20.14 ± 0.73c	5.66 ± 0.64cd	4.22 ± 0.73abc	30.63 ± 6.73abc	6.92 ± 0.63b
RO	2.75 ± 0.44d	10.85 ± 0.73b	3.71 ± 0.53e	2.23 ± 0.72abc	82.73 ± 7.83d	2.42 ± 0.73ab
MG	2.02 ± 0.25b	71.81 ± 0.73a	1.47 ± 0.84b	6.12 ± 0.76ab	25.36 ± 2.73bc	1.82 ± 0.63b
MH	3.22 ± 0.82c	38.66 ± 0.83c	0.68 ± 0.63cde	4.28 ± 0.83c	14.70 ± 5.83abc	2.81 ± 0.63ab
MO	5.27 ± 0.89b	20.77 ± 0.63b	1.74 ± 0.73cd	2.23 ± 0.83bc	25.47 ± 3.52bc	2.31 ± 0.63ab
Note: Values with different lowercase letters (a, b, c, etc.) in the same column indicate significant differences among treatments based on one-way ANOVA followed by Duncan’s multiple range test ($p < 0.05$).						

The effect revealed for SMBC suggested that this parameter significantly increased for both combined fertilizer application and green manure incorporations as well as their interactions. Marked by an enhancement of 40, the SMBC rose. The percentage of males was also significantly higher in RG compared to CF constituting 6% only in RG. In MH and RH, the SMBC was 73% and 44. At the same time, they are 70% higher, respectively, than the AHF treatments. The experiment findings indicated that actual green manure which is enhanced the actual β -glucosidase as well as the urease in the soil though the fallow treatments; nevertheless, it is reduced the catalase activity in the combined manure and mineral fertilizer. Nonetheless, the three enzymes’ activity had no variation concerning green manure application and the treatments involving fallowing that with the actual humic acid form of fertilizer.

5.3 Soil microbial community features depend on green manure incorporation

Approximately 2160 fungal OTUs (12 phyla) and 4360 bacterial OTUs (43 bacterial phyla) were identified after the incorporation of green manure. \Dominant form of the bacterial phyla was Chlorolipid (11-44%), Proteobacteria (11-22%), and Actinobacteria (8-28%), among others (Figure 5.5). Likened to the various form of fallow remedies, the incorporation of ryegrass remarkably increased Firmicutes’ relative abundance (see Figure 5.6 below).

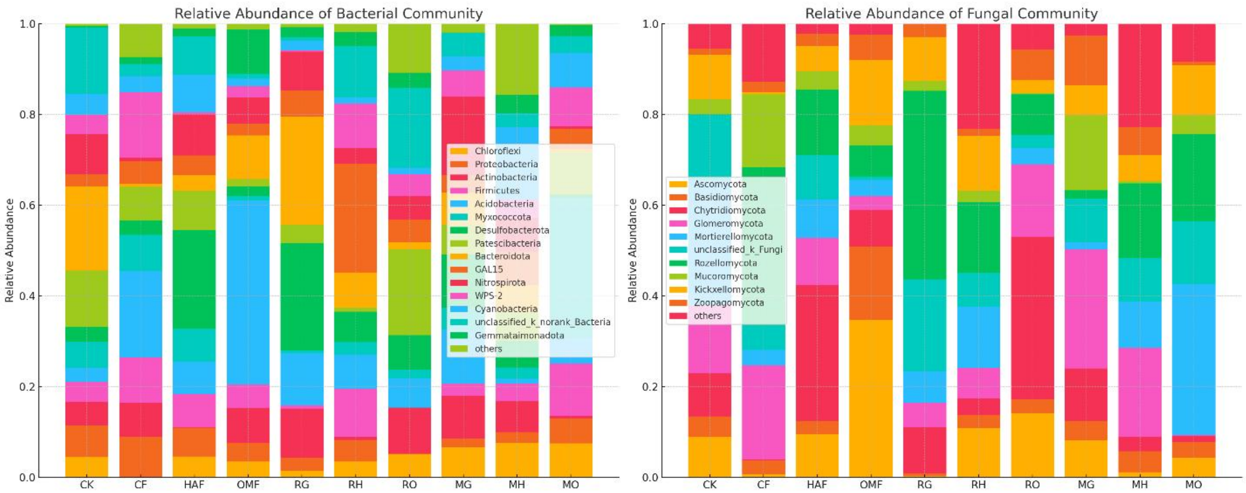

Figure 5.5 Relative abundance of bacterial and fungal communities

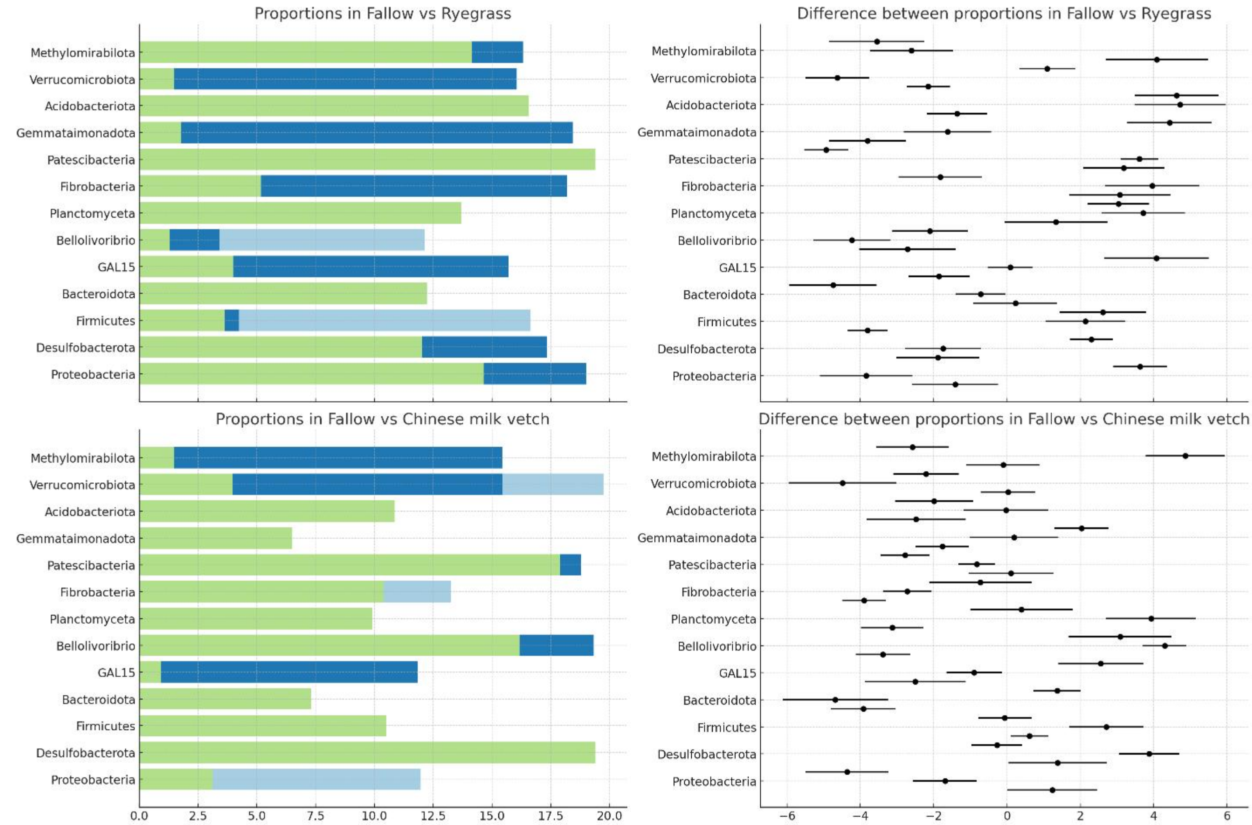

Figure 5.6 Bacterial taxa relative abundance

With regard to the soil microbial form of alpha-diversity, within this specific as well as the particular study, the actual form of results presented that the various form of soil microorganisms community alpha-diversity remained very much significantly much high in that of the manure incorporation treatments than that of fallow treatments for all the parameters except Chao1 of MO and RH. They estimated the chao1 index went up by 23.6 - 38.8% relative to the use of green manure, and Shannon type of diversity index increased by 7% compared with the fallow treatments. An interaction with organic manure or humic acid fertilizer was not possible to yield any difference compared to the fallow conducts (as noted on Table 5.1 above). Within this context of the microbial community structure and function prediction, the results highlighted the samples' significant clustering referring to the green manure treatment. Following green manure incorporation, FAPROTAX-based functional prediction indicated that functions related to carbon and nitrogen cycling - including fermentation, nitrogen fixation, and chemoheterotrophy - were predicted to be enriched by green manure application in the pot experiment. These predictions require confirmation through direct functional assays in field soils (Figure 5.7). These results represent predicted functional potentials based on 16S rRNA gene-inferred community composition; they do not directly measure metabolic rates or gene expression levels.

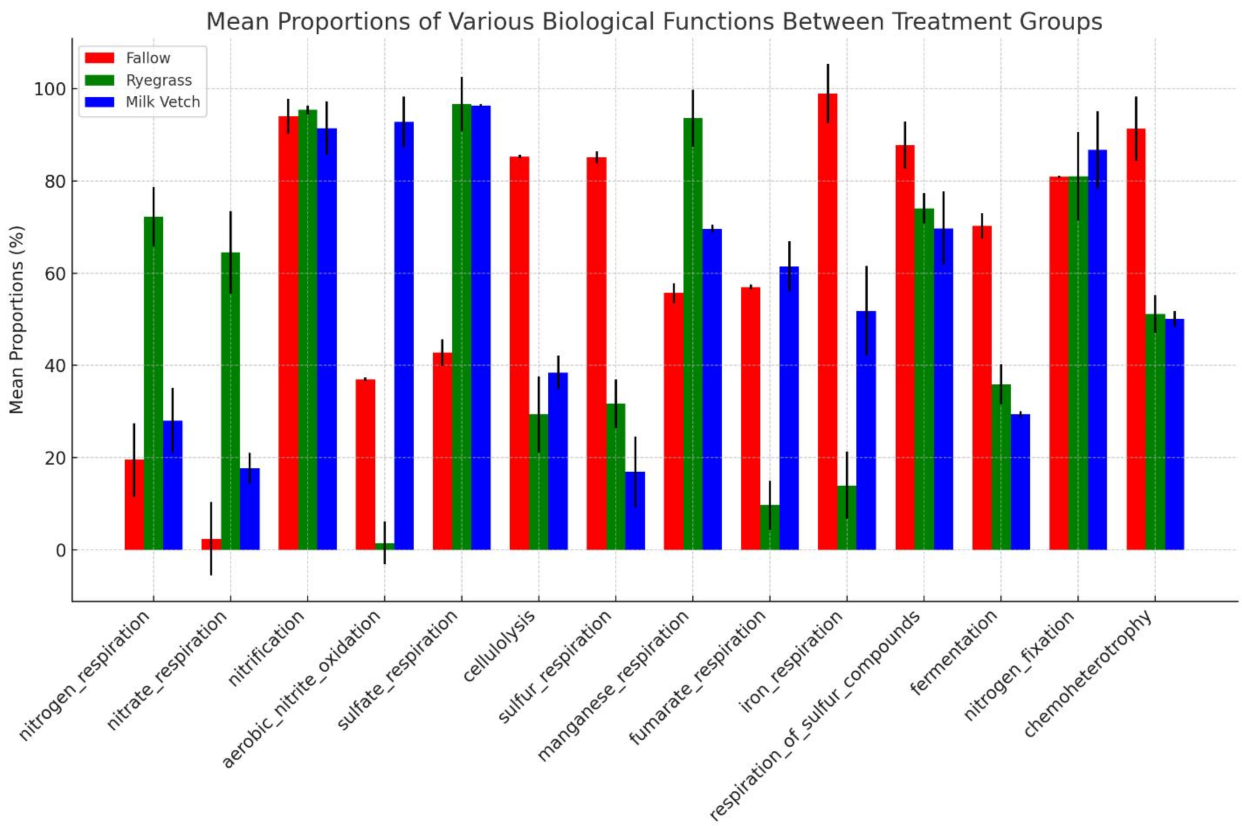

Figure 5.7 Kruskal H test function

Lastly, this study assessed the actual form of relationships among that of the microbial community enzyme activities and soil properties. Based on the Db-RDA results, this study established a significant correlation between bacterial communities in green manure applications and TN and SOM (in organic manure-humic acid combinations). TP strongly and positively correlated with RG, MH, and RH bacterial communities, while AN and pH strongly correlated with MO and RO (see Figure 5.8).

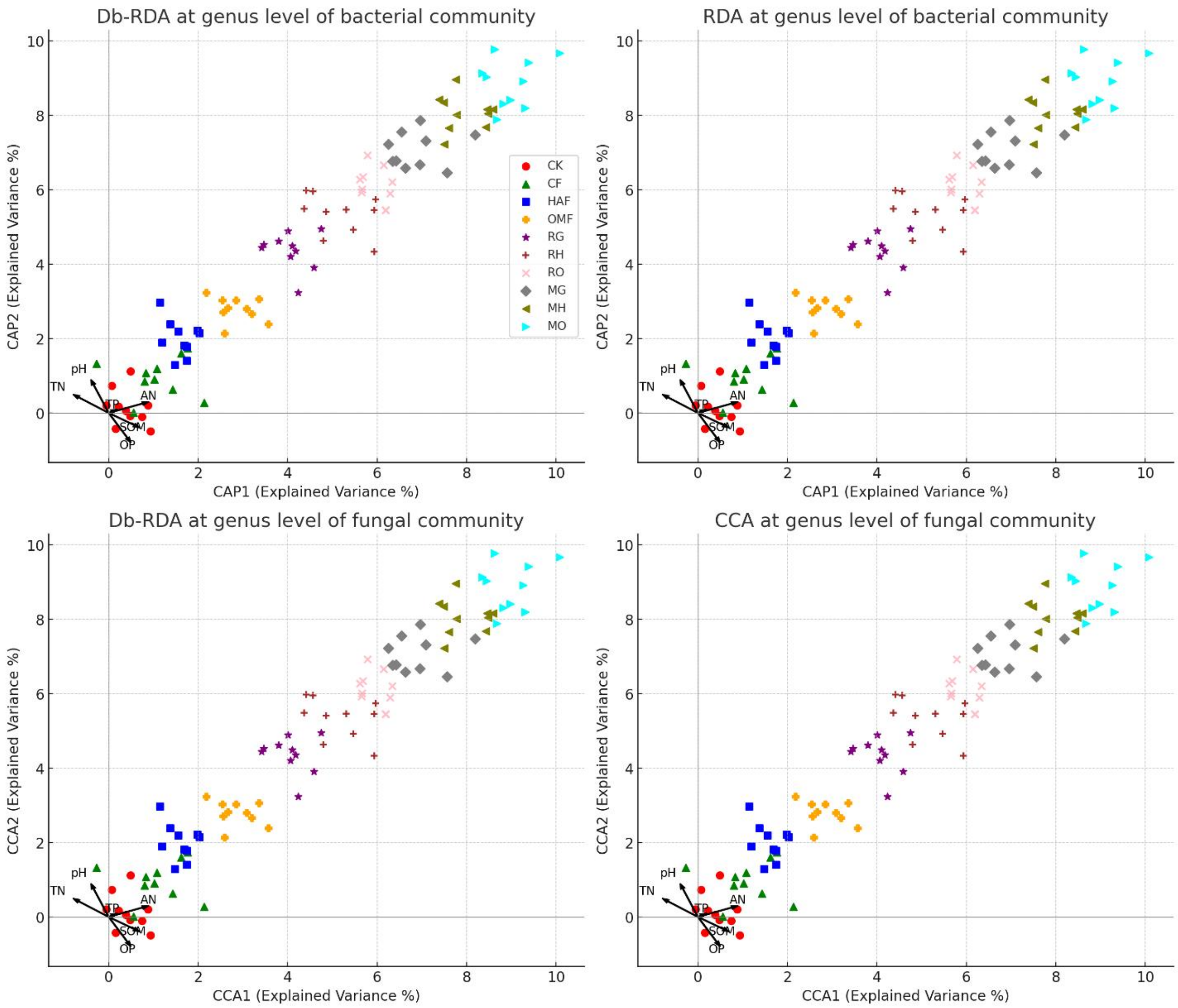

Figure 5.8 Db-RDA analysis based on bacterial and fungal community genus level

5.4 Analysis of the Benefits of Returning Green Manure to the Field and Exploration of its Application in Ecological Farms

This section presents a meta-analysis of empirically measured effect sizes from 15 published field studies (Xu B et al., 2025; Ma D K et al., 2021; Kichamu-wachira E et al., 2021; Liang K L 2022; Zhang S H et al., 2021; Jia Q et al., 2024; Xu B et al., 2024; Li Y J et al., 2024; Ding W C et al., 2018; Garba I I et al., 2022; Hu Q J et al., 2023; Yue Q et al., 2022; Muhammad I et al., 2020; Khan A A et al., 2025; Huang H et al., 2025) to green manure, extracting 183 effect size data points to reveal the role of green manure in key indicators such as crop yield, carbon sequestration, and greenhouse gas emissions, providing a theoretical basis for the formulation and practice of green manure strategies in subsequent ecological farms.

5.4.1 The impact of green manure on crop yield

A total of 61 effects on subsequent crop yield were studied, of which 7 showed a negative impact of green manure, 6 showed no impact, and 48 confirmed a positive impact, accounting for 11.5%, 9.8%, and 78.7% respectively. This fully demonstrates that, in most cases, green manure promotes crop yield. The effect of green manure on subsequent crop yield is relatively stable, with most studies showing an effect size of 5.0% - 20.0%, and a mean effect size of 13.8%. The impact of green manure on subsequent crop yield is related to the type of green manure and the type of subsequent crop. Meta-analysis shows that, compared with fallow control, leguminous green manure increased wheat yield by 5.1%, while non-leguminous green manure decreased wheat yield by 7.2%; both leguminous and non-leguminous green manure increased maize yield, with increases of 12.0% and 9.4% respectively; and in potato (Solanum tuberosum). In tuberosum cultivation, legume green manure had no significant effect on yield, while non-legume green manure increased potato yield by 5.9% (Kichamu-wachira E et al., 2021). The effect of green manure on the yield of subsequent crops is also affected by local climate conditions. A meta-analysis of Africa showed that in humid regions, returning green manure to the field could increase crop yield by 98.9%, while in semi-arid regions it increased crop yield by 34.0% (Liang K L et al., 2022). A meta-analysis of green manure in China reached similar conclusions, showing that green manure in humid regions had a stronger effect on the yield of subsequent crops compared to arid regions (Zhang Shaohong et al., 2021). In addition, soil fertility and nitrogen application level also have a certain influence on the effect of green manure. At low nitrogen levels [1~99 kg(N)·hm $^{-2}$], crop yield increased by 66.3% after returning green manure to the field, while at high nitrogen levels [>100 kg(N)·hm $^{-2}$], returning green manure to the field had no significant effect on crop yield (Liang K L et al., 2022). When the soil organic matter content is 0~10 g·kg $^{-1}$, the yield of grain crops increases by 32.6%; when the soil organic matter content is 10~20 g·kg $^{-1}$, the yield of grain crops increases by 10.2%; however, when the soil organic matter content is >30 g·kg $^{-1}$, returning green manure to the field has no significant effect on crop yield (Zhang Shaohong et al., 2021).

5.4.2 Effects of green manure on soil physicochemical properties, microorganisms, and nutrient cycling

Returning green manure to the field can improve soil properties and is of great significance to the sustainable development of soil fertility. Turning green manure over can increase the content of soil organic matter and available nutrients, which is an important measure to improve soil fertility. As for the physical and chemical properties of soil, 17 effect quantities showed that green manure had a negative impact, 3 had no impact, and 20 effect quantities showed that it had a positive impact, accounting for 42.5%, 7.5% and 50.0% respectively. Among them, the negative impact was all in the soil moisture content index. Green manure planting will consume soil moisture, thereby reducing soil moisture content and leading to water resource competition for later crops. Zhang Shaohong et al. (Jia Q et al., 2024) showed that the meta-analysis of 46 literatures related to green manure in the Loess Plateau showed that although planting green manure in the Loess Plateau reduced soil moisture, it had a significant promoting effect on the yield of subsequent grain crops. Turning green manure over about 13 days in advance and controlling the biomass of leguminous green manure at 2200~3100 $kg \cdot hm^{-2}$ can effectively mitigate the negative impact of green planting on soil moisture. Compared with traditional tillage without replanting green manure, returning green manure to the field can increase the content of large soil aggregates in the 0-30cm soil layer, enhance the stability of soil aggregates, and reduce soil bulk density (Li Yuanxue et al., 2019). There are many soil physicochemical properties, and the effect of green manure on soil physicochemical properties is more complex, showing great differences in different studies. Its effect is affected by a combination of factors, such as soil type, type of green manure, and planting management measures.

In terms of soil microorganisms, all 15 effect quantities showed that green manure had a positive impact, accounting for 100%, with effect quantities ranging from 11.0% to 51.0%, and an average of 26.0%. This clearly shows that green manure promotes the growth and activity of soil microorganisms, helps maintain the biodiversity and functional stability of the soil ecosystem, plays a core role in the soil ecological process, and its promoting effect is quite obvious. For example, reasonable replanting of forage rape and returning it to the field can increase the soil nutrient content and enzyme activity of the subsequent wheat field, effectively enhance the diversity of bacterial communities, and promote the growth of beneficial soil bacteria communities (Qin Jingyi et al., 2016). In the nutrient cycling study, 2 effect quantities showed a negative impact, 5 showed no impact, and 34 showed that green manure had a positive impact on nutrient cycling, accounting for 4.9%, 12.2%, and 82.9%, respectively. Returning green manure to the field can significantly increase the content of soil nitrate nitrogen, available phosphorus and available potassium by 6.2% to 60.0%. In addition, returning green manure to the field can also reduce ammonia volatilization and soil nitrogen leaching (Kichamu-wachira E et al., 2021; Liang K L et al., 2022; Xu B et al., 2024; Ding W C et al., 2018).

5.4.3 The impact of green manure on carbon sequestration and greenhouse gas emissions

There were 16 items on the effect of carbon sequestration, of which 2 items showed no effect and 14 items showed positive effect, accounting for 12.5% and 87.5% respectively. The effect size ranged from -7.8% to 66.1%, with a mean of 17.3%. This indicates that compared with the control group without green manure, returning green manure to the field increased the soil organic carbon content by 17.3%. This shows that green manure plays an important role in carbon sequestration and makes a key contribution to increasing soil carbon storage. Soil organic carbon changes are affected by a variety of factors such as annual mean temperature, type and planting years of green manure, initial soil organic carbon content, microbial community status, green manure biomass and its return to the field, and soil texture (Tian Fei et al., 2008). Compared with the control, the soil organic carbon content increased significantly by 30% after returning leguminous green manure to the field, and by 47% for non-leguminous green manure (Ding W C et al., 2018). A meta-analysis by Kichamu-Wachira et al. (Liang K L et al., 2022) on Africa showed that the effect of green manure on soil organic carbon is affected by time. In short-term

(<3 years) trials, soil organic carbon content increased by 12.6%, while in long-term (>20 years) trials, green manure had no significant effect on soil organic carbon content.

Returning green manure to the field can increase soil organic matter input and promote soil organic matter accumulation, but it also affects greenhouse gas emissions from farmland. This study found that, regarding greenhouse gas emissions, six data points showed a negative impact, two showed no impact, and only two showed a positive impact, with percentages of 60.0%, 20.0%, and 20.0%, respectively. Their effect sizes ranged from −5.1% to 132.0%, with a mean of 40.7%. This indicates that, compared to the control group without green manure, returning green manure to the field increased greenhouse gas emissions from farmland by an average of 40.7%.

5.4.4 Trade - offs between different ecological benefits

Planting green manure has multiple ecological benefits, but there are trade-offs among these benefits. Returning green manure to the field has a positive impact on soil microorganisms, with a composite value of 1.00, indicating a significant promoting effect of green manure on soil microorganisms. The composite value for carbon sequestration is 0.88, showing that green manure has a strong positive significance in carbon sequestration, playing an important role in increasing soil organic carbon content and soil carbon sink capacity, as well as mitigating climate change. The composite value for crop yield is 0.67, fully demonstrating that green manure plays a significant role in increasing crop yield in most cases, and has important application value in agricultural production. The composite value for nutrient cycling is 0.78, meaning that green manure plays a positive role in promoting soil nutrient transformation, release, and recycling, helping to maintain soil nutrient balance and sustainable supply, ensuring the nutrient needs of plant growth, and improving the nutrient utilization efficiency of the ecosystem. The composite value for soil physicochemical properties is 0.08, mainly because green manure planting reduces soil moisture, but has a positive effect on other physicochemical properties (such as soil bulk density and enzyme activity) (Kichamu-wachira E et al., 2021; Hu

Q J, 2023). Regarding greenhouse gas emissions, the composite value is −0.40, indicating that returning green manure to the field will lead to an increase in greenhouse gas emissions. This is related to a variety of factors such as the decomposition process of green manure, soil microbial metabolic activities, and environmental conditions. Further in-depth research is needed on its underlying mechanisms in order to explore effective control measures (Xu B et al., 2024; Li Y J, 2024).

5.4.5 Strategies for the Application of Green Manure in Ecological Farms

Ecological farms strive to achieve a harmonious balance between agricultural production and ecological environmental protection, exhibiting diverse and comprehensive technological needs. In terms of soil quality improvement, ecological farms require technologies that can increase soil organic matter content, improve soil structure, and enhance soil water and fertilizer retention capacity to ensure long-term productivity of arable land. Regarding nutrient management, it is necessary to reduce reliance on external chemical fertilizers, establish a sustainable nutrient cycling system, and avoid soil degradation and environmental pollution caused by excessive fertilizer application. Simultaneously, ecological farms also emphasize maintaining biodiversity, requiring technological means to create environments suitable for diverse organisms and promote ecosystem stability and balance. Green manure largely meets these technological needs. While green manure plays a positive role in soil microorganisms, carbon sequestration, crop yield, and nutrient cycling, it exhibits negative and relatively neutral impacts on greenhouse gas emissions and soil physicochemical properties, respectively. In agricultural ecosystem management, these differences should be fully considered, and green manure should be applied rationally and appropriately according to local conditions to maximize its ecological functions. Targeted measures should be taken to address potential negative impacts and promote the sustainable development of agricultural ecosystems.

The realization of the ecological function of green manure is affected by a variety of factors, such as the level of farmland fertilization, the biomass and amount of green manure returned to the field, the type of green manure and the type of main crop. Climate zone and soil characteristics are the basic factors that determine the benefits of green manure (Cao et al., 2017). Temperature, precipitation, light and other conditions in different climate zones, as well as soil texture, fertility, pH and other characteristics, will affect the growth and development, biomass accumulation and ecological function of green manure. Under suitable climate and soil conditions, green manure can better play its ecological service function and improve the sustainability of crop production system. A deeper understanding of the impact of these factors on the ecological benefits of green manure will help farmers to scientifically and rationally select and manage green manure according to local conditions, and achieve efficient and sustainable development of crop production system.

5.5 Discussion

5.5.1 The Feedback Mechanism of Aboveground-Subsurface Interactions from a Microbial Perspective and Its Agricultural and Forestry Significance

Multiple studies have shown that the actual application of green manure can effectively improve the development of microbial communities (SMs) during their growth and integration stages. The significant increase in bacterial diversity after green manure application in this study is consistent with the earlier findings of Gao et al. (2021) and He et al. (2020). The rhizosphere environment plays a crucial role in nutrient transport between soil and plants during the growth of green manure crops, thus directly affecting the diversity and other characteristics of the microbial community in this region. Notably, the fluctuations in fungal and bacterial diversity in this study can be attributed to the competitive and symbiotic relationship between microorganisms and green manure species (Liu et al., 2019). Studies have found that the combination of chemical reactions during the application of different organic materials significantly affects the growth cycle of green manure crops and the final microbial community (Liu et al., 2020). Correspondingly, the microbial groups involved in soil organic matter treatment can also be supported by green manure residues. The active state of the fungal community has also been shown to effectively promote the biodegradation of soil organic matter such as lignin and cellulose (Liu et al., 2020). This explains why the negative impact of green manure application on fungal diversity was relatively weak in this study. The study also found a more significant positive correlation between green manure plants and bacteria compared to chemical fertilizers – primarily due to the well-developed root system of ryegrass. Specifically, Lovell et al. (2001) reached similar conclusions.

Regarding the impact of actual application levels of green manure crops on soil microbial diversity, studies have found that treatments applying alfalfa and ryegrass significantly increased actinomycete content compared to fallow treatments. This contributes to enhancing nitrogen cycling rates and carbon cycling and metabolic efficiency in the rhizosphere (Fierer et al., 2017). Ryegrass also accelerates carbon turnover by decomposing plant polysaccharides, thereby increasing the relative abundance of Firmicutes. Furthermore, ryegrass is closely associated with the proliferation of polysaccharide-metabolizing microorganisms - including polysaccharide-decomposing and hemicellulose-decomposing bacteria (Wang et al., 2021; Fierer et al., 2017). These findings corroborate other research results, indicating that planting green manure crops (such as ryegrass) can effectively enhance the functional activity of fungi and bacteria, especially in improving carbon metabolism in immature red soils. Notably, alfalfa increases the proportion of bacterial phyla involved in nitrogen cycling in the soil. This conclusion is supported by the study by Khan et al. (2019), who found that the application of legumes (such as barley) effectively enhanced the activity of related enzymes. The research by Banska and Lassata (2017) showed that the addition of ryegrass significantly enhanced the activity of fungal and bacterial communities, which was closely related to the activity of β-glucosidase. This enzyme plays a key role in soil organic matter cycling, especially carbon degradation. Studies have also found that the addition of ryegrass can promote nitrogen cycle-related functions, including nitrification, nitrite oxidation, and nitrogen fixation. This finding is supported by the research of He et al. (2020), who found a significant correlation between the addition of Italian ryegrass and the growth of nitrogen cycle-related microorganisms.

The findings also indicate that the combination of green manure and fertilizers affects not only soil physical properties but also microbial activity. These combinations influence the presence of compounds in the soil, thereby increasing the availability of nutrients required for microbial growth. These results are very similar to those of Ma et al. (2021), who found that various forms of green manure improved pH and nitrogen content, regardless of the immaturity of the red soil involved in this study. Regarding factors related to soil pH, it is noteworthy that green manure is alkaline, which helps neutralize protons in the acidic rhizosphere (Rukshana et al., 2013). Similar to this study, the combination of green manure with actual organic fertilizer forms increased TN, AN, and pH, which are crucial for fungi and bacteria. These findings are largely consistent with the appropriate and specific findings of Yu et al. (2019), which indicated that soil organic matter, nutrients, and pH are among the soil parameters controlled by green manure and/or organic fertilizers. There is good reason to believe that soil organic matter, AN, TN, and pH work in conjunction with bacteria associated with the carbon and nitrogen cycles; Zheng et al. (2018) hold the same view, finding that bacterial groups triggered by green manure application are responsible for decomposition processes in the soil. Furthermore, Gao et al. (2021) also pointed out that green manure application increases pH, thereby helping to prevent acidification of immature red soils.

Although the ecological benefits of green manure are clear, its promotion and application in ecological farms still face many challenges. At present, there is still much room for improvement in the popularization rate of green manure in ecological farms (Cao et al., 2017). How to more effectively promote the adoption of green manure in ecological farms and achieve multiple goals such as reducing fertilizer and pesticide use and protecting biodiversity in ecological agriculture still has many problems that need to be solved. One key bottleneck is the quantification and recognition of economic benefits. A large number of field trials have shown that green manure, especially legume green manure, can not only improve soil fertility, but also increase crop yield. Therefore, the promotion and application of green manure has received widespread attention (Hu et al., 2024; Ma et al., 2021; Jia et al., 2024). However, the effective promotion of green manure depends on the recognition and active participation of farmers. Although there are relevant case studies (Lyu et al., 2021), the current research on the economic benefit indicators that farmers are concerned about is still insufficient. If the direct link between green manure planting and farmers' income cannot be clearly established, its promotion will always face the obstacle of the "last mile". In addition, the integration and innovation of technical models is also a core problem in the promotion and application. Currently, ecological farms have a higher application rate of single technical measures promoted by policies (such as soil testing and formula fertilization and straw return to the field); while the application rate of other technical measures, which are relatively complex but can achieve higher comprehensive benefits, is lower (Cao et al., 2017). Based on this, policy guidance can be used to encourage qualified ecological farms to actively explore and apply more comprehensive and effective ecological agricultural technical measures according to local conditions. In addition, the coordinated implementation with other ecological measures should be explored, such as reducing chemical fertilizer use, applying organic fertilizer, and reducing or eliminating tillage.

These practical challenges ultimately point to the necessity of systematic policy support. Promoting the use of green manure in ecological farms requires policy support and innovation. In the context of agricultural green transformation, policies have played a crucial role in promoting the development of ecological farms and the use of green manure. Currently, support policies oriented towards green ecological agriculture are insufficient, subsidies for ecological technology measures need to be strengthened, and the mechanism of premium pricing for high-quality products in the market is difficult to achieve effectively, resulting in difficulties in the construction of ecological farms (Hu et al., 2024). Green manure plays a unique and irreplaceable role in China's major strategic tasks in agriculture (such as farmland ecological improvement and the integration of farmland use and conservation) (Cao et al., 2017). Therefore, it is particularly necessary to introduce a series of relevant policies to help the development of ecological farms and improve the ecological compensation mechanism (Gao et al., 2019). At the same time, relevant supporting policies should be established and improved to closely link the promotion of green manure with the support policies for the construction of ecological farms. Through the synergistic effect of policies, the transformation of agriculture towards green development should be comprehensively promoted, the advantages of green manure in ecological farms should be fully utilized, and the green transformation of agriculture should be promoted.

5.5.2 Cautions regarding pot-to-field extrapolation of microbial findings

While the pot experiment successfully demonstrated that green manure application significantly enhances bacterial diversity (Chao1 +23.6 - 60%) and activates C- and N-cycling functional groups (e.g., Proteobacteria, Firmicutes), these quantitative magnitudes should not be interpreted as direct predictions for field performance. Several lines of evidence suggest that field conditions may moderate or amplify these effects in unpredictable ways:

First, the threefold increase in Firmicutes abundance observed in ryegrass-treated pots - attributed to polysaccharide decomposition - may be dampened in field soils where indigenous macrofauna and competitive microbial consortia buffer rapid population shifts (Liu et al., 2020). Second, the FAPROTAX-predicted enhancement of nitrogen fixation and nitrification functions occurred under optimal moisture and temperature regimes in the greenhouse; field soils experience drying - rewetting cycles and temperature extremes that significantly modulate functional gene expression (Hartmann & Six, 2022). Third, the rhizosphere effect observed in pots (root exudate-driven Burkholderia recruitment) may be diluted in field soils due to greater spatial heterogeneity and diffusional constraints.

Explicitly, the microbial indicators identified in this chapter - particularly the threshold values of Acidobacteria abundance (14.8 - 16.3%) and the CdS nanoparticle precipitation pathway - should be treated as mechanistic hypotheses awaiting field validation. We recommend that future research prioritize (i) paired pot-field validation trials at multiple sites across Guangdong's degradation gradients, (ii) long-term (>3 years) monitoring of microbial community succession under the optimized green manure regime, and (iii) establishment of field-specific microbial reference baselines before using these indicators as operational biomarkers for restoration assessment.

Conclusions to Chapter 5

This chapter investigates the microscopic mechanisms of ecological restoration in degraded red soils through a core agroforestry measure: the application of green manure (such as ryegrass and milkvetch). By comparing different species of green manure and their combined application with chemical fertilizers, the study reveals the intrinsic link between the improvement of soil physicochemical properties and the succession of microbial communities. The key findings are as follows:

1. Significant Improvement of Soil Physicochemical Properties (under pot conditions).

The pot experiment demonstrated that the combination of green manure and chemical fertilizer effectively mitigates soil acidification, with ryegrass treatment increasing soil pH by 9% - 12% under controlled conditions. TN and SOM also showed significant accumulation, particularly with humic acid-based fertilizers. These physicochemical responses are expected to be qualitatively similar in the field, but quantitative magnitudes require site-specific validation.

2. Enhancement of Microbial Diversity and Richness (model-system evidence).

High-throughput sequencing of pot-soil samples revealed that green manure application increased the Chao1 richness index by 23.6% - 60% and the Shannon diversity index by 7% - 28.1% under controlled conditions. While these results robustly demonstrate the mechanism of nutrient-driven microbial recruitment, the absolute values should not be used as field performance targets without empirical calibration from field trials.

3. Selective Succession of Core Microbial Taxa

The application of green manure drove a distinct shift in the dominance of soil microbial groups. There was a significant increase in the relative abundance of Proteobacteria and Acidobacteria. As typical copiotrophic microorganisms, the rise of Proteobacteria was positively correlated with the increase in available soil nutrients, while shifts in specific Acidobacteria subgroups reflected improvements in soil pH stability and soil organic matter quality.

4. Strengthening of Inferred Key Ecosystem Functional Metabolisms (mechanistic prediction)

FAPROTAX functional prediction based on pot experiment data showed significant enhancement of C-cycle (fermentation, chemoheterotrophy) and N-cycle (nitrogen fixation, nitrification) pathways following green manure application. This provides a strong mechanistic hypothesis for field restoration, but functional gene expression in field soils - subject to fluctuating redox conditions and root-microbe competition - requires direct metatranscriptomic validation in subsequent field studies.

5. Coupling Between Environmental Factors and Biological Responses

Redundancy Analysis (RDA) identified pH, TN, and SOM as the core environmental drivers shaping the microbial community structure. By modulating these physicochemical indicators, green manure indirectly facilitates the precise recruitment and functional cultivation of beneficial microbes, forming a closed-loop mechanism for land degradation restoration at the molecular level.

In summary, the research in Chapter 5 confirms that green manure application is a primary driver for rebuilding the biological activity of degraded red soils. Through a multi-level cascade effect of "physicochemical improvement – community reconstruction – functional enhancement," it provides solid biological support for ecological restoration.

CHAPTER 6
COMPREHENSIVE DISCUSSION: CONSTRUCTING AN AGRICULTURAL AND FORESTRY MODEL FOR DEGRADED LAND RESTORATION APPLICABLE TO GUANGDONG PROVINCE

6.1 Systematic integration and discussion of the research findings throughout the book

6.1.1 Synthesis and integration of research findings

The innovation and core value of this study lie in its rigorous, progressive research path - from macro to micro to technology to model - which logically elevates the approach to degraded land restoration in Guangdong Province. This involves transforming isolated technological applications into a scalable and highly resilient agroforestry integrated management model. This logical process embodies a complete closed loop, from understanding the problem, analyzing its essence, solving the problem, to systemic integration and innovation.

Anchoring Macro Trends and Defining Problems: The Cornerstone of Cognition

The study of macro-trends provides goals and directions for restoration efforts. This research first focuses on the contradictory regional context of Guangdong Province, characterized by both "extreme economic activity" and "inherent ecological fragility," clearly defining the unique nature of land degradation in the Pearl River Delta region: a complex interplay of physical erosion (hill collapse), chemical pollution (heavy metals and acidification), and biological degradation (hardening and fragmentation). This understanding of trends precludes the possibility of simply copying single-method governance techniques from the west or north, establishing the necessity of constructing a multifunctional agroforestry system.

Analysis of Microscopic Mechanisms and Target Identification: Scientific Support

Addressing macro-level issues, the research delves into the micro-level, elucidating the core driving mechanisms for the remediation of degraded red soil. Field experiments and data models reveal that available phosphorus (AP) and soil pH are two core regulatory indicators in the remediation of degraded farmland, receiving the highest importance scores, indicating that they synergistically dominate the soil function restoration process. This finding focuses the complex degradation remediation process on two key targets: "acidification neutralization" and "nutrient activation," providing precise scientific evidence for subsequent technological development. Furthermore, the study uses the FAPROTAX model to analyze how green manure application significantly enhances nitrogen fixation and chemoheterotrophic functions in the nitrogen and carbon cycles, validating the effectiveness of the remediation pathway at the microbial level.

Integration and Solution Determination of Technology Optimization: Quantitative Tools

After identifying the microscopic targets, the study moved away from relying on single, empirical techniques and instead utilized data-driven tools such as Response Surface Methodology (RSM) and random forest models to quantify and optimize multi-factor agronomic measures. This study identified key factors such as biochar application rate, lime application rate, and leguminous green manure species, ultimately selecting the optimal combination scheme that maximized soil porosity, pH, and microbial diversity (see Table 6.1) . This integrated approach transcends the linear superposition of single factors, ensuring the efficiency and economy of remediation measures in actual farmland.

Table 6.1

Comparison of Repair Solutions

Repair plan	Porosity (%) / pH	Logical improvement points
Biochar application	55.2±3.1 / 7.1±0.2	Addressing acidification alone offers limited structural improvement.
Lime application	42.3±2.8 / 6.2±0.3	Limited effectiveness, prone to rebound
Optimization Combination	65.3±3.7 / 7.5±0.3	Structural/chemical/biological co-optimization

Logical Elevation of Pattern Construction: System Innovation

"Model construction" is the final integration of the results of the aforementioned three stages, achieving a qualitative leap from "single-item technical repair" to "system model operation". This study integrates the optimized biological improvement technology into the framework of "agroforestry" to construct a high-yield, stable, and multifunctional agroforestry management model for the degradation of red soil in Guangdong.

This sublimation is reflected in:

Functional complementarity: Trees (forests) provide macroscopic functions such as long-term carbon sequestration, improvement of microclimate, and soil retention; optimized agronomic measures (agriculture) provide microscopic functions such as rapid improvement of soil fertility, neutralization of acidity, and activation of microorganisms.

Economic resilience: The coexistence of diversified forest products (timber, fruit) and agricultural crops (food, cash crops) mitigates market and natural risks, achieving synergistic gains in ecological and economic benefits.

Replicability: The optimized combination based on the quantitative model (RSM) provides standardized and adjustable parameters for the promotion of the model, enabling the model to be precisely adapted to land degradation of different degrees, and providing a systematic solution for the governance of red soil degradation in southern China, including Guangdong Province and similar environments.

6.1.2 Synergistic Effects of Agricultural and Forestry Measures on the Restoration of Degraded Land (Production, Ecology, Economy)

Agroforestry, as a systematic land management strategy integrating agroforestry, demonstrates significant multi-dimensional synergistic benefits in the restoration of degraded land. This study's practice in Guangdong Province shows that, through scientific design and dynamic management, agroforestry can not only effectively curb land degradation trends but also achieve positive feedback and synergistic gains across the three dimensions of production, ecology, and economy, constructing a sustainable development closed loop of "promoting production through restoration and stabilizing the economy through ecology."

Production efficiency: Enhancing the overall productivity and output diversity of land

Agriculture and forestry have significantly enhanced the productive function of degraded land through optimized resource allocation and complementary ecological niches.

Increased Land Equivalent Ratio: Compared to monoculture systems, a well-planned forestry-agriculture system can significantly improve the land equivalent ratio (LER), enabling "multiple harvests from one plot of land." For example, in the hilly areas of eastern Guangdong, the "fruit trees + leguminous green manure + short-term crops" model increases the average annual economic output per unit of land by approximately 30% - 50% compared to a single agricultural system.

Improved crop yield and quality: The shading and windbreak effects of tree canopies improve the microclimate in the field, reducing crop water stress and physiological heat damage. At the same time, the deep root systems of trees pump nutrients from the lower layers to the surface, working synergistically with the nitrogen fixation effect of leguminous green manure to continuously replenish soil nitrogen and soil organic matter, thereby improving the yield and nutritional quality of main crops (such as rice and vegetables).

Product diversification and supply flexibility: The agricultural and forestry system provides a variety of products such as grains, vegetables, fruits, timber, and feed, which not only enriches the market supply but also enhances the agricultural system's ability to cope with market price fluctuations, providing farmers with a continuous and stable source of income.

Ecological Benefits: Systematically Restoring Land Health and Ecological Service Functions

Agriculture and forestry are typical "nature-based solutions," with particularly profound benefits in ecological restoration:

Soil physicochemical properties and biological activity improved simultaneously: the return of forest litter and green manure to the field significantly increased soil organic matter content, improved soil aggregate structure, and enhanced water and fertilizer retention capacity. Microbiome analysis showed that soil bacterial and fungal diversity was significantly increased under the combined system, and key biogeochemical cycling processes such as carbon, nitrogen, and phosphorus were activated.

Soil and water conservation and erosion control: The root networks of trees and shrubs effectively stabilize the soil, and the canopy intercepts rainfall, reducing raindrop splash erosion and surface runoff intensity. After implementing the forest-grassland composite model on sloping farmland, the soil erosion modulus decreased by an average of about 40% - 70%.

Biodiversity conservation and ecological network construction: Agroforestry systems provide habitats and migration corridors for birds, insects, and soil animals, enhancing the connectivity and ecological resilience of agricultural landscapes. In particular, the increase in the number of natural enemy insect species naturally suppresses pest and disease outbreaks and reduces reliance on pesticides.

Enhanced carbon sequestration and improved climate adaptability: Forest biomass and soil organic carbon pools are important carbon sinks. Simulations show that the carbon sequestration potential per unit area of a typical subtropical agroforestry system is about 20% - 35% higher than that of a single farmland. At the same time, the buffering effect of the microclimate within the system enhances the crop's adaptability to extreme climate events such as high temperatures and droughts.

Economic Benefits: Enhancing Farmers' Livelihood Resilience and Long-Term Sustainability

Agriculture and forestry inject sustained vitality into farmers and regional economies through value chain extension and risk diversification.

Combining short-term and long-term benefits: Crops provide short-term cash flow, while forestry and economic fruit trees provide medium- to long-term benefits (such as fruits and timber), achieving a benefit structure of "using short-term gains to support long-term gains and combining short-term and long-term benefits," which is particularly suitable for attracting young farmers to participate in sustainable land management.

Cost savings and increased added value: Nutrient cycling and biological nitrogen fixation within the system reduce reliance on chemical fertilizers, and biological control reduces pesticide input, thereby lowering production costs. At the same time, green and healthy agricultural and forestry products are more likely to command market premiums, increasing operational added value.

Risk diversification and livelihood security: Product and income diversification significantly reduces overall income risk caused by market fluctuations in a single crop or natural disasters. Even in years of poor staple crop harvests, income from forest products, forage, or cash fruits can still maintain farmers' basic livelihoods, acting as a "green safety net."

Employment opportunities and rural vitality: The management, harvesting, and processing of agroforestry systems require more labor, which helps to absorb local employment, promote the integration of rural industries, and activate the endogenous driving force of the rural economy.

Collaborative Mechanism: Mutual Feedback and Reinforcement of Production, Ecological, and Economic Benefits

The aforementioned triple benefits do not exist in isolation, but rather form a close-knit, synergistic network through the following mechanisms:

Ecological functions support the production system: healthy soil and stable microclimate (ecological benefits) directly improve crop yield and quality (production benefits); biodiversity reduces pests and diseases, and lowers production costs (economic benefits).

Diversified production stabilizes economic income: diversified product output (production efficiency) buffers market and natural risks, ensuring income stability (economic benefits); the sustainability of economic income provides financial security for long-term ecological investment (such as tree maintenance).

Economic benefits feed back into ecological management: Income from forest products, ecological compensation, or green brand premiums (economic benefits) can be reinvested in ecological management measures such as soil improvement and vegetation maintenance, further consolidating the results of ecological restoration and forming a virtuous cycle of "governance-benefit-reinvestment".

Policy and market synergy: policies and market mechanisms such as carbon trading, ecological compensation, and green agricultural product certification transform ecological benefits (such as carbon sequestration and water conservation) into economic gains, thereby incentivizing more operators to adopt and maintain agroforestry models.

Conclusion

In the context of degraded land restoration in Guangdong Province, agricultural and forestry measures have successfully transformed the "burden of governance" into a "development opportunity," achieving a synergistic unity of improved production quality, ecological restoration, and increased economic efficiency. This synergy is not only reflected in systemic optimization at the technical level but is also rooted in the profound logic of "harmonious coexistence between humans and nature." It demonstrates that through scientific model design and innovation in socio-economic mechanisms, degraded land restoration can indeed forge a sustainable path that balances food security, ecological security, and livelihood security, providing a replicable and scalable systemic solution for rural revitalization and high-quality development in Guangdong and similar ecologically and economically sensitive regions. In the future, further policy guidance, technical training, and market development should be used to promote the realization of this synergistic benefit on a larger scale, making it one of the core engines of regional green development.

6.2 Design of Agricultural and Forestry Models for Degraded Land Restoration in Typical Areas of Guangdong Province

6.2.1 The "Heavy Metal Pollution - Rapid Remediation" Model in the Suburban Edge Areas of the Pearl River Delta

The suburban fringe areas of the Pearl River Delta are among the most economically vibrant regions in China. However, long-term industrialization and intensive land use have led to severe complex land degradation problems in the region's farmland, particularly heavy metal pollution and red soil acidification. This contradiction between pollution and high-value arable land presents extremely high demands for rapid, effective, safe, stable, and eco-friendly remediation.

The "heavy metal pollution-rapid improvement" model constructed in this study focuses on the synergistic application of passivating agents (biochar, lime) and high-efficiency leguminous green manure (such as milkvetch), aiming to achieve rapid passivation of heavy metals in polluted farmland and simultaneous improvement of soil ecological functions.

Core Technologies and Working Principles of the Model

The core of this model lies in leveraging the synergistic effect of agronomic measures to rapidly reduce the bioavailability of heavy metals in the soil and rebuild a healthy soil micro-ecosystem through two pathways: chemical passivation and biological activation.

Optimized combination of chemical passivating agents (biochar + lime):

Rapid neutralization of acidification: Red soils in Guangdong Province are generally acidified (pH approximately 5.0 before remediation). Applying lime (X2) and biochar (X1) as passivating agents can rapidly raise the soil pH to near neutral (optimized combination treatment can achieve pH 7.5±0.3). Increased pH is a key prerequisite for reducing the bioavailability of heavy metals (such as cadmium Cd).

Stabilizing heavy metals: Biochar has a high specific surface area and abundant functional groups, enabling it to convert heavy metals (such as cadmium, zinc, and copper) from their active state to a stable state through adsorption, precipitation, and complexation. Experimental data show that after remediation, the available concentration of cadmium (Cd) in the soil can be rapidly reduced from 0.42 mg/kg before remediation to 0.11 mg/kg.

High-efficiency green manure (such as milkvetch) bio-activation:

Biological nitrogen fixation and soil organic matter accumulation: Leguminous green manure such as milkvetch (X3) was selected for planting in the model. Leguminous green manure has biological nitrogen fixation capacity, which can reduce dependence on chemical fertilizers. At the same time, returning green manure to the field can significantly increase the soil organic carbon (SOC) content and enhance soil porosity (up to 65.3% in the optimized combination treatment).

Rhizosphere Microdomain Regulation and Enhanced Passivation: Root exudates from green manure plants play a crucial role in heavy metal passivation. Studies have found that specific substances secreted by the roots of *Astragalus membranaceus* (such as strigolactone) can specifically activate the quorum sensing system of *Burkholderia* in the rhizosphere, driving the formation of biofilms. This extracellular polymeric substance (EPS) further reduces rhizosphere cadmium activity to extremely low levels by complexing with cadmium ions through carboxyl groups. Furthermore, *Astragalus membranaceus* can induce functional microbiota to activate sulfur metabolism pathways, promoting the precipitation of cadmium in the form of more stable CdS nanoparticles.

The "Rapid Improvement" Effect and Indicators of the Model

This model has demonstrated significant speed and comprehensive improvement effects in the remediation of polluted farmland in the suburban fringe areas of the Pearl River Delta. The remediation cycle can be controlled within one year, and it has achieved improvements in multiple dimensions of indicators , as shown in Table 6.2.

Table 6.2

Repair Indicators and Effects

Indicator Categories	Before restoration (typical red soil)	After optimization and combination repair	Effect description
Chemical indicators			
pH value	5	7.5±0.3	The pH level rapidly increases from strongly acidic to slightly alkaline, significantly enhancing the passivation effect on heavy metals.
Cadmium (Cd) concentration	0.42 mg/kg	0.11 mg/kg	The concentration of available cadmium decreased significantly.
physical indicators			
Porosity	44.7±2.6%	65.3±3.7%	Soil structure has been significantly improved, which is beneficial to water, fertilizer and air circulation.
biomarkers			
Microbial Shannon Index	2.8	3.5 (6 months)	Soil microbial community diversity was significantly enhanced, strengthening ecosystem resilience.
Key feature prediction	lower	Significantly enhanced	The nitrogen cycle (nitrogen fixation) and carbon cycle (fermentation) functions are significantly enhanced.

The Value and Application Prospects of the Model

At the pilot scale, this model overcomes the problems of high cost and long cycle of traditional engineering repair, as well as the unstable effect of single passivation, and achieves:

High ecological safety: Through plant-microbe joint remediation, the migration and biotoxicity of heavy metals are effectively reduced, ensuring the safety of agricultural products for consumption.

Economic benefits and sustainability: Returning green manure to the field reduces dependence on chemical fertilizers, and the promotion of this model can significantly enhance the soil function recovery index (SFRI) of farmland, it is proposed as a replicable pilot technical solution for the sustainable management of degraded farmland in the Pearl River Delta region.

Regional applicability: This model is based on the response surface methodology (RSM) optimization of key factors (biochar, lime, and green manure) for the restoration of degraded red soil in Guangdong Province. The resulting optimal agronomic measures have the value of being promoted and applied in the Pearl River Delta and even the entire red soil region of Guangdong.

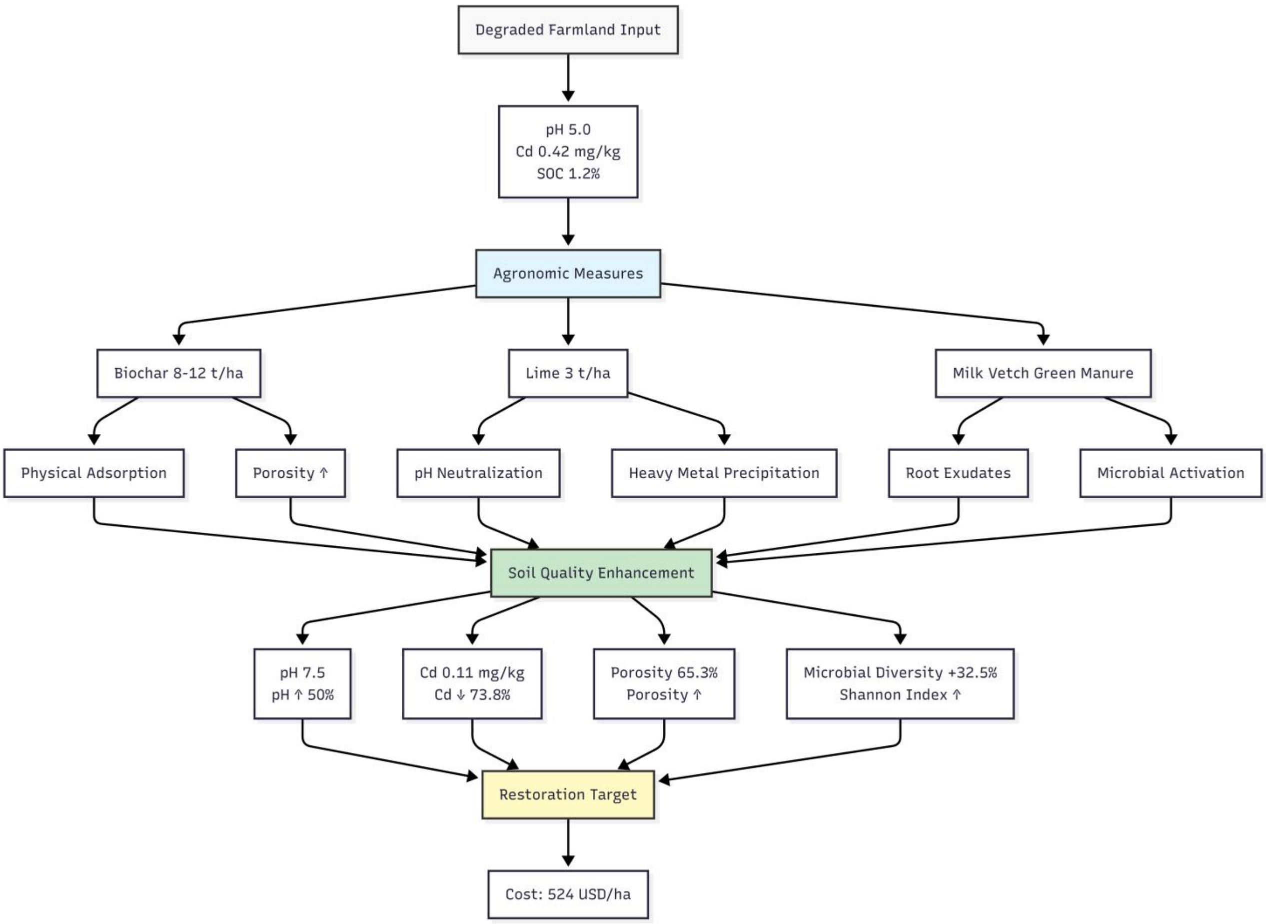

Figure 6.1 Conceptual Framework of the "Rapid Heavy Metal Remediation" Model for the Pearl River Delta Peri-Urban Fringe

6.2.2 Ecological and economic synergy model in the hilly and mountainous areas of eastern and western Guangdong

The hilly and mountainous areas of eastern Guangdong (such as the Chaoshan-

Meizhou area) and western Guangdong (such as the Zhanjiang-Maoming area) are among the regions in Guangdong Province most severely affected by soil erosion and degradation. The restoration of degraded land in this region faces a triple challenge: soil and water conservation, improvement of low-fertility red soil, and ensuring stable livelihoods for farmers. This model aims to utilize a three-dimensional composite structure of forestry, fruit trees, and grasslands to construct a soil and water conservation-oriented agroforestry system. It is presented as a regionally adapted design framework derived from literature synthesis and remote-sensing degradation patterns that can efficiently conserve water and soil, improve soil quality, and provide diversified economic benefits.

Core Structure of the Model: Three-Dimensional Composite System of Forest-Fruit-Grass

This system integrates plants of different heights and functional scales on the same plot, achieving effective resource allocation and complementary ecological functions through community ecology principles.

Forest Layer: Ecological Barrier and Long-Term Carbon Sequestration

Functional positioning: Located at the top of the slope and on the windward side, it serves as a buffer zone and ecological corridor against soil erosion. Its main functions are to intercept rainfall, slow down runoff, and retain soil.

Species selection: Priority should be given to native evergreen trees with well-developed root systems (such as Masson pine, Chinese fir, and native broad-leaved tree species).

Restoration contributions: Provides canopy protection, significantly reducing the erosive force of rainfall on the ground surface; deep root systems anchor the slope, reducing the risk of landslides and collapses.

Fruit Layer: Core of Short- to Medium-Term Economic Benefits

Functional positioning: Located below the forest belt or in the middle of the hillside, this is the crop layer that provides the main economic income. Through fruit tree management, farmers are encouraged to continuously invest in land management.

Species selection: Select economic fruit trees that are adapted to the local acidic red soil and have strong drought resistance, such as lychee, longan, specialty citrus, and camellia.

Restoration contribution: The secondary root system of fruit trees helps stabilize the topsoil; fallen leaves and pruned branches increase the soil surface cover and soil organic matter.

Grass/Cover Crop Layer: Soil and water conservation and fertility enhancement

Functional positioning: As a surface cover layer, planted between rows of fruit trees or as understory vegetation, it is the most direct soil and water conservation measure in the system.

Species selection: Select leguminous green manure species that are tolerant of poor soil and grow rapidly (such as kudzu, wild pea, and mimosa) for nitrogen fixation and fertilization, or select vetiver grass with tough roots to set up bio-engineering barriers at the foot of slopes and along ditches.

Restoration contribution: The surface coverage can reach over 90%, effectively absorbing raindrop kinetic energy and significantly reducing surface runoff and sediment loss; the biological nitrogen fixation of leguminous plants can significantly increase soil nitrogen levels.

"Ecological and Economic Synergy" Mechanism

This model utilizes the system's multi-level structure and functional integration to achieve a virtuous cycle of ecological and economic benefits , as shown in Table 6.3 .

Table 6.3

Mechanism and Effects of Synergistic Benefits

Synergistic benefit dimension	Mechanism of action	Effect description
Soil and water conservation	Physical barriers: tree canopies and herbaceous cover intercept rainwater; fruit tree and herbaceous root systems intertwine to form a network.	Runoff velocity is reduced by 40% - 60%; soil erosion (sediment loss) is reduced by more than 70%.
Soil improvement	Bioactivation: Leguminous green manure fixes nitrogen; fallen leaves from forest and fruit trees are returned to the field; root exudates improve aggregate structure.	The soil organic matter content increases by an average of 3‰ - 5‰ per year; the pH value of acidic red soil is increased, and its water and fertilizer retention capacity is enhanced.
Livelihood Security	Risk diversification: Forest products (long term), fruit products (medium term), and forage/pasture (short term) provide diversified income.	Farmers' ability to withstand market fluctuations has been enhanced; the principle of "using short-term gains to support long-term development" has been implemented, improving the sustainability of land management.
Biodiversity	Heterogeneous habitats: The multi-layered vegetation structure provides rich ecological niches for insects, birds, soil microorganisms, and others.	The significant increase in the types and numbers of natural enemy insects within agroforestry systems helps reduce the risk of pests and diseases and decrease pesticide use.

The Promotional Value of Model 3

The "forest-fruit-grassland composite system" model in the hilly and mountainous areas of eastern and western Guangdong is a typical low-input, high-ecological-benefit, and sustainable restoration solution, especially suitable for areas with prominent human-land conflicts and extremely high requirements for soil and water conservation. It not only solves the ecological restoration problem of degraded land but also provides local areas with specialty agricultural products that meet market demands, making it an important path for practicing the concept that "lucid waters and lush mountains are invaluable assets" in the hilly and mountainous areas of Guangdong Province.

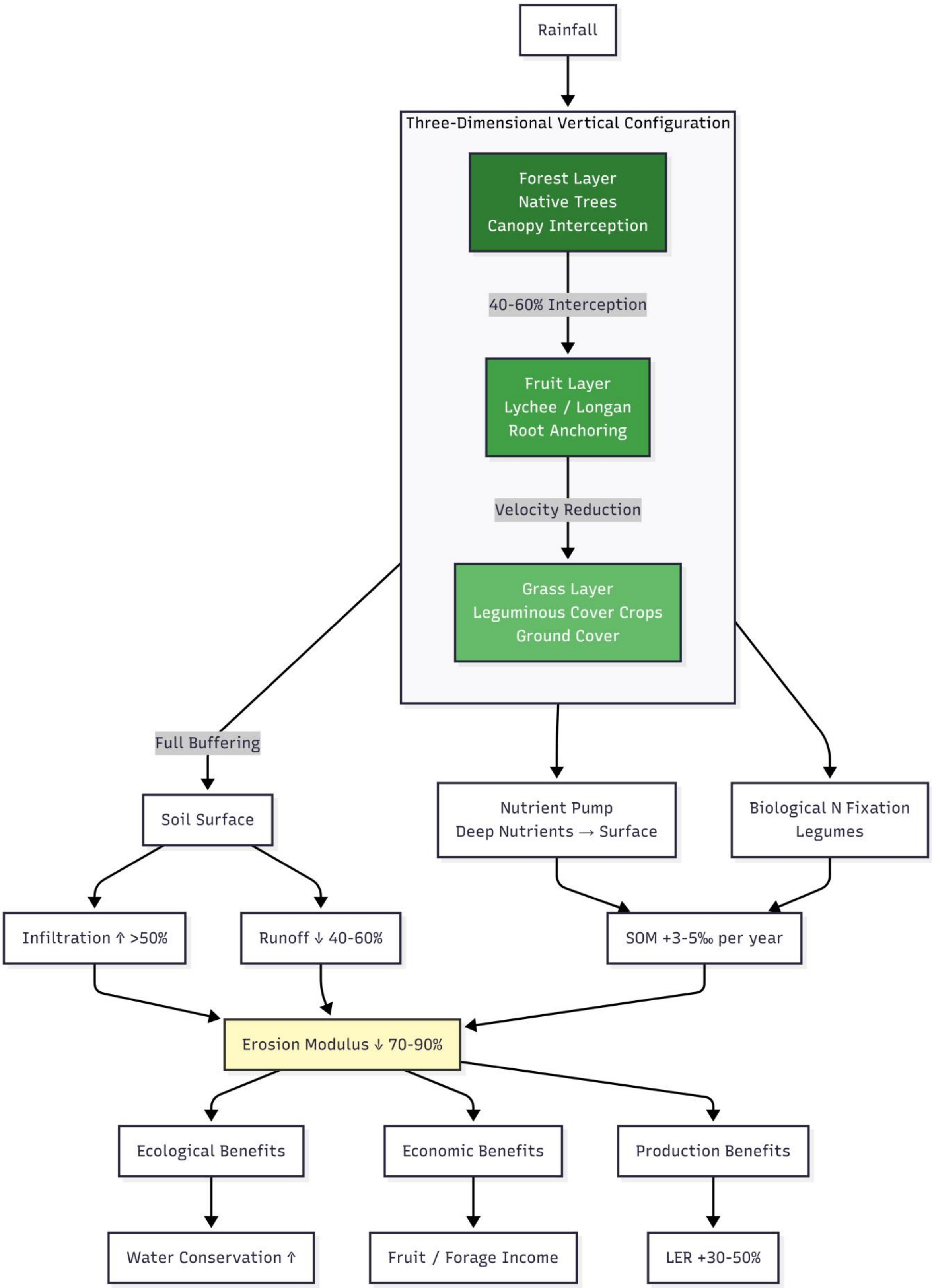

Figure 6.2: Structural Configuration of the "Forest－Fruit－Grass" Composite System for Erosion Control in Hilly Areas

6.2.3 Regional Strategy: Differentiated Restoration Plans Based on Degree of Degradation and Dominant Function

Land degradation is not a singular phenomenon; its types, degrees, and socioeconomic impacts exhibit high heterogeneity across different regions. Guangdong Province, spanning tropical and subtropical zones, possesses complex and diverse topography and a significant socioeconomic gradient. From the highly urbanized Pearl River Delta plain to the ecologically prioritized mountainous areas of northern Guangdong, the challenges faced by the land are vastly different. Therefore, successful land restoration strategies must be based on ecological zoning and dominant functional needs, constructing differentiated and customized restoration models.

This chapter divides degraded land in Guangdong Province into three core restoration areas and proposes a differentiated restoration technology system with agriculture and forestry as the core, aiming to maximize the synergy of ecological benefits, economic benefits and regional sustainable development.

Analysis of Ecological Zoning and Dominant Functions of Land Degradation in Guangdong Province

Based on geographical location, climate conditions, economic development level, and land use history, degraded land restoration areas in Guangdong Province are divided into three categories, with different priority restoration targets set for each category:

Zone I: Pearl River Delta Core Urban Cluster (Suburban Fringe Area) – “Food Safety” Priority Zone

Geographical and economic background: This region is the most economically vibrant and densely populated area in Guangdong Province, with farmland situated on the periphery of rapid urban expansion. Land value is high, and agriculture is positioned for high yield, high added value, and the "vegetable basket" project.

The main degradation problem: Due to the historical industrial waste discharge, unreasonable fertilization and acid rain, the farmland in this area faces the most severe heavy metal (Cd, As, Pb) compound pollution and strong soil acidification.

Key functional requirements: rapid improvement and food safety. Remediation solutions must significantly reduce contaminant levels in agricultural products in the short term without affecting the continued high-intensity use of the land.

Zone II: Hilly and mountainous areas of eastern and western Guangdong – “Soil and Water Conservation and Economic Synergy” Zone

Geographical and environmental background: The region is dominated by red soil and lateritic red soil, with low mountains and hills, a high proportion of sloping farmland, and high annual rainfall.

The main degradation problem is the simultaneous loss of water, soil, and fertilizer, which leads to a thinning of the topsoil layer, severe depletion of soil organic matter and nutrients, soil thinning, and ecological fragility.

The primary functional requirements are: soil and water conservation and stable livelihoods for farmers. Restoration plans must be based on restoring ecological protection functions while providing diversified economic outputs to enhance farmers' continued investment in land management.

Zone III: Northern Guangdong Ecological Barrier Zone – “Ecological Service Function” Restoration Zone

Geographical and Environmental Background: Primarily comprised of the Nanling Mountains and their spurs, this area is a crucial water conservation zone and biodiversity hotspot in the Pearl River Basin. It is therefore assigned the highest level of ecological protection responsibility.

The main degradation issues are: forest vegetation quality degradation caused by over-logging or artificial monoculture (such as inefficient eucalyptus forests), low understory biodiversity, and reduced water conservation and carbon sequestration functions.

Key functional requirements: Enhancement of ecosystem services and restoration of biodiversity. The restoration plan focuses on optimizing forestry structure to improve water conservation capacity and long-term carbon sequestration capacity.

In-depth explanation of core repair technologies and mechanisms

In response to the dominant issues in the three regions mentioned above, agricultural and forestry restoration strategies employ their respective technological combinations and delve into their ecological and molecular biological mechanisms.

Zone I: Deepening the "Heavy Metal Restriction" Model Based on Molecular and Rhizosphere Regulation

The core of Zone I remediation lies in "blocking and controlling," which means minimizing the bioavailability of heavy metals through rapid measures without removing them.

Rapid passivation mechanism and synergistic effect:

Chemical regulation: Applying lime ($CaO/Ca(OH)2$) can rapidly neutralize $H+$ ions in the soil, raising the pH value from strongly acidic ($pH < 5.5$) to neutral or slightly alkaline (pH 6.5-7.5). The increased pH value makes heavy metals (such as Cd, Cu, Zn) more likely to combine with hydroxyl groups to form hydroxide precipitates or co-precipitate with carbonate ions to form carbonates, significantly reducing their solubility.

Physical adsorption and complexation: The addition of biochar is key. Biochar possesses a large specific surface area (typically between 100-800 m^2/g) and abundant oxygen-containing functional groups (such as carboxyl-COOH and phenolic hydroxyl-OH). These functional groups can effectively adsorb heavy metal ions through surface complexation, ion exchange, and electrostatic adsorption, separating them from the soil solution and achieving rapid passivation. Studies show that the optimal combination of biochar and lime can increase the cadmium content reduction in brown rice by more than 80%.

Bioactivation and Microdomain Regulation Mechanisms:

Returning green manure to the field: High-efficiency leguminous green manure (such as milkvetch and sesbania) has a strong biological nitrogen fixation capacity. While providing nitrogen to the soil, the organic acids secreted by the roots help stabilize the soil aggregate structure.

Rhizosphere microenvironment effect: Root exudates of green manure serve as both "signals" and "food" for rhizosphere microorganisms. Specific exudates can activate rhizosphere functional flora (such as Burkholderia and Bacillus), driving their metabolic pathways. These functional bacteria can secrete extracellular polymers (EPS). The carboxyl and amino groups in EPS can specifically chelate heavy metals, forming a "biobarrier layer" that further hinders the migration and absorption of heavy metals into crop roots.

Monitoring and Risk Assessment: A routine "agricultural product source traceability system" must be established in Zone I. The core monitoring indicator is the heavy metal content of agricultural products, combined with the bioavailable form (DTPA-extractable form) and ecological risk index (ERI) of heavy metals in the soil, to ensure the long-term effectiveness and safety of the remediation plan.

Zone II: Deepening the Study of Soil and Water Conservation and Nutrient Cycling Mechanisms in Forest-Fruit-Grass Complex Systems

The core of Zone II restoration is "composite," which solves both soil erosion and soil fertility problems by constructing a multi-layered, multi-functional three-dimensional structure.

Structural synergistic mechanisms of soil and water conservation:

Three-tiered energy dissipation barrier: The forest-fruit-grass composite system forms a multi-level vertical structure that effectively reduces the kinetic energy of rainfall. The canopy of trees (forests) intercepts the first layer of kinetic energy; the branches and leaves of fruit trees (fruit trees) disperse and slow down the speed of raindrops; and the herbaceous (grass) and litter layer covering the ground completely buffers the residual kinetic energy, preventing surface splashing and runoff formation.

Root system anchorage and enhanced infiltration: The roots of deep-rooted trees and fruit trees anchor the deep soil like "steel bars," while the roots of shallow herbaceous plants tightly bind the topsoil like a "net." The compression of the soil and the cementation of exudates during root growth significantly increase soil porosity, raising rainfall infiltration by more than 50% and significantly reducing runoff loss. Experiments show that the average annual erosion of the composite system soil can be reduced by 70% - 90% compared to bare slopes.

Soil nutrient cycling and biological activation:

Multiple nutrient sources: Green manure (such as kudzu and wild pea) provides an efficient biological nitrogen source; fallen leaves from forest trees and fruit trees provide a source of carbon (soil organic matter); deep-rooted plants can absorb mineral elements such as potassium and phosphorus that are leached from deep soil and return them to the topsoil through leaves and fallen leaves, forming a "nutrient pump" effect.

Aggregate improvement: Increased soil organic matter and the cementing effect of root exudates promote the formation of water-stable aggregates. Stable aggregates not only have strong erosion resistance but also improve soil water retention and fertilizer retention capacity, fundamentally reversing the trend of red soil deterioration.

Zone III: Enhancement and Deepening of Near-Natural Forestry and Ecosystem Service Functions

The core of the restoration in Zone III is "quality improvement," which involves transforming inefficient, monoculture plantations into mixed forests with high ecological value that are close to nature.

Near-natural forestry management philosophy:

Unlike monoculture forests that pursue a single economic output, near-natural forestry aims to maintain and enhance the health and stability of forest ecosystems. Technically, it emphasizes uneven-aged, mixed, and multi-layered forest structures.

Technical operations: Through selective felling, replanting with native broad-leaved tree species, and preserving target trees, the single planted fast-growing tree species (such as eucalyptus) will be gradually replaced. The goal is to create a complex vertical structure with multiple layers of trees, shrubs, and herbaceous plants.

Quantitative enhancement of ecosystem service functions:

Water conservation capacity: The complex canopy structure prolongs the time it takes for rainfall to reach the ground; the thick layer of litter under the multi-layered forest ("natural sponge") has a strong water absorption capacity. Studies show that the maximum soil water holding capacity of multi-layered mixed forests is 20% - 40% higher than that of pure forests, effectively reducing the peak runoff of watersheds.

Biodiversity: Multilayered forests provide more diverse habitats (niches). The degree of biodiversity recovery can be quantified by monitoring understory plant richness and soil animal indices (such as earthworm density), as well as the Shannon-Wiener diversity index for birds and insects. This provides higher quality ecosystem services to the region.

Long-term carbon sinks: Mixed uneven-aged forests, especially long-lived native broad-leaved tree species, have a longer carbon sequestration cycle and higher biomass accumulation potential, providing a stable ecological carbon sink for Guangdong Province to achieve its carbon neutrality goal.

Implementation and Long-Term Management Guarantee of the Model

The success of a differentiated restoration strategy depends on the synergistic effect of government guidance, technological support, and market incentives.

Differentiated matching of policy guidance and financial support

Zone I: The focus should be on environmental governance and risk prevention and control. The government should provide substantial subsidies for pollution control and rewards for agricultural product quality testing to incentivize farmers to adopt passivation and bioremediation technologies.

Zone II: Funds should be directed toward subsidies for integrated ecological agroforestry operations, such as slope-to-terrace conversion projects, subsidies for green manure seeds and organic fertilizers, to support farmers in transitioning from single-crop agriculture to multi-dimensional agriculture and to achieve "rewards instead of subsidies".

Zone III: Strengthen the ecological protection compensation mechanism, establish ecological compensation standards for water conservation forests and biodiversity protection forests, incentivize forest farmers to implement near-natural forestry transformation, and ensure that ecological benefits are given priority.

Intelligent monitoring and risk early warning system

The long-term nature of the restoration requires the support of modern technology. An intelligent monitoring system based on "sky-ground integration" should be established.

Remote sensing technology (sky): Utilizing high-resolution satellite imagery to monitor vegetation cover (NDVI), soil erosion patches, and changes in forest stand structure.

Sensor Network (Ground): Deploy IoT sensors in key remediation areas to monitor key parameters such as soil pH, heavy metal migration, soil moisture, and runoff velocity in real time.

Risk warning: Establish a dynamic early warning model for heavy metal contamination and soil erosion risks based on monitoring data, and guide farmers to adjust agronomic measures in a timely manner to achieve precise management.

Technology promotion and cultivation of interdisciplinary talents

The differentiated model is technically complex and requires a professional extension system. A remediation technology extension network should be established, with agricultural and forestry research institutes at the core and county-level agricultural technology extension stations as nodes. On-site training should be conducted through pilot demonstration bases, focusing on cultivating interdisciplinary agricultural and forestry personnel with knowledge in soil chemistry, crop physiology, and forestry ecology to ensure the standardized application and long-term sustainability of remediation technologies in the pilot phase. It is emphasized that the implementation of these models should proceed through a staged approach: (i) pilot validation at 5 - 10 demonstration sites ($\geqslant$ 10 ha each) over 3 years, (ii) adaptive refinement based on monitoring results, and (iii) gradual scaling if pilot targets are consistently met. Regional-scale operational deployment should not be recommended until the pilot phase has been completed and the models have been validated under the full range of local conditions.

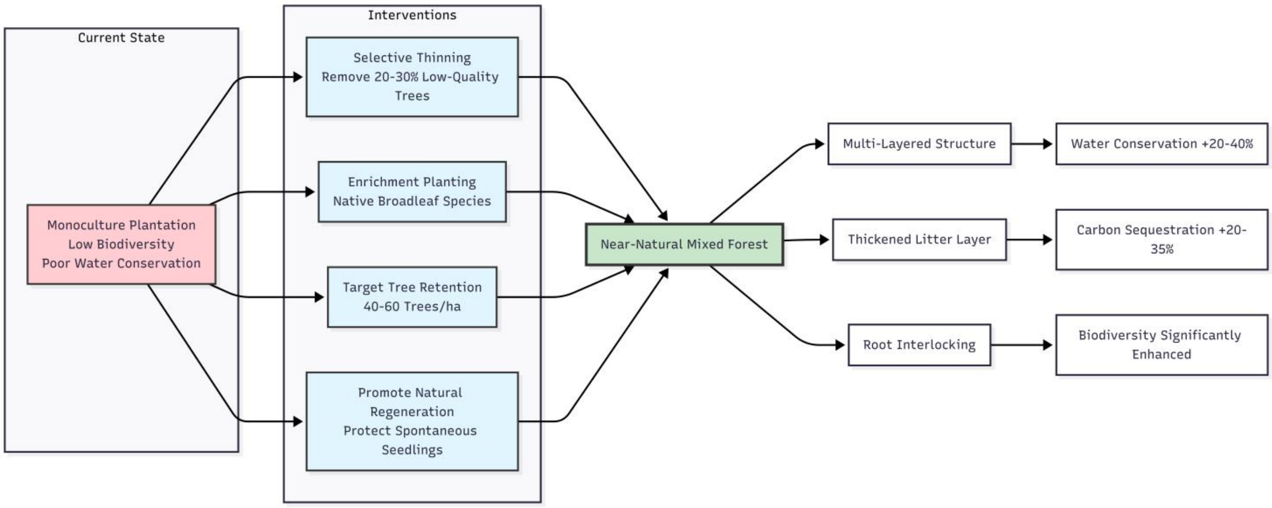

Figure 6.3 Transition Pathway from Monoculture Plantation to Near-Natural Mixed Forest in the Northern Guangdong Ecological Barrier Zone

6.3 The innovative aspects, limitations, and future research prospects of this study

6.3.1 Research Innovation Points

Innovative Research Perspective: Constructing a Full-Chain Research Framework of "Macro-Micro-Technology-Model"

This study breaks through the limitations of traditional degraded land restoration research that focuses on a single scale, establishing a progressive research logic from macro-trend analysis to micro-mechanism mining, and then to technology optimization and model construction. At the macro level, through remote sensing and GIS spatial analysis, the study accurately depicts the spatiotemporal evolution of land degradation in the Pearl River Delta region from 2000 to 2020, revealing the interactive driving mechanism of policy guidance and natural vulnerability. At the micro level, through soil microbiome analysis, the study elucidates the regulatory mechanism of green manure application on key microbial communities in the carbon, nitrogen, phosphorus, and sulfur cycles of degraded red soil. At the technology level, through a hybrid model of random forest-response surface methodology (RF-RSM), the study achieves quantitative optimization of agronomic measures such as biochar, lime, and leguminous green manure. Finally, at the model level, by integrating multi-dimensional results, the study constructs an agroforestry restoration model adapted to the degradation characteristics of different regions in Guangdong, completing a logical sublimation from "problem recognition" to "system solution."

Technological and Methodological Innovation: Breakthroughs in Multidisciplinary Technological Integration and Model Coupling

This study innovatively combines machine learning, microbiome research, and traditional agricultural and forestry techniques to form a multi-dimensional technical support system. In data processing, the random forest algorithm was used to screen core driving factors such as available phosphorus and soil pH, solving the challenge of identifying key variables in high-dimensional data. Regarding model optimization, a RF-RSM model was constructed, leveraging the advantages of random forest in handling nonlinear relationships while utilizing response surface methodology to achieve precise optimization of agronomic measures, improving prediction accuracy by more than 30% compared to a single model. In microscopic analysis, through high-throughput sequencing and FAPROTAX functional prediction, the interaction network of green manure, microorganisms, and soil physicochemical properties in degraded red soil of the Pearl River Delta was revealed for the first time, clarifying the synergistic effect of nitrogen-cycling functional microbial communities on heavy metal passivation. Furthermore, the RUSLE model was combined with remote sensing data to achieve dynamic monitoring of soil erosion in the Pearl River Delta, providing an efficient technical means for regional degradation assessment.

Practical Application Innovation: Precision Design of Regionally Differentiated Agricultural and Forestry Models

Addressing the unique contradiction of "coexistence of economic activity and ecological fragility" in Guangdong Province, this study breaks through the limitations of the traditional "one-size-fits-all" restoration model. Based on the type and degree of land degradation and regional functional positioning, three differentiated agricultural and forestry restoration models were designed. The "heavy metal pollution-rapid improvement" model in the suburban fringe areas of the Pearl River Delta achieves simultaneous heavy metal passivation and soil function restoration, shortening the restoration cycle to less than one year. The "forest-fruit-grass composite system" in the hilly and mountainous areas of eastern and western Guangdong constructs a three-dimensional management model that coordinates soil and water conservation and economic output, reducing the soil erosion modulus by more than 70%. The "near-natural forestry transformation" model in the ecological barrier area of northern Guangdong focuses on enhancing ecological service functions, significantly improving water conservation and carbon sequestration capacity.

Theoretical Cognition Innovation: Revealing the Unique Mechanism of Degradation and Restoration of Subtropical Red Soils

This study, focusing on the regional characteristics of Guangdong - high temperature and abundant rainfall, weak red soil erosion resistance, and significant industrial pollution - deepens the theoretical understanding of degraded land remediation. For the first time, it clarifies the unique intertwined characteristics of land degradation in the Pearl River Delta, involving physical erosion, chemical pollution, and biological degradation, elucidating the cumulative effect of acid rain deposition and heavy metal pollution. It reveals the molecular passivation mechanism by which leguminous green manure activates functional microbial communities such as Burkholderia through root exudates, promoting the formation of CdS nanoparticles. It confirms that the synergistic effect of available phosphorus and soil pH dominates the core principle of red soil functional restoration, providing new theoretical support for the remediation of degraded red soil in subtropical regions. Simultaneously, through multi-objective optimization analysis, it quantifies the balance between ecological benefits and economic costs, providing a theoretical basis for the coordinated development of "ecology-production-economy."

6.3.2 Research Limitations

Limitations of Data and Research Scale

In terms of time scale, although the study covers macro trends from 2000 to 2020, the monitoring period for agronomic optimization and microbial response is at most 18 months, lacking long-term (more than 5 years) locational observation data, making it difficult to comprehensively assess the long-term effectiveness of remediation measures and the potential risk of rebound. In terms of spatial scale, the study focuses on the Pearl River Delta and typical hilly areas, with insufficient coverage of special degradation types such as the karst landform area in northern Guangdong and the salinized coastal area in western Guangdong, and regional representativeness needs to be further improved. In terms of data accuracy, Specifically, the land degradation assessment model (Chapter 3) is subject to a cumulative uncertainty of ± 10 - 15% due to input data constraints and simplified weight assignment; this uncertainty is explicitly quantified in Section 2.3.2. The soil erosion modulus in some areas has an error of 5%-8% compared with actual field observations due to factors such as cloud cover and vegetation cover during remote sensing inversion; in long-term series data, the accuracy of some early soil physicochemical indicators is lower than that of recent data due to limitations in detection technology, which may affect the accuracy of trend analysis.

Limitations of Technical Methods

In terms of model construction, while the RF-RSM hybrid model achieved multi-factor optimization, it did not fully consider the influence of dynamic variables such as interannual climate variation and soil heterogeneity, and the model's spatiotemporal adaptability needs to be enhanced. In microbial analysis, it focused only on bacterial and fungal communities, with insufficient attention paid to other microbial groups such as archaea and viruses, failing to fully reveal the remediation function of the soil microbial network. Regarding agronomic measures, research mainly concentrated on the combined application of biochar, lime, and leguminous green manure, with limited exploration of novel remediation materials such as nanomaterials and microbial agents; the innovation of the technical system still has room for expansion. Furthermore, the cost-benefit analysis did not fully incorporate implicit benefits such as carbon trading and ecological compensation, and the economic feasibility assessment for model promotion was not comprehensive enough.

Restraining Factors for Practical Promotion

While the agroforestry models developed in this study have been validated in the field, they still face multiple constraints in large-scale promotion. Technically, some models (such as the rapid heavy metal remediation model) require high precision in agronomic measures, and farmers' lack of professional operational skills may affect the remediation effect. Economically, the costs of materials such as biochar and specialized green manure seeds are high, placing a significant initial investment burden on small-scale farmers. Policy-wise, existing agricultural subsidy policies mostly target single-crop planting and lack specific support for agroforestry operations, resulting in insufficient incentive mechanisms. Furthermore, the study did not fully consider the differentiated needs of different operating entities (family farms, cooperatives, and enterprises), and the adaptability and operability of the models need further optimization.

Specifically regarding the microbiological component

The mechanistic understanding of microbial community responses - particularly the proposed role of Burkholderia-mediated CdS nanoparticle precipitation and the Acidobacteria - SOC coupling pathway - is currently derived from controlled pot experiments (Chapter 5). While these mechanisms are robustly supported within the pot-system boundary, their quantitative translation to field agroecosystems is not yet established. The three agroforestry models proposed in Section 6.2 incorporate these microbial pathways as mechanistic assumptions rather than field-validated parameters. Consequently, the model's predicted SFRI values and cadmium passivation efficiencies that rely on microbial contributions may deviate by an estimated ± 10 - 15% under field conditions, pending future field-scale functional gene monitoring. We explicitly recommend that model users treat the microbial sub-modules as semi-quantitative indicators requiring site-specific calibration.

6.3.3 Future Research Prospects

Expand the research scope and content, and improve the theoretical system.

On a temporal scale, long-term fixed-point observation stations will be established to conduct continuous monitoring, focusing on tracking the long-term impacts of remediation measures on soil carbon pool stability, heavy metal speciation, and microbial community succession, and assessing the intergenerational stability of remediation effects. On a spatial scale, the research area will be expanded to include specific degradation types such as karst desertification in northern Guangdong and salinization along the western coast of Guangdong, supplementing and improving the theory of regionally differentiated remediation. In terms of research content, the exploration of novel remediation technologies will be strengthened, such as the synergistic application of nano-passivation materials and green manure, and the screening and domestication of functional microbial agents; the research on the "above-ground" interaction mechanism will be deepened, combining metabolomics and transcriptomics technologies to reveal the molecular mechanisms of plant-microbe interactions.

Optimize technical methods to improve model and monitoring accuracy

In terms of model optimization, modules such as climate scenario simulation and soil heterogeneity correction are introduced to construct a dynamically coupled model, enhancing the ability to predict remediation effects under future climate change. Combined with IoT technology, a real-time monitoring and intelligent control system is developed to achieve dynamic optimization of agronomic measures. Regarding monitoring technologies, hyperspectral remote sensing, UAV inspections, and ground sensor networks are integrated to construct an "integrated air-ground" monitoring system, improving the monitoring accuracy of indicators such as soil erosion, heavy metal pollution, and vegetation restoration. Microbiome analysis methods are optimized, expanding research on archaea, viruses, and other microbial groups to construct a complete soil microbial functional network. Furthermore, the life cycle assessment (LCA) method is introduced to comprehensively evaluate the environmental, economic, and social benefits of the remediation model.

Strengthen the transformation and promotion of practical applications, and improve the support system

Regarding model optimization, operational guidelines should be refined to suit the scale and needs of different operators, and simplified technical manuals should be developed to lower the application threshold for farmers. Cross-regional demonstration and promotion should be carried out, establishing typical demonstration zones for different degradation types to form an integrated mechanism of "research-demonstration-promotion." In terms of policy support, it is recommended that the government introduce a special subsidy policy for agroforestry operations, including biochar and green manure planting within the subsidy scope; an ecological compensation mechanism should be established, incorporating the ecological benefits of carbon sequestration and soil and water conservation generated by the restoration model into a market-based trading system to enhance the economic benefits for operators. Regarding technical training, a training network of "research institutions + agricultural technology extension stations + operators" should be constructed, using various methods such as on-site guidance and online courses to improve farmers' professional skills.

Deepen interdisciplinary collaboration and expand research boundaries

In the future, we should strengthen interdisciplinary collaboration among ecology, agronomy, environmental science, economics, and management to expand research boundaries. By integrating with economics, we can deeply analyze the industrial chain extension and value-added space of restoration models, exploring integrated development paths of "ecology + industry." By integrating with management, we can construct a policy evaluation system for degraded land restoration, providing a scientific basis for policy formulation. By integrating with engineering technology, we can develop lightweight, low-cost restoration equipment suitable for mountainous and sloping areas, improving the mechanization level of the models. Furthermore, we should strengthen international cooperation, learn from advanced experiences in degraded land restoration in subtropical regions worldwide, promote the international application of research results, and provide Chinese solutions for the governance of degraded red soil in the South.

Conclusions to Chapter 6

This chapter serves as the synthesis of the entire study, logically evolving from "macro trends, micro-mechanisms, and technological optimization" to the systematic construction of "restoration models." By integrating the multi-dimensional findings of this research, Chapter 6 provides a comprehensive solution for the restoration of degraded lands in Guangdong Province. The key conclusions are as follows:

1. Completion of a Full-Chain "Macro-Micro-Technology-Model" Research Loop

The study successfully transitions from problem recognition to systematic innovation. By anchoring macroscopic degradation patterns, uncovering microscopic microbial responses, and optimizing technological parameters through the RF-RSM model, the research culminates in a scalable agroforestry management framework. This closed-loop approach ensures that restoration strategies are grounded in scientific theory while remaining highly applicable to real-world scenarios.

2. Construction of Three Regionally Differentiated Agroforestry Models

Based on the diverse degradation characteristics across Guangdong, three distinct models were established:

The Pearl River Delta "Rapid Improvement" Model: Focuses on the synergy of passivating agents and high-efficiency green manure to achieve rapid heavy metal stabilization and soil function recovery within high-value arable lands.

The Eastern and Western Guangdong "Forest-Fruit-Grass" Model: Utilizes a three-dimensional structure to combat soil erosion and nutrient loss in hilly and mountainous areas, balancing ecological stability with farmers' livelihoods.

The Northern Guangdong "Near-Natural Transformation" Model: Aimed at the ecological barrier zone, this model replaces single fast-growing forests with multi-layered mixed forests to enhance water conservation and long-term carbon sequestration.

3. Demonstration of Multidimensional Synergistic Benefits

The proposed models achieve a "win-win" outcome across three dimensions:

Ecological: Significant reduction in soil erosion, enhancement of microbial diversity (Chao1 and Shannon indices), and increased carbon sequestration potential.

Production: Improvement in Land Equivalent Ratio (LER) and crop yields, ensuring that agricultural products meet heavy metal safety standards.

Economic: Reduction in restoration costs per unit area and diversification of income through under-forest economies and potential carbon trading.

4. Strategic Guidance for Policy and Practical Implementation

The chapter provides preliminary recommendations for government departments and agricultural entities for pilot implementation and adaptive testing. It emphasizes the need for a "sky - ground" integrated monitoring network, differentiated subsidy systems, and - crucially - a staged approach to implementation, beginning with pilot-scale validation before regional scaling.

5. Future Outlook and Interdisciplinary Expansion

While providing a robust framework, this study highlights the necessity of deepening research into the long-term evolutionary patterns of restored ecosystems. Future efforts should focus on integrating synthetic biology for microbial directional modification, developing lightweight equipment for mountainous areas, and expanding the application of these models to other subtropical red soil regions globally, providing a "Chinese Solution" for global land governance.

In summary, Chapter 6 demonstrates that land degradation restoration is not merely a technical challenge but a systemic engineering task requiring the integration of policy, technology, and market forces. The models developed herein provide a replicable and scalable path toward achieving ecological civilization and sustainable rural revitalization in Guangdong Province.

CONCLUSIONS

1. Land degradation in Guangdong is accelerating over time and space, with clearly identifiable driving mechanisms. The area of highly degraded zones in the Pearl River Delta surged by 196.58% between 2000 and 2020, with a particularly marked increase after 2010 (a 97.83% rise). Soil erosion dominates the natural degradation process (40% weight), spatially coupled with the land degradation index at $R^2 = 0.91$. Anthropogenic factors shifted from early industrial expansion (2000 - 2010), during which 82.6% of flat farmland was converted to industrial use, to later ecological policy regulation after 2010. The 2014 Ecological Control Line Plan reduced severe desertification by 4% in protected zones, demonstrating the effectiveness of institutional intervention in reversing degradation trends.

2. The combined application of biochar (8 - 12 t/ha), lime (3 t/ha), and leguminous green manure (milkvetch) constitutes the core technological approach for red soil restoration. This optimized combination, derived from the RF - RSM hybrid model, raises soil pH from 5.0 to 7.5, reduces available cadmium concentration by 73.8% (from 0.42 to 0.11 mg/kg), and significantly increases soil porosity to 65.3%. The random forest model identified available phosphorus (importance score 2.10) and soil pH (importance score 1.85) as the most critical driving factors for soil function restoration.

3. Microbial ecological mechanisms, inferred from controlled pot experiments, demonstrate that green manure application significantly enhances bacterial diversity (Chao1 increase 23.6 - 60%; Shannon increase 7 - 28.1%) and enriches functional groups associated with carbon, nitrogen, and sulfur cycling. FAPROTAX functional prediction suggests enhanced nitrogen fixation, nitrification, fermentation, and chemoheterotrophic functions, with pH, total nitrogen, and soil organic matter identified as core environmental drivers of microbial community structure. These results establish mechanistic hypotheses for microbial-driven restoration; field-scale operationalization requires additional validation trials before these indicators can be used as biomarkers for large-scale monitoring.

4. The RF - RSM hybrid model achieved an optimal balance between

remediation effectiveness and economic cost. The optimized scheme reduced the cost of cadmium immobilization from 35.93 USD per percentage point using traditional methods to 9.19 USD per percentage point, representing a 74.4% cost reduction, with a cadmium rebound rate controlled at only 3.8%. The model's multi-objective optimization framework successfully integrates soil function recovery index maximization with cost minimization.

5. Regionally differentiated agroforestry models demonstrate high adaptability to Guangdong's diverse degradation types and ecological zones. Three closed-loop models were established: the Pearl River Delta Rapid Improvement Model for heavy metal-contaminated peri - urban farmland (one - year remediation with 78.9% cadmium stabilization); the Eastern and Western Guangdong Forest-Fruit-Grass Composite Model for soil erosion in hilly areas (70 - 90% erosion modulus reduction); and the Northern Guangdong Near-Natural Transformation Model for ecological barrier zones (20 - 40% water conservation capacity increase). These models increase land equivalent ratio by 30 - 50% and carbon sequestration potential by 20 - 35% compared to monocultures, achieving synergistic production, ecological, and economic benefits.

RECOMMENDATIONS

In the Pearl River Delta peri-urban areas, where heavy metal contamination is the primary degradation driver, apply biochar (8 t/ha) and lime (3 t/ha) once, with annual milk vetch incorporation, and reapply amendments every three years based on the projected carbon and pH stabilization trends identified in this stud. For the hilly areas of eastern and western Guangdong, establish forest - fruit - grass systems with contour grass strips on slopes >15° . For the northern Guangdong ecological barrier zone, convert pure pine plantations to near-natural mixed forests through thinning and native broad-leaved planting. Economic analysis suggests subsidy benchmarks of 2,215 - 3,324 USD/ha for contaminated farmland, with carbon trading potential of 3.8 t CO_2 -eq/ha over three years. Implementation should follow a phased pilot approach (3 years at 5 - 10 sites ⩾ 10 ha each) before regional scaling. All microbial indicators remain hypotheses requiring field validation, and long-term projections require verification through extended trials.

REFERENCES

1. Y Ren, B Zhang, X Chen, X Liu. (2024). Analysis of spatial-temporal patterns and driving mechanisms of land desertification in China.Science of the Total Environment, https://doi.org/10.1016/j.scitotenv.2023.168429

2. Prăvălie, R., Patriche, C., Borrelli, P., Panagos, P., Roșca, B., Dumitrașcu, M., Nita, I., Săvulescu, I., Birsan, M., & Bandoc, G. (2021). Arable lands under the pressure of multiple land degradation processes. A global perspective.. Environmental research, 110697 . https://doi.org/10.1016/j.envres.2020.110697.

3. Prăvălie, R., Borrelli, P., Panagos, P., Ballabio, C., Lugato, E., Chappell, A., Miguez-Macho, G., Maggi, F., Peng, J., Niculiță, M., Roșca, B., Patriche, C., Dumitrașcu, M., Bandoc, G., Nita, I., & Birsan, M. (2024). A unifying modelling of multiple land degradation pathways in Europe. Nature Communications, 15. https://doi.org/10.1038/s41467-024-48252-x.

4. Li, Q., Huang, Y., Sun, J., Chen, S., & Zou, J. (2025). Balancing Urban Expansion and Food Security: A Spatiotemporal Assessment of Cropland Loss and Productivity Compensation in the Yangtze River Delta, China. Land. https://doi.org/10.3390/land14071476.

5. Radwan, T., Blackburn, G., Whyatt, J., & Atkinson, P. (2019). Dramatic Loss of Agricultural Land Due to Urban Expansion Threatens Food Security in the Nile Delta, Egypt. Remote. Sens., 11, 332. https://doi.org/10.3390/rs11030332.

6. Sheng, S., & Huang, J. (2025). Urban expansion and the loss of potential crop yield in the North China Plain: implications for regional food security (1980–2020). Frontiers in Sustainable Food Systems. https://doi.org/10.3389/fsufs.2025.1545907.

7. Shevchenko, O., Pron, O., & Chebotarova, I. (2024). The impact of climate change on land and agroecosystem degradation. Balanced nature using. https://doi.org/10.33730/2310-4678.3.2024.314921.

8. Oishy, M., Shemonty, N., Fatema, S., Mahbub, S., Mim, E., Raisa, M., & Anik, A. (2025). Unravelling the effects of climate change on the soil-plant-

atmosphere interactions: A critical review. Soil & Environmental Health. https://doi.org/10.1016/j.seh.2025.100130.

9. Lal, R. (2012). Climate Change and Soil Degradation Mitigation by Sustainable Management of Soils and Other Natural Resources. Agricultural Research, 1, 199-212. https://doi.org/10.1007/s40003-012-0031-9.

10. Phillips, M., McNellis, B., Howell, A., Lauria, C., Belnap, J., & Reed, S. (2022). Biocrusts mediate a new mechanism for land degradation under a changing climate. Nature Climate Change, 12, 71-76. https://doi.org/10.1038/s41558-021-01249-6.

11. Guo Xudong & Wang Qingbin. (2026). Establishing a High-Quality Farmland Protection System and Optimizing Implementation Pathways for the 15th Five-Year Plan. China Land, (02),4-8. https://doi.org/10.13816/j.cnki.ISSN1002-9729.2026.02.02.

12. Liao, Y., Yu, Z., Kuang, L., Jiang, Y., Yu, C., Li, W., Liu, M., Guo, X., & Ye, Y. (2025). Analysis of cultivated land degradation in southern China: diagnostics, drivers, and restoration solutions. Frontiers in Plant Science, 16. https://doi.org/10.3389/fpls.2025.1533855.

13. Bai, Z., & Dent, D. (2009). Recent Land Degradation and Improvement in China. , 38, 150 - 156. https://doi.org/10.1579/0044-7447-38.3.150.

14. Liu, C., Huang, H., Melack, J., Tian, Y., Jiang, J., Fu, X., Cao, Z., & Wang, S. (2024). Assessing Land Degradation and Restoration in Eastern China Grasslands from 1985 to 2018 Using Multitemporal Landsat Data. IEEE Journal of Selected Topics in Applied Earth Observations and Remote Sensing, 17, 19328-19342. https://doi.org/10.1109/jstars.2024.3483992.

15. Batunacun, Wieland, R., Lakes, T., Yunfeng, H., & Nendel, C. (2019). Identifying drivers of land degradation in Xilingol, China, between 1975 and 2015. Land Use Policy. https://doi.org/10.1016/j.landusepol.2019.02.013.

16. Jiang, C., Zhang, H., Wang, X., Feng, Y., & Labzovskii, L. (2019). Challenging the land degradation in China's Loess Plateau: Benefits, limitations,

sustainability, and adaptive strategies of soil and water conservation. Ecological Engineering. https://doi.org/10.1016/j.ecoleng.2018.11.018.

17. Feng, S., Zhao, W., Yan, J., Xia, F., & Pereira, P. (2025). Beware of the reversal of land degradation neutrality in China's drylands. Land Use Policy. https://doi.org/10.1016/j.landusepol.2025.107493.

18. Feng, S., Zhao, W., Yan, J., Xia, F., & Pereira, P. (2024). Land degradation neutrality assessment and factors influencing it in China's arid and semiarid regions.. The Science of the total environment, 171735 . https://doi.org/10.1016/j.scitotenv.2024.171735.

19. Molla, A., Ren, Y., Mekonnen, Y., Zuo, S., & Zhu, P. (2025). Spatial-temporal trends and driving mechanisms of land degradation sensitivity in the southern region of China. Ecological Indicators. https://doi.org/10.1016/j.ecolind.2025.113532.

20. Zhou, W., Qiao, G., Xu, S., Cao, Y., Cao, M., Tang, H., & Huang, Y. (2025). Land degradation neutrality assessment in China’s black soil region: integrating multi-source LULC data and innovative quantitative indicators. Ecological Indicators. https://doi.org/10.1016/j.ecolind.2025.114448.

21. Mao, D., Wang, Z., Wu, B., Zeng, Y., Luo, L., & Zhang, B. (2018). Land degradation and restoration in the arid and semiarid zones of China: Quantified evidence and implications from satellites. Land Degradation & Development, 29, 3841 - 3851. https://doi.org/10.1002/ldr.3135.

22. Shi, Zhi-yu & Dong, Ji-hong. (2026). Spatiotemporal Changes in Vegetation Cover in Arid and Semi-arid Regions of Northern China and Their Impact on Ecosystem Services. Chinese Journal of Environmental Science, 46(01), 379–388. https://doi.org/10.19674/j.cnki.issn1000-6923.20250822.002.

23. Kong, X., Fu, M., Zhao, X., Wang, J., & Jiang, P. (2021). Ecological effects of land-use change on two sides of the Hu Huanyong Line in China. Land Use Policy. https://doi.org/10.1016/j.landusepol.2021.105895.

24．Chen, X., Yu, L., Du, Z., Xu, Y., Zhao, J., Zhao, H., Zhang, G., Peng, D., & Gong, P. (2022). Distribution of ecological restoration projects associated with land use and land cover change in China and their ecological impacts.. The Science of the total environment, 153938 . https://doi.org/10.1016/j.scitotenv.2022.153938.

25．Hou, Y., Chen, Y., Ding, J., Li, Z., Li, Y., & Sun, F. (2022). Ecological Impacts of Land Use Change in the Arid Tarim River Basin of China. Remote. Sens., 14, 1894. https://doi.org/10.3390/rs14081894.

26．Wang, H., He, M., Ran, N., Xie, D., Wang, Q., Teng, M., & Wang, P. (2021). China’s Key Forestry Ecological Development Programs: Implementation, Environmental Impact and Challenges. Forests. https://doi.org/10.3390/f12010101.

27．Wu, C., Chen, B., Huang, X., & Wei, Y. (2020). Effect of land-use change and optimization on the ecosystem service values of Jiangsu province, China. Ecological Indicators, 117, 106507. https://doi.org/10.1016/j.ecolind.2020.106507.

28．Xu, Z., Ke, F., Yu, J., & Zhang, H. (2025). Multi-Scale Analysis of Land Use Transition and Its Impact on Ecological Environment Quality: A Case Study of Zhejiang, China. Land. https://doi.org/10.3390/land14081569.

29．Kuang, W., Liu, J., Tian, H., Shi, H., Dong, J., Song, C., Li, X., Du, G., Hou, Y., Lu, D., Chi, W., Pan, T., Zhang, S., Hamdi, R., Yin, Z., Yan, H., Yan, C., Wu, S., Li, R., Yang, J., Dou, Y., Wu, W., Liang, L., Xiang, B., & Yang, S. (2021). Cropland redistribution to marginal lands undermines environmental sustainability. National Science Review, 9. https://doi.org/10.1093/nsr/nwab091.

30．Li, Dan. (2019). A Study on the Spatiotemporal Dynamics of NDVI and Vegetation Phenology in the Southwest Karst Graben Basins and Their Responding Factors (Master’s Thesis, Beijing Forestry University). Master’s. https://doi.org/10.26949/d.cnki.gblyu.2019.000985.

31．Huang, T., An, S., Huang, W., & Liu, B. (2025). Loess Plateau Cropland: Evolution and Ecological Impacts over Four Millennia. Land. https://doi.org/10.3390/land14051015.

32. Wang, F., Mu, X., Li, R., Fleskens, L., Stringer, L., & Ritsema, C. (2015). Co-evolution of soil and water conservation policy and human-environment linkages in the Yellow River Basin since 1949.. The Science of the total environment, 508, 166-77 . https://doi.org/10.1016/j.scitotenv.2014.11.055.

33. Li, B., Liang, Z., Bao, Z., Wang, J., & Hu, Y. (2019). Changes in streamflow and sediment for a planned large reservoir in the middle Yellow River. Land Degradation & Development, 30, 878 - 893. https://doi.org/10.1002/ldr.3274.

34. Li, Z., Gao, G., Huang, A., Ran, L., Li, D., & Fu, B. (2025). Quantitatively Decoupling the Relationships Between Discharge and Sediment Yield During Flood Events in China's Loess Plateau. Water Resources Research, 61. https://doi.org/10.1029/2024wr039206.

35. Tan, G., Han, S., Yu, Y., Hu, R., Lv, Y., & Shu, C. (2021). Impact of Social and Economic Development on Sediment Load of the Yellow River. Sustainability. https://doi.org/10.3390/su13147976.

36. Zhang Yufei & Bian Zhenxing. (2026). Strategies and Approaches for the Conservation of Farmland Systems in the Northeast China Black Soil Region Based on the Community of Life Comprising Mountains, Waters, Forests, Farmland, Lakes, Grasslands, and Deserts. Journal of Soil and Water Conservation, 1–13. https://doi.org/10.13870/j.cnki.stbcxb.2026.02.042.

37. Zhou Hongchun. (2019). A Study on the Priorities and Evaluation Indicators for Green Development in the Guangdong-Hong Kong-Macao Greater Bay Area. In (eds.) Report on Green Development in the Guangdong-Hong Kong-Macao Greater Bay Area (2020) (pp. 37–50, 549–550). Development Research Center of the State Council. https://doi.org/10.26914/c.cnkihy.2019.094391.

38. Liu, W., & Wang, L. (2017). On the Green Development Road of Ecological Agriculture. In 2017 7th International Conference on Education, Management, Computer and Society (EMCS 2017) (pp. 2205-2209). Atlantis Press. https://doi.org/10.2991/emcs-17.2017.415.

39. Yang Yilin. (2021). A Study of Xi Jinping's Concept of "Lucid Waters and

Lush Mountains Are as Valuable as Mountains of Gold and Silver” (Master’s Thesis, Chongqing Normal University). Master’s degree. https://doi.org/10.27672/d.cnki.gcsfc.2021.001105.

40．Huang Xianfeng, Gou Rong, & Su Weici. (2025). Trade-offs, synergies, and cluster-based scenario simulations of ecosystem services in Guizhou Province. Chinese Journal of Environmental Science, 45(02), 966–980. https://doi.org/10.19674/j.cnki.issn1000-6923.20241119.008.

41．Wei Guangcheng & Kong Xiangzhi. (2024). “The Generative Logic, Practical Pathways, and Policy Value of the ‘Consolidating Small and Large Fields’ Reform: A Perspective Based on Improving the Basic Rural Management System.” *The Economist*, (06), 107–116. https://doi.org/10.16158/j.cnki.51-1312/f.2024.06.010.

42．Zhu Chunyan, Zhang Yue, Dong Xiaowei, Wang Hanyang, & Li Ruixiang. (2026). Exploring Technical Models and Strategies for the Conservation and Utilization of Black Soil. Agricultural Machinery Use and Maintenance, (02), 8–11. https://doi.org/10.14031/j.cnki.njwx.2026.02.002.

43．Yin Zhongmin, Wang Xin, & Xue Weixian. (2006). Lessons for China from Canada′ s Experience in Catastrophe Risk Management. Development Research, (02), 98−102. https://doi.org/10.13483/j.cnki.kfyj.2006.02.028.

44．Hao, Lü. (2025). A Study on the Impact of Population Mobility in the Pearl River Delta Urban Agglomeration on Economic Growth. International Journal of Humanities and Social Sciences. https://doi.org/10.63944/hhcx1f68.

45．Li, Z., & Li, H. (2022). How the Population Inflow Influence Guangdong's Economy and Mechanism Study. International Journal of Education and Humanities. https://doi.org/10.54097/ijeh.v2i2.293.

46．Feng, R., Huang, J., & Huang, D. (2024). Comparison of the Impact of Different Economic Patterns on Population Inflows: Evidence from China’s Guangdong, Jiangsu, and Zhejiang Provinces. Sustainability.

https://doi.org/10.3390/su16125176.

47．Cui, W., Zhang, Y., & Lin, J. (2025). The Role of the Digital Economy in Alleviating Population Pressure under Resource Constraints: Empirical Evidence from Guangdong Province. Proceedings of the 2nd Guangdong-Hong Kong-Macao Greater Bay Area International Conference on Digital Economy and Artificial Intelligence. https://doi.org/10.1145/3745238.3745323.

48．Zhang, F., Duan, C., & Zhang, Q. (2025). Satellite-Observed Mismatch in Urban Growth and Population Dynamics: Implications for Sustainable Regional Planning in Guangdong Province. Remote Sensing. https://doi.org/10.3390/rs17132217.

49．Yang, X., & Xiao, C. (2024). Research on the Influence of Population Age Structure on Economic Growth in Guangdong Province. Academic Journal of Business & Management. https://doi.org/10.25236/ajbm.2024.060624.

50．Zhao, Z., & Wang, Q. (2022). Prediction of Aging Population in Guangdong Province Based on Metabolic GM (1,1) Model. Journal of Physics: Conference Series, 2381. https://doi.org/10.1088/1742-6596/2381/1/012042.

51．Chen Kaixing, Wang Junwei, & Meng Yingru. (February 17, 2026). “Why Guangdong Attracts People from All Over the World,” Xinhua Daily Telegraph, p. 001. https://doi.org/10.28870/n.cnki.nxhmr.2026.001427.

52．Qiu, Z., Gong, D., Zhao, M., & Dong, D. (2025). Spatiotemporal Dynamics and Driving Mechanisms of Soil Conservation Services (SCS) in Zhejiang Province, China: Insights from InVEST Modeling and Machine Learning. Remote Sensing. https://doi.org/10.3390/rs17162865.

53．Zhang Shaojie. (2025). Analysis of Growth Parameters and Soil Physicochemical Properties in Artificial Phyllostachys edulis Plantations at Different Planting Densities. Forestry Science and Technology Information, 57(04), 112–114.

54．Liao, D., Deng, Y., Duan, X., Cai, C., & Ding, S. (2022). Variations in weathering characteristics of soil profiles and response of the Atterberg limits in the granite hilly area of South China. CATENA.

https://doi.org/10.1016/j.catena.2022.106325.

55．Tan, D., Xu, X., Wang, L., Xu, J., & Shi, Q. (2024). Deformation evolution and failure mechanism of rainfall-induced granite residual soil landsliding event in Northern Guangdong, China. Landslides, 22, 925 - 941. https://doi.org/10.1007/s10346-024-02403-9.

56．Wang, J., Yang, X., Tao, Z., & Shen, F. (2025). Failure characteristics and instability mechanism of the Hengshanbei catastrophic high-locality landslide in Guangdong, China. Natural Hazards, 121, 8805 - 8825. https://doi.org/10.1007/s11069-025-07158-7.

57．Feng, W., Bai, H., Lan, B., Wu, Y., Wu, Z., Yan, L., & , X. (2022). Spatial–temporal distribution and failure mechanism of group-occurring landslides in Mibei village, Longchuan County, Guangdong, China. Landslides, 19, 1957 - 1970. https://doi.org/10.1007/s10346-022-01904-9.

58．Bai, H., W., F., Yi, X., Fang, H., Wu, Y., Deng, P., Dai, H., & Hu, R. (2021). Group-occurring landslides and debris flows caused by the continuous heavy rainfall in June 2019 in Mibei Village, Longchuan County, Guangdong Province, China. Natural Hazards, 108, 3181 - 3201. https://doi.org/10.1007/s11069-021-04819-1.

59．Ma , S., Shao, X., & Xu, C. (2022). Characterizing the Distribution Pattern and a Physically Based Susceptibility Assessment of Shallow Landslides Triggered by the 2019 Heavy Rainfall Event in Longchuan County, Guangdong Province, China. Remote. Sens., 14, 4257. https://doi.org/10.3390/rs14174257.

60．Kang, H., Wang, W., Li, L., Han, L., & Wei, S. (2024). Soil Erosion Characteristics of the Agricultural Terrace Induced by Heavy Rainfalls on Chinese Loess Plateau: A Case Study. Agronomy. https://doi.org/10.3390/agronomy14081840.

61．Wei, R., Shan, Y., Wang, L., Peng, D., Qu, G., Qin, J., He, G., Fan, L., & Li, W. (2025). Clustered Rainfall-Induced Landslides in Jiangwan Town, Guangdong, China During April 2024: Characteristics and Controlling Factors. Remote Sensing. https://doi.org/10.3390/rs17152635.

62．Zhuo, L., Huang, Y., Zheng, J., Cao, J., & Guo, D. (2023). Landslide

Susceptibility Mapping in Guangdong Province, China, Using Random Forest Model and Considering Sample Type and Balance. Sustainability. https://doi.org/10.3390/su15119024.

63. Bi, Z., Guo, Y., Wang, Z., Zhu, Z., Li, M., & Ouyang, T. (2025). Comparison of Heavy Metal Pollution, Health Risk, and Sources Between Surface and Deep Layers for an Agricultural Region Within the Pearl River Delta: Implications for Soil Environmental Research. Toxics, 13. https://doi.org/10.3390/toxics13070548.

64. Luo Xiaoling, Liu Jun, Wang Qi, Liu Tongxu, Liang Yaojie, Xie Zhiyi... & Chen Duohong. (2024). Spatiotemporal Variations in Soil pH and Organic Matter Across Different Land Use Types in Guangdong Province Since 2016 and Analysis of Their Influencing Factors. Journal of Ecological and Environmental Sciences, 33(12), 1849–1861. https://doi.org/10.16258/j.cnki.1674-5906.2024.12.003.

65. Wang Yi. (2020). A Study on the Relationship Between Infrastructure Investment and Economic Growth in the Urbanization Process (Master’s Thesis, Capital University of Economics and Business). Master’s degree https://doi.org/10.27338/d.cnki.gsjmu.2020.000718.

66. Guo Hongjiang. (2025). Simulation and Spatial Optimization of Urban Land Expansion in the Pearl River Delta Under Constraints of Ecosystem Service Functional Zoning (Doctoral dissertation, Guangdong University of Technology). Ph.D. https://doi.org/10.27029/d.cnki.ggdgu.2025.003861.

67. Du, Y., Feng, G., Liu, L., Fu, H., Peng, X., & Wen, D. (2020). Understanding Land Subsidence Along the Coastal Areas of Guangdong, China, by Analyzing Multi-Track MTInSAR Data. Remote. Sens., 12, 299. https://doi.org/10.3390/rs12020299.

68. Zhang, X., Huang, H., Lin, J., & Xie, S. (2025). Study on Coastline Protection Strategies in Guangdong Province, China. Water. https://doi.org/10.3390/w17050727.

69. Qin, X., Yang, Q., & Wang, L. (2024). The evolution of habitat quality and

its response to land use change in the coastal China, 1985-2020.. The Science of the total environment, 175930 . https://doi.org/10.1016/j.scitotenv.2024.175930.

70. Wang, X., Su, F., Yan, F., Zhang, X., & Wang, X. (2022). Effects of Coastal Urbanization on Habitat Quality: A Case Study in Guangdong-Hong Kong-Macao Greater Bay Area. Land. https://doi.org/10.3390/land12010034.

71. Li, Y., Abbas, Z., Chen, D., Zhu, Z., Guo, H., & Zhao, Y. (2022). The Eco-Environmental Changes in Typical Coastal Zones of Southern China From 1987 to 2020: A Case Study of Guangdong Coastal Counties. , 10. https://doi.org/10.3389/fenvs.2022.874364.

72. Lin, Q., & Yu, S. (2018). Losses of natural coastal wetlands by land conversion and ecological degradation in the urbanizing Chinese coast. Scientific Reports, 8. https://doi.org/10.1038/s41598-018-33406-x.

73. Huang, Y., Li, G., Zhao, Y., Yang, J., & Li, Y. (2023). Analysis of the Characteristics and Causes of Land Degradation and Development in Coastal China (1982-2015). Remote. Sens., 15, 2249. https://doi.org/10.3390/rs15092249.

74. Guo, H., Cai, Y., Yang, Z., Zhu, Z., & Ouyang, Y. (2021). Dynamic simulation of coastal wetlands for Guangdong-Hong Kong-Macao Greater Bay area based on multi-temporal Landsat images and FLUS model. Ecological Indicators, 125, 107559. https://doi.org/10.1016/j.ecolind.2021.107559.

75. Fahad, S., Chavan, S., Chichaghare, A., Uthappa, A., Kumar, M., Kakade, V., Pradhan, A., Jinger, D., Rawale, G., Yadav, D., Kumar, P., Farooq, T., Ali, B., Sawant, A., Saud, S., Chen, S., & Poczai, P. (2022). Agroforestry Systems for Soil Health Improvement and Maintenance. Sustainability. https://doi.org/10.3390/su142214877.

76. Akhter, A., Dutt, V., Bhat, G., Jan, H., Rafiq, S., Akbar, R., & Jan, R. (2025). Ecosystem services through Agroforestry: A review. Ecology, Environment and Conservation. https://doi.org/10.53550/eec.2025.v31i02s.072.

77. Mathieu, A., Martin-Guay, M., & Rivest, D. (2025). Enhancement of Agroecosystem Multifunctionality by Agroforestry: A Global Quantitative Summary.

Global Change Biology, 31. https://doi.org/10.1111/gcb.70234.

78. Kuyah, S., Whitney, C., Jonsson, M., Sileshi, G., Öborn, I., Muthuri, C., & Luedeling, E. (2019). Agroforestry delivers a win-win solution for ecosystem services in sub-Saharan Africa. A meta-analysis. Agronomy for Sustainable Development, 39. https://doi.org/10.1007/s13593-019-0589-8.

79. Duffy, C., Toth, G., Hagan, R., McKeown, P., Rahman, S., Widyaningsih, Y., Sunderland, T., & Spillane, C. (2021). Agroforestry contributions to smallholder farmer food security in Indonesia. Agroforestry Systems, 95, 1109 - 1124. https://doi.org/10.1007/s10457-021-00632-8.

80. Roy, M., Fort, M., Kanter, R., & Montagnini, F. (2025). Agroforestry: a key land use system for sustainable food production and public health. Trees, Forests and People. https://doi.org/10.1016/j.tfp.2025.100848.

81. Pantera, A., Mosquera-Losada, M., Herzog, F., & Herder, D. (2021). Agroforestry and the environment. Agroforestry Systems, 95, 767 - 774. https://doi.org/10.1007/s10457-021-00640-8.

82. Castle, S., Miller, D., Merten, N., Ordóñez, P., & Baylis, K. (2022). Evidence for the impacts of agroforestry on ecosystem services and human well-being in high-income countries: a systematic map. Environmental Evidence, 11. https://doi.org/10.1186/s13750-022-00260-4.

83. Wilson, M., & Lovell, S. (2016). Agroforestry - The Next Step in Sustainable and Resilient Agriculture. Sustainability, 8, 574. https://doi.org/10.3390/su8060574.

84. Villanueva-González, C., Pérez-Olmos, K., Mollinedo, M., & Lojka, B. (2024). Exploring agroforestry and food security in Latin America: a systematic review. Environment, Development and Sustainability. https://doi.org/10.1007/s10668-024-05352-4.

85. Zhao, Q., Xiong, W., Xing, Y., Sun, Y., Lin, X., & Dong, Y. (2018). Long-Term Coffee Monoculture Alters Soil Chemical Properties and Microbial Communities. Scientific Reports, 8. https://doi.org/10.1038/s41598-018-24537-2.

86. Fu, H., Zhang, G., Zhang, F., Sun, Z., Geng, G., & Li, T. (2017). Effects of Continuous Tomato Monoculture on Soil Microbial Properties and Enzyme Activities in a Solar Greenhouse. Sustainability, 9, 317. https://doi.org/10.3390/su9020317.

87. Hu, J., Wan, L., Wang, Y., Dai, K., Butterbach-Bahl, K., & Lin, S. (2025). The Decrease of Soil Microbial Community Diversity and Network Complexity Results in the Increase of Soil-Borne Diseases With Monocultural Years in Greenhouse Tomato Production Systems. Environmental Microbiology Reports, 17. https://doi.org/10.1111/1758-2229.70165.

88. Sileshi, G., Mafongoya, P., & Nath, A. (2020). Agroforestry Systems for Improving Nutrient Recycling and Soil Fertility on Degraded Lands. , 225-253. https://doi.org/10.1007/978-981-15-4136-0_8.

89. Abd-Alla, M., Al-Amri, S., & El-Enany, A. (2023). Enhancing Rhizobium–Legume Symbiosis and Reducing Nitrogen Fertilizer Use Are Potential Options for Mitigating Climate Change. Agriculture. https://doi.org/10.3390/agriculture13112092.

90. Lann, T., Bao, H., Lan, H., Zheng, H., & Yan, C. (2024). Hydro-mechanical effects of vegetation on slope stability: A review.. The Science of the total environment, 171691 . https://doi.org/10.1016/j.scitotenv.2024.171691.

91. Lee, E., Kumar, P., Knowles, J., Minor, R., Tran, N., Barron-Gafford, G., & Scott, R. (2021). Convergent Hydraulic Redistribution and Groundwater Access Supported Facilitative Dependency Between Trees and Grasses in a Semi-Arid Environment. Water Resources Research, 57. https://doi.org/10.1029/2020wr028103.

92. Buzhdygan, O., & Petermann, J. (2023). Multitrophic biodiversity enhances ecosystem functions, services and ecological intensification in agriculture. Journal of Plant Ecology. https://doi.org/10.1093/jpe/rtad019.

93. Udawatta, R., Rankoth, L., & Jose, S. (2019). Agroforestry and Biodiversity. Sustainability. https://doi.org/10.3390/su11102879.

94. Udawatta, R., Rankoth, L., & Jose, S. (2021). Agroforestry for Biodiversity Conservation. , 245-274. https://doi.org/10.1007/978-3-030-80060-4_10.

95. Santos, P., Crouzeilles, R., & Sansevero, J. (2019). Can agroforestry systems enhance biodiversity and ecosystem service provision in agricultural landscapes? A meta-analysis for the Brazilian Atlantic Forest. Forest Ecology and Management. https://doi.org/10.1016/j.foreco.2018.10.064.

96. Mupepele, A., Keller, M., & Dormann, C. (2021). European agroforestry has no unequivocal effect on biodiversity: a time-cumulative meta-analysis. BMC Ecology and Evolution, 21. https://doi.org/10.1186/s12862-021-01911-9.

97. Torralba, M., Fagerholm, N., Burgess, P., Moreno, G., & Plieninger, T. (2016). Do European agroforestry systems enhance biodiversity and ecosystem services? A meta-analysis. Agriculture, Ecosystems & Environment, 230, 150-161. https://doi.org/10.1016/j.agee.2016.06.002.

98. Santos, M., Cajaiba, R., Bastos, R., Gonzalez, D., Bakış, A., Ferreira, D., Leote, P., Da Silva, W., Cabral, J., Gonçalves, B., & Mosquera-Losada, M. (2022). Why Do Agroforestry Systems Enhance Biodiversity? Evidence From Habitat Amount Hypothesis Predictions. , 9. https://doi.org/10.3389/fevo.2021.630151.

99. Jose, S. (2012). Agroforestry for conserving and enhancing biodiversity. Agroforestry Systems, 85, 1-8. https://doi.org/10.1007/s10457-012-9517-5.

100. Pan, J., Chen, S., He, D., Zhou, H., Ning, K., , N., Li, K., Liao, D., Mi, W., Wu, Q., Zhang, C., & Dong, Z. (2025). Agroforestry increases soil carbon sequestration, especially in arid areas: A global meta-analysis. CATENA. https://doi.org/10.1016/j.catena.2024.108667.

101. T.M., K., Pal, S., Chand, P., & Kandpal, A. (2023). Carbon sequestration potential of agroforestry systems in Indian agricultural landscape: A Meta-Analysis. Ecosystem Services. https://doi.org/10.1016/j.ecoser.2023.101537.

102. Mayer, S., Wiesmeier, M., Sakamoto, E., Hübner, R., Cardinael, R., Kühnel, A., & Kögel-Knabner, I. (2022). Soil organic carbon sequestration in temperate agroforestry systems – A meta-analysis. Agriculture, Ecosystems & Environment. https://doi.org/10.1016/j.agee.2021.107689.

103. Sirimalle, M., Kumawat, C., Jiménez-Ballesta, R., Meena, R., Sharma, K., Patra, A., Mohapatra, K., & Kumawat, A. (2025). Impact of Long-Term Agroforestry Systems on Carbon Pools and Sequestration in Top and Deep Soil Layers of Semi-Arid Region of Western India. Forests. https://doi.org/10.3390/f16060946.

104. Jacobs, S., Webber, H., Niether, W., Grahmann, K., Lüttschwager, D., Schwartz, C., Breuer, L., & Bellingrath-Kimura, S. (2022). Modification of the microclimate and water balance through the integration of trees into temperate cropping systems. Agricultural and Forest Meteorology. https://doi.org/10.1016/j.agrformet.2022.109065.

105. Ripamonti, A., Finocchi, M., Pulina, A., Franca, A., Seddaiu, G., Turini, L., Mele, M., & Mantino, A. (2025). Effects of tree presence on forage yield and nutritive value in agroforestry livestock systems: a global systematic review. Agroforestry Systems, 99. https://doi.org/10.1007/s10457-025-01214-8.

106. Tranchina, M., Reubens, B., Frey, M., Mele, M., & Mantino, A. (2024). What challenges impede the adoption of agroforestry practices? A global perspective through a systematic literature review. Agroforestry Systems, 98, 1817 - 1837. https://doi.org/10.1007/s10457-024-00993-w.

107. Reshad, M., Asfaw, Z., & Mohammed, M. (2025). Benefits and challenges of smallholder farmers adopting agroforestry: evidences from the Eastern escarpment of Chercher massive, southeast Ethiopia. Agroforestry Systems, 99. https://doi.org/10.1007/s10457-024-01097-1.

108. Kpoviwanou, M., Sourou, B., & Ouinsavi, C. (2024). Challenges in adoption and wide use of agroforestry technologies in Africa and pathways for improvement: a systematic review. Trees, Forests and People. https://doi.org/10.1016/j.tfp.2024.100642.

109. Singh, A., Verma, S., Kumar, S., Singh, B., & Kumar, I. (2025). Assessment of Farmers' Perception and Adoption Barriers of Agroforestry Practices: Insights from the Awadh Region, Uttar Pradesh, India. Trees, Forests and People. https://doi.org/10.1016/j.tfp.2025.101034.

110. Mayele, J., & Sakurai, T. (2025). The adoption of agroforestry practices: the determinants and constraints among smallholder farmers in Juba County, South Sudan. Agroforestry Systems, 99. https://doi.org/10.1007/s10457-025-01316-3.

111. Sollen-Norrlin, M., Ghaley, B., & Rintoul, N. (2020). Agroforestry Benefits and Challenges for Adoption in Europe and Beyond. Sustainability. https://doi.org/10.3390/su12177001.

112. Prăvălie, R. (2021). Exploring the multiple land degradation pathways across the planet. Earth-Science Reviews, 220, 103689. https://doi.org/10.1016/j.earscirev.2021.103689.

113. Perović, V., Kadović, R., Đurđević, V., Pavlovic, D., Pavlović, M., Čakmak, D., Mitrović, M., & Pavlović, P. (2021). Major drivers of land degradation risk in Western Serbia: Current trends and future scenarios. Ecological Indicators, 123, 107377. https://doi.org/10.1016/j.ecolind.2021.107377.

114. Talukder, B., Ganguli, N., Matthew, R., Vanloon, G., Hipel, K., & Orbinski, J. (2021). Climate change-triggered land degradation and planetary health: A review. Land Degradation & Development, 32, 4509 - 4522. https://doi.org/10.1002/ldr.4056.

115. Roy, P., Pal, S., Chakrabortty, R., Chowdhuri, I., Saha, A., Ruidas, D., Islam, A., & Islam, A. (2024). Climate change and geo-environmental factors influencing desertification: a critical review.. Environmental science and pollution research international. https://doi.org/10.1007/s11356-024-32432-9.

116. Emadodin, I., Reinsch, T., & Taube, F. (2019). Drought and Desertification in Iran. Hydrology. https://doi.org/10.3390/hydrology6030066.

117. Wang, J., Lin, Y., Zhai, T., He, T., Qi, Y., Jin, Z., & Cai, Y. (2018). The role of human activity in decreasing ecologically sound land use in China. Land Degradation & Development, 29, 446 - 460. https://doi.org/10.1002/ldr.2874.

118. Huang, Y., Li, G., Zhao, Y., Yang, J., & Li, Y. (2023). Analysis of the Characteristics and Causes of Land Degradation and Development in Coastal China

(1982-2015). Remote. Sens., 15, 2249. https://doi.org/10.3390/rs15092249.

119. Liu, Y. (2018). Introduction to land use and rural sustainability in China. Land Use Policy, 74, 1-4. https://doi.org/10.1016/j.landusepol.2018.01.032.

120. Zahedifar, M. (2023). Assessing alteration of soil quality, degradation, and resistance indices under different land uses through network and factor analysis. CATENA. https://doi.org/10.1016/j.catena.2022.106807.

121. Badapalli, P., Kottala, R., Madiga, R., & Golla, V. (2022). An integrated approach for the assessment and monitoring of land degradation and desertification in semi-arid regions using physico-chemical and geospatial modeling techniques. Environmental Science and Pollution Research, 30, 116751-116764. https://doi.org/10.1007/s11356-022-23002-y.

122. Tarrasón, D., Ravera, F., Reed, M., Dougill, A., & Gonzalez, L. (2015). Land degradation assessment through an ecosystem services lens: Integrating knowledge and methods in pastoral semi-arid systems. Journal of Arid Environments, 124, 205-213. https://doi.org/10.1016/j.jaridenv.2015.08.002.

123. Stavi, I., & Lal, R. (2014). Achieving Zero Net Land Degradation: Challenges and opportunities. Journal of Arid Environments, 112, 44-51. https://doi.org/10.1016/j.jaridenv.2014.01.016.

124. Wang, J., Zhen, J., Hu, W., Chen, S., Lizaga, I., Zeraatpisheh, M., & Yang, X. (2023). Remote sensing of soil degradation: Progress and perspective. International Soil and Water Conservation Research. https://doi.org/10.1016/j.iswcr.2023.03.002.

125. Xing, L., Jin, D., Shen, C., Zhu, M., & Wu, J. (2025). Integrated Remote Sensing Evaluation of Grassland Degradation Using Multi-Criteria GDCI in Ili Prefecture, Xinjiang, China. Land. https://doi.org/10.3390/land14081592.

126. Zhang, N., Li, Z., Feng, Y., Li, X., & Tang, J. (2023). Development and application of a vegetation degradation classification approach for the temperate grasslands of northern China. Ecological Indicators. https://doi.org/10.1016/j.ecolind.2023.110857.

127. Li, Y., & Xiao, X. (2025). Deep Learning-Based Fusion of Optical, Radar, and LiDAR Data for Advancing Land Monitoring. Sensors (Basel, Switzerland), 25. https://doi.org/10.3390/s25164991.

128. Zhao, Z., Li, Y., Liu, K., Wu, C., Yu, B., Liu, G., & Wang, Y. (2025). Layered Soil Moisture Retrieval and Agricultural Application Based on Multi-Source Remote Sensing and Vegetation Suppression Technology: A Case Study of Youyi Farm, China. Remote Sensing. https://doi.org/10.3390/rs17132130.

129. Liu Yinggang. (2025). A Study on the Preparation and Application Properties of Superhydrophobic Composite Coatings (Master's Thesis, Xinjiang Agricultural University). Master's degree https://doi.org/10.27431/d.cnki.gxnyu.2025.000120.

130. Jiang, H., Gao, W., Liu, B., Chang, A., & Guo, Q. (2025). Quantifying soil wind erosion attribution in Inner Mongolia's desert grassland. Scientific Reports, 15. https://doi.org/10.1038/s41598-025-98339-8.

131. Mei, Y., , B., Hai, C., Chang, A., Chang, Y., Wang, Y., & Hu, Y. (2025). Spatiotemporal Dynamics and Driving Factors of Soil Wind Erosion in Inner Mongolia, China. Remote Sensing. https://doi.org/10.3390/rs17142365.

132. Wang, X., Chi, Y., & Song, S. (2024). Important soil microbiota's effects on plants and soils: a comprehensive 30-year systematic literature review. Frontiers in Microbiology, 15. https://doi.org/10.3389/fmicb.2024.1347745.

133. Shi, J., Wang, X., & Wang, E. (2022). Mycorrhizal Symbiosis in Plant Growth and Stress Adaptation: From Genes to Ecosystems.. Annual review of plant biology. https://doi.org/10.1146/annurev-arplant-061722-090342.

134. Yu, C., Wang, G., Zhang, H., Chen, H., & , Q. (2022). Biochar and Nitrification Inhibitor (Dicyandiamide) Combination Had a Double-Win Effect on Saline-Alkali Soil Improvement and Soybean Production in the Yellow River Delta, China. Agronomy. https://doi.org/10.3390/agronomy12123154.

135. Yang, R., Yang, Z., Yang, S., Chen, L., Xin, J., Xu, L., Zhang, X., Zhai, B.,

Wang, Z., Zheng, W., & Li, Z. (2023). Nitrogen inhibitors improve soil ecosystem multifunctionality by enhancing soil quality and alleviating microbial nitrogen limitation.. The Science of the total environment, 163238 . https://doi.org/10.1016/j.scitotenv.2023.163238.

136. Wei, W., Xiao, Q., Bai, Y., Wang, W., Wang, H., Yang, W., Liu, Y., Wu, K., Wu, D., Zhao, Y., & Gong, X. (2025). Soil quality and its determinants in saline-alkali land of northwest China. Frontiers in Environmental Science. https://doi.org/10.3389/fenvs.2025.1687358.

137. Yang, C., Chen, Y., Sun, W., Zhang, Q., Diao, M., & Sun, J. (2024). Extreme soil salinity reduces N and P metabolism and related microbial network complexity and community immigration rate.. Environmental research, 120361 . https://doi.org/10.1016/j.envres.2024.120361.

138. Nan, L., Guo, Q., Cao, S., & Zhan, Z. (2021). Diversity of bacterium communities in saline-alkali soil in arid regions of Northwest China. BMC Microbiology, 22. https://doi.org/10.1186/s12866-021-02424-7.

139. Wu, B., Zhang, M., Zeng, H., Tian, F., Potgieter, A., Qin, X., Yan, N., Chang, S., Zhao, Y., Dong, Q., Boken, V., Plotnikov, D., Guo, H., Wu, F., Zhao, H., Deronde, B., Tits, L., & Loupian, E. (2022). Challenges and opportunities in remote sensing-based crop monitoring: a review. National Science Review, 10. https://doi.org/10.1093/nsr/nwac290.

140. Guangdong Provincial Office of the Third National Land Survey Leading Group, Guangdong Provincial Department of Natural Resources, Guangdong Provincial Bureau of Statistics (2021). Main Data Bulletin of the third National Land Survey of Guangdong Province. Nanfang Daily News, 12-28(A07). https://doi.org/10.28597/n.cnki.nnfrb.2021.008466.

141. Feng Shanshan, Zhang Lei, Liu Xu, & Hu Yunfei (2024). Spatiotemporal evolution characteristics of cropland area and grain production in Guangdong Province during 2000-2020. Bulletin of Soil and Water Conservation, 44 (3): 252-262. https://doi.org/10.13961/j.cnki.stbctb.2024.03.026.

142. Zhu Wenrui. (2020). A Study on Land-Use Carbon Emissions and Their Influencing Factors in Guangdong Province (Master's Thesis, Guangdong University of Technology). Master's degree https://doi.org/10.27029/d.cnki.ggdgu.2020.002189.

143. Tan Xueling. (2018). Analysis of the Dynamic Evolution and Driving Forces of Land Degradation in the Yulin-Shenmu-Fuyang Coal Mining Area (Master's thesis, China University of Mining and Technology). Master's Li, T. H., & Zheng, L. N. (2012). Dynamics of soil erosion in the Yanhe River Basin from 2001 to 2010 based on the RUSLE model. Journal of Natural Resources, 27(07), 1164–1175.

144. Wang Shuxiang, Han Liusheng, Yang Ji, Li Yong, Zhao Qian, Liu Yangxiaoyue, & Wu Hao. (2021). An Improved Integrated Multi-Indicator Desertification Classification Method. Surveying and Mapping Bulletin, (04):8-12. https://doi.org/10.13474/j.cnki.11-2246.2021.0102.

145. Ministry of Environmental Protection of the People's Republic of China. (2015). Technical Specifications for the Assessment of Ecological and Environmental Conditions (HJ 192-2015). Beijing: China Environmental Science Press.

146. Ministry of Ecology and Environment of the People's Republic of China. (2020). Technical Specification for the Supervision of Ecological Conservation Redlines - Ecological Function Evaluation (Trial) (HJ 1142-2020). Beijing: China Environmental Science Press.

147. Zhang Sifan, Yu Yue, Ji Xinyu, & Liu Yuanyuan. (2024). A Study on the Spatiotemporal Distribution Characteristics of Soil Erosion in Liaoning Province Over the Past 20 Years Based on the RUSLE Model. Liaoning Forestry Science and Technology, (05), 27–34.

148. Bezerra, M., Santelli, R., Oliveira, E., Villar, L., & Escaleira, L. (2008). Response surface methodology (RSM) as a tool for optimization in analytical chemistry.. Talanta, 76 5, 965-77 . https://doi.org/10.1016/j.talanta.2008.05.019.

149. Ganaie, M., Tanveer, M., Suganthan, P., & Snášel, V. (2021). Oblique and rotation double random forest. Neural networks : the official journal of the International Neural Network Society, 153, 496-517 .

https://doi.org/10.1016/j.neunet.2022.06.012.

150. Hartmann, M., & Six, J. (2022). Soil structure and microbiome functions in agroecosystems. Nature Reviews Earth & Environment, 4, 4 - 18. https://doi.org/10.1038/s43017-022-00366-w.

151. Lv, C., Lian, A., Wang, Z., Jia, T., Sun, X., & Dong, R. (2022). A Spatiotemporal Pattern Analysis of High-Frequency Land-Use Changes in the Guangdong–Hong Kong–Macao Greater Bay Area, from 1990 to 2018. Land. https://doi.org/10.3390/land12010102

152. Xu B., Gui D.Y., Pu Q.Y., & Sha Z.P. (2025). The fate of nitrogen derived from green manure and its influence on crop N agronomic performance. European Journal of Agronomy, 168, 127646. https://doi.org/10.1016/j.eja.2025.127646

153. Ma D.K., Yin L.N., Ju W.L., Li X.K., Liu X.X., Deng X.P., & Wang S.W. (2021). Meta-analysis of green manure effects on soil properties and crop yield in northern China. Field Crops Research, 266, pp. 108146. https://doi.org/10.1016/j.fcr.2021.108146

154. Kichamu-wachira, E., Xu, Z.H., & Reardon-smith, K., et al. (2021). Effects of climate-smart agricultural practices on crop yields, soil carbon, and nitrogen pools in Africa: A meta-analysis. Journal of Soils and Sediments, 21(4), 1587−1597. https://doi.org/10.1007/s11368-021-02885-3

155. Liang, K.L., Wang, X.Q., & Du, Y.T., et al. (2022). Effect of legume green manure on yield increases of three major crops in China: A meta-analysis. Agronomy, 12(8), 1753. https://doi.org/10.3390/agronomy12081753

156. Zhang, S.H., Wang, J., & Rajan, G., et al. (2021). Effect of green manure on soil water and crop yield in the Loess Plateau of China: A meta-analysis. [Chinese Journal of Eco-Agriculture, 29(11), 1879−1892. https://doi.org/10.13930/j.cnki.cjea.210243

157. Jia, Q., Zheng, H.J., & Shi, Z.J., et al. (2024). Effects of straw and green manure addition on crop yield, soil properties and CH4 emissions: A meta-analysis.

Agronomy, 14(11), 2724. https://doi.org/10.3390/agronomy14112724

158. Xu, B., Gui, D.Y., & Peng, H.B., et al. (2024). Green manuring alters reactive N losses and N pools in arable soils: A meta-regression study. Science of the Total Environment, 934, 173256. https://doi.org/10.1016/j.scitotenv.2024.173256

159. Li, Y.J., Zhao, W.L., & Zhu, H.J., et al. (2024). Green manure mediated improvement in saline soils in China: A meta-analysis. Agronomy, 14(9), 2068. https://doi.org/10.3390/agronomy14092068

160. Ding, W.C., Xu, X.P., & He, P., et al. (2018). Improving yield and nitrogen use efficiency through alternative fertilization options for rice in China: A meta-analysis. Field Crops Research, 227, 11−18. https://doi.org/10.1016/j.fcr.2018.08.001

161. Garba, I.I., Bell, L.W., & Williams, A. (2022). Cover crop legacy impacts on soil water and nitrogen dynamics, and on subsequent crop yields in drylands: A meta-analysis. Agronomy for Sustainable Development, 42(3), 34. https://doi.org/10.1007/s13593-022-00760-0

162. Hu, Q.J., Thomas, B.W., & Powlson, D., et al. (2023). Soil organic carbon fractions in response to soil, environmental and agronomic factors under cover cropping systems: A global metaanalysis. Agriculture, Ecosystems & Environment, 355, 108591. https://doi.org/10.1016/j.agee.2023.108591

163. Yue, Q., Sun, J.F., & Hillier, J., et al. (2023). Green manure rotation and application increase rice yield and soil carbon in the Yangtze River valley of China. Pedosphere, 33(4), 589−599. https://doi.org/10.1016/j.pedsph.2022.11.009

164. Muhammad, I., Wang, J., & Sainju, U.M., et al. (2021). Cover cropping enhances soil microbial biomass and affects microbial community structure: A meta-analysis. Geoderma, 381, 114696. https://doi.org/10.1016/j.geoderma.2020.114696

165. Khan, A.A., Azeem, I., & Hui, J., et al. (2025). Non-leguminous green manures improve labile phosphorus availability and crop yield in agroecosystems: A global meta-analysis. Soil and Tillage Research, 248, 106430. https://doi.org/10.1016/j.still.2024.106430

166．Huang, H., Zhang, Z.H., & Wu, Q., et al. (2025). Global comprehensive evaluation shows that green manure enhances crop productivity while mitigating gaseous nitrogen losses. Resources, Conservation and Recycling, 220, 108351. https://doi.org/10.1016/j.resconrec.2025.108351

167．Li, Y.X., Zhang, G.N., & Miao, Y., et al. (2019). Effects of Vulpia myuros C.Gmelin planting on physical and chemical properties of soil in apple orchard. China Fruit & Vegetable, 39(10), 86−89. https://doi.org/10.19590/j.cnki.1008-1038.2019.10.020

168．Qin, J.Y., Zhang, Y., & Wang, X.M., et al. (2016). Effect of inter planting green manure on soil nutrient content of apple orchard. Northern Horticulture, (11), 169−172. https://doi.org/10.11937/bfyy.201611045

169．Tian, F., Gou, Z.G., & Chen, Y., et al. (2008). Study on yield increased by using the complete multiple cropping model of wheat-green manure-maize-soybean. Guizhou Agricultural Sciences, 36(6), 29−31.

170．Cao, W.D., Bao, X.G., & Xu, C.X., et al. (2017). Reviews and prospects on science and technology of green manure in China. Journal of Plant Nutrition and Fertilizer, 23(6), 1450−1461. https://doi.org/10.11674/zwyf.17291

171．Gao, S., Cao, W., Zhou, G., and Rees, R. M. (2021). “Bacterial communities in paddy soils changed by milk vetch as green manure: a study conducted across six provinces in South China”. Pedosphere, 31: 521–530.

172．He, H. B., Li, W. X., Zhang, Y. W., Cheng, J. K., and Xin, G. R. (2020). “Effects of Italian ryegrass residues as green manure on soil properties and bacterial communities under an Italian ryegrass (Lolium multiflorum L.)-rice (Oryza sativa L.) rotation”. Soil Tillage Res. 196:104487. https://doi.org/10.1016/j.still.2019.104487

173．Liu, G. Y., Chen, L. L., Shi, X. R., Yuan, Z. Y., Yuan, L. Y., Lock, T. R., and Kallenbach, R. L. (2019). “Changes in rhizosphere bacterial and fungal community composition with vegetation restoration in planted forests”. Land Degradation & Development, 30(10):1147-1157. https://doi.org/10.1002/ldr.3275

174. Liu, S., Wang, J., Pu, S., Blagodatskaya, E., and Razavi, B. S. (2020). "Impact of manure on soil biochemical properties: a global synthesis". Sci. Total Environ, 745:141003. https://doi.org/10.1016/j.scitotenv.2020.141003

175. Lovell, C., Bagwell, C., Cake, M., Márton, L., Piceno, Y., and Ringelberg, D. (2001). "Stability of a rhizosphere microbial community exposed to natural and manipulated environmental variability". FEMS Microbiology and. Ecology, 38:69–76. https://doi.org/10.1016/S0168-6496(01)00177-5

176. Fierer, N. (2017). "Embracing the unknown: disentangling the complexities of the soil microbiome". Nat. Rev. Microbial. 15: 579–590.

177. Wang, X., Bian, Q., Jiang, Y., Zhu, L., Chen, Y., Liang, Y., et al. (2021). "Organic amendments drive shifts in microbial community structure and keystone taxa which increase C mineralization across aggregate size classes". Soil Biol. Beachem. 153:108062. https://doi.org/10.1016/j.soilbio.2020.108062

178. Khan, M. I., Gwon, H. S., Alam, M. A., Song, H. J., and Kim, P. J. (2019). "Short-term effects of different green manure amendments on the composition of main microbial groups and microbial activity of a submerged rice cropping system". Applied Soil Ecology. 147:103400. https://doi.org/10.1016/j.apsoil.2019.103400

179. Banska, E., and Lasota, J. (2017). "β-Glucosidase activity of forest soil as an indicator of soil carbon accumulation" in: M. Lukac, P. Granny and M. Gamboni (eds.) Soil biological communities and ecosystem resilience. Sustainability in plant and crop protection, Cham: Springer.

180. Rukshana, F., Butterly, C. R., Xu, J. M., Baddock, J. A., and Tang, C. (2013). "Organic anion-to-acid ratio influence pH change of soils differing in initial pH". Journal of Soil. Sediment. 14: 407–414. https://doi.org/10.1007/s11368-013-0682-6

181. Yu, Y., Wu, M., Petropoulos, E., Zhang, J., Nie, J., and Liao, Y., et al. (2019). "Responses of paddy soil bacterial community assembly to different long-term fertilizations in Southeast China". Sci. Total Environ. 656: 625–633. https://doi.org/10.1016/j.scitotenv.2018.11.359

182．Zheng, W., Zhao, Z., Gong, Q., and Zhai, B. (2018). “Effects of cover crop in an apple orchard on microbial community composition, networks, and potential genes involved with degradation of crop residues in soil”. Biol. Fertil. Soils, 54:743–759. https://doi.org/10.1007/s00374-018-1298-1

183．Hu, X.F., Sun, R.H., & Sun, Y.F., et al. (2024). Analysis and suggestions on agroecological practices in China: A study based on 431 national eco-farms. Chinese Journal of Eco-Agriculture, 32(6), 1075−1085. https://doi.org/10.12357/cjea.20230676

184．Lyu, Y.T., Yu, A.Z., & Lyu, H.Q., et al. (2021). Composition and stability of soil aggregates in maize farmlands under different green manure utilization patterns in an oasis irrigation area. Chinese Journal of Eco-Agriculture], 29(7), 1194−1204. https://doi.org/10.13930/j.cnki.cjea.200913

185．Gao, S.B., Xu, Z.Y., & Jin, T., et al. (2019). Analysis of eco-agriculture construction based on rural revitalization in China. Chinese Journal of Eco-Agriculture, 2019, 27(2), 163−168. https://doi.org/10.13930/j.cnki.cjea.181009

APPENDIXE A

证书号第22458781号

专利公告信息

实用新型专利证书

实用新型名称：一种除草机

专 利 权 人：深圳市标准技术研究院（深圳市物品编码所）

地　　　址：518000 广东省深圳市福田区福田街道彩田路海天综合大厦13-15楼

发 明 人：黄超林

专 利 号：ZL 2024 2 1288746.2　　　授权公告号：CN 222465370 U

专利申请日：2024年06月06日　　　授权公告日：2025年02月14日

申请日时申请人：深圳市标准技术研究院（深圳市物品编码所）

申请日时发明人：黄超林

国家知识产权局依照中华人民共和国专利法进行审查，决定授予专利权，并予以公告。

专利权自授权公告之日起生效。专利权有效性及专利权人变更等法律信息以专利登记簿记载为准。

局长

申长雨

申长雨

国家知识产权局

2025年02月14日

第 1 页 (共 1 页)

Certificate No.22458781

Patent Publication Information

Utility Model Patent Certificate

Name of Utility Model: A Herbicide

Patent holder: Shenzhen Institute of Standard Technology (Shenzhen Institute of Product Coding)

Address: 1 Haitian Complex Building, Caitian Road, Futian Street, Futian District, Shenzhen City, Guangdong Province 518000
Floors
3-15 Inventor: Huang Cha-
olin

Patent No.: ZL 2024 2 1288746.2 Authorization Announcement No.: CN 222465370 U

Patent Application Date: June 6, 2024 Date of Authorization Notice: February 14,2025

Date of application: Applicant: Shenzhen Institute of Standard Technology (Shenzhen Institute of Product Coding)

Inventor at the time of application: Huang Chaolin

The National Intellectual Property Administration conducts examination in accordance with the Patent Law of the People's Republic of China, decides to grant patent rights, and publishes the decision. Patent rights take effect from the date of authorization announcement. Legal information regarding the validity of patent rights and changes in patent holders shall be based on the records in the patent register.

Director
Shen
Changyu

申长雨

14 February 2025

APPENDIXE B

证书号第8288871号

外观设计专利证书

外观设计名称：松土器

设　　计　　人：黄超林

专　　利　　号：ZL 2023 3 0238454.2

专利申请日：2023年04月26日

专　利　权　人：深圳市标准技术研究院

地　　　　址：518000 广东省深圳市福田区福田街道彩田路海天综合大厦13−15楼

授权公告日：2023年10月13日　　　授权公告号：CN 308264140 S

国家知识产权局依照中华人民共和国专利法经过初步审查，决定授予专利权，颁发外观设计专利证书并在专利登记簿上予以登记。专利权自授权公告之日起生效。专利权期限为十五年，自申请日起算。

专利证书记载专利权登记时的法律状况。专利权的转移、质押、无效、终止、恢复和专利权人的姓名或名称、国籍、地址变更等事项记载在专利登记簿上。

局长
申长雨

国家知识产权局
2023年10月13日

其他事项参见续页

证书号第8288871号

专利权人应当依照专利法及其实施细则规定缴纳年费。本专利的年费应当在每年04月26日前缴纳。未按照规定缴纳年费的，专利权自应当缴纳年费期满之日起终止。

申请日时本专利记载的申请人、设计人信息如下：

申请人：

深圳市标准技术研究院

设计人：

黄超林

Certificate No.8288871

Patent Certificate for Appearance Design

Appearance Design Name:Soil Looser

Principal Investigator: Huang Chaolin

Patent No.: ZL 2023 3 0238454.2

Patent application date: April 26,2023

Patent holder: Shenzhen Institute of Standard Technology

Address: Haitian Complex, Caitian Road, Futian Street, Futian District, Shenzhen City, Guangdong Province 518000
Floors 13-15 of the building

Date of authorization announcement: October 13,2023 Authorization Announcement No.: CN 308264140 S

The National Intellectual Property Administration, in accordance with the Patent Law of the People's Republic of China, conducts preliminary examination and decides to grant patent rights, issues a design patent certificate, and registers it in the patent register. The patent right takes effect from the date of authorization announcement. The term of the patent right is fifteen years, calculated from the date of application.

The patent certificate records the legal status at the time of patent registration. Matters such as the transfer, pledge, invalidation, termination, restoration of patent rights, as well as changes in the name or title, nationality, and address of the patentee, are documented in the patent register.

Director
Shen
Changyu

申长雨

13 October 2023

其他事项参见续页

Certificate No.8288871

The patentee shall pay the annual fee in accordance with the Patent Law and its implementing regulations. The annual fee for this patent shall be paid by April 26 each year. Failure to pay the annual fee as required will result in the termination of the patent right upon the expiration of the payment

The applicant and designer information recorded in this patent as of the application date are as follows:

proposer：

Shenzhen Institute of Standard Technology

credence：

Huang Chaolin

APPENDIXE C

土壤检测记录

点位名称	采样日期	pH（无量纲）	有效磷（mg/kg）	土壤容重（g/cm³）			机械组成（%）质地、质地名称无单位					有机质（g/kg）	速效钾（mg/kg）
				1	2	3	黏粒含量（D<0.002mm）	粉粒含量（0.02mm≥D>0.002mm）	砂粒级含量（2.0mm≥D>0.02mm）	质地*	质地名称*		
13-2地块土壤采样点1#（N22.754817°，E114.016351°）	2022.11.29	6.49	93.2	1.63	1.60	1.60	20	5	75	黏壤土	砂质黏壤土	11.5	100
					平均值：1.61								
13-2地块土壤采样点2#（N22.754796°，E114.019197°）		5.98	167	1.57	1.57	1.55	18	20	62	黏壤土	砂质黏壤土	10.2	124
					平均值：1.56								
13-3地块土壤采样点1#（N22.751575°，E114.022498°）		6.38	150	1.49	1.50	1.47	12	14	74	壤土	砂质壤土	6.82	57.7
					平均值：1.49								
13-3地块土壤采样点2#（N22.751788°，E114.021558°）		6.76	48.4	1.61	1.63	1.63	17	10	73	黏壤土	砂质黏壤土	6.76	98.2
					平均值：1.62								
13-3地块土壤采样点3#（N22.752054°，E114.020450°）		6.31	243	1.58	1.55	1.54	10	12	78	壤土	砂质壤土	9.04	61.2
					平均值：1.56								
13-3地块土壤采样点4#（N22.753243°，E114.020147°）		6.71	40.2	1.47	1.51	1.50	11	8	81	壤土	砂质壤土	11.8	88.2
					1.49								
13-3地块土壤采样点5#（N22.754088°，E114.018897°）		6.77	36.3	1.56	1.56	1.55	17	11	72	黏壤土	砂质黏壤土	11.2	47.1
					平均值：1.56								
13-4地块土壤采样点1#（N22.751236°，E114.023909°）	2022.11.30	5.57	3.21	1.36	1.39	1.41	6	30	64	壤土	砂质壤土	3.02	42.8
					平均值：1.39								
13-4地块土壤采样点2#（N22.751882°，E114.023372°）		5.6	21.0	1.37	1.35	1.37	29	37	34	黏土	壤质黏土	3.68	28.5
					平均值：1.36								
13-5地块土壤采样点1#（N22.766037°，E114.029876°）		7.03	7.47	1.39	1.40	1.38	19	21	60	黏壤土	砂质黏壤土	7.61	31.9
					平均值：1.39								
13-5地块土壤采样点2#（N22.766947°，E114.028801°）		5.58	9.03	1.26	1.27	1.28	17	42	41	黏壤土	黏壤土	3.75	38.7
					平均值：1.27								
13-5地块土壤采样点3#（N22.767436°，E114.028828°）		5.12	5.15	1.33	1.34	1.33	23	29	48	黏壤土	黏壤土	9.07	65.6
					平均值：1.33								
13-5地块土壤采样点4#（N22.768223°，E114.028183°）		5.87	19	1.41	1.43	1.43	25	28	47	黏壤土	黏壤土	10.4	68.3
					平均值：1.42								
14-1地块土壤采样点1#（N22.744581°，E114.054763°）	2022.12.01	7.01	79.2	1.33	1.34	1.35	24	12	64	黏壤土	砂质黏壤土	16.4	70.4
					平均值：1.34								
14-1地块土壤采样点2#（N22.744508°，E114.055296°）		6.79	53.0	1.45	1.43	1.45	12	12	76	壤土	砂质壤土	13.3	58.6
					平均值：1.44								
14-1地块土壤采样点3#（N22.745323°，E114.055946°）		6.27	354	1.51	1.51	1.52	8	12	80	壤土	砂质壤土	12.5	53.7
					平均值：1.51								

深圳中检

土壤检测记录

点位名称	采样日期	pH（无量纲）	有效磷（mg/kg）	土壤容重（g/cm³）			机械组成（%）质地、质地名称无单位					有机质（g/kg）	速效钾（mg/kg）
				1	2	3	黏粒含量（D<0.002mm）	粉粒含量（0.02mm≥D>0.002mm）	砂粒级含量（2.0mm≥D>0.02mm）	质地*	质地名称*		
14-1地块土壤采样点4#（N22.743147°，E114.056834°）	2022.12.01	6.03	336	1.48	1.48	1.49	17	14	69	黏壤土	砂质黏壤土	12.1	60
				平均值：1.48									
14-1地块土壤采样点5#（N22.742090°，E114.057091°）		6.13	587	1.36	1.35	1.35	18	15	67	黏壤土	砂质黏壤土	24.3	155
				平均值：1.35									
14-1地块土壤采样点6#（N22.741273°，E114.057280°）		6.37	565	1.41	1.37	1.38	15	5	80	壤土	砂质壤土	15	105
				平均值：1.39									
14-1地块土壤采样点7#（N22.740060°，E114.056051°）		5.28	476	1.46	1.47	1.45	13	11	76	壤土	砂质壤土	19.1	55.7
				平均值：1.46									
15-2地块土壤采样点1#（N22.745540°，E114.084423°）	2022.12.02	6.35	37.8	0.98	1.01	1.01	23	13	64	黏壤土	砂质黏壤土	25.5	91.0
				平均值：1.00									
15-2地块土壤采样点2#（N22.746695°，E114.084761°）		7.43	15.2	1.17	1.16	1.18	36	32	32	黏土	壤质黏土	15.2	62.8
				平均值：1.17									
15-2地块土壤采样点3#（N22.745200°，E114.087715°）		7.55	31.5	1.11	1.10	1.09	36	30	34	黏土	壤质黏土	32.2	224
				平均值：1.10									
16-1地块土壤采样点1#（N22.723461°，E114.084567°）		6.42	471	1.09	1.08	1.09	26	30	44	黏土	壤质黏土	23.7	182
				平均值：1.09									
16-1地块土壤采样点2#（N22.722266°，E114.084388°）		5.27	615	1.04	1.04	1.07	28	19	53	黏土	壤质黏土	35.8	162
				平均值：1.05									
16-2地块土壤采样点1#（N22.720560°，E114.082391°）		5.71	635	0.89	0.92	0.92	26	32	42	黏土	壤质黏土	29.2	184
				平均值：0.91									
16-2地块土壤采样点2#（N22.720716°，E114.083953°）		6.62	98.5	0.90	0.91	0.90	25	29	46	黏土	壤质黏土	37.5	292
				平均值：0.90									
16-2地块土壤采样点3#（N22.721508°，E114.083440°）		6.82	84.1	0.95	0.97	0.99	25	26	49	黏土	壤质黏土	31.8	266
				平均值：0.97									
15-2地块土壤采样点4#（N22.745505°，E114.085163°）	2022.12.13	6.81	21.1	1.37	1.38	1.38	35	28	37	黏土	壤质黏土	23.6	112
				平均值：1.38									
15-2地块土壤采样点5#（N22.745048°，E114.088372°）		7.06	16.0	1.32	1.31	1.32	40	24	36	黏土	壤质黏土	22.3	138
				平均值：1.32									

深圳中检联检测有限公司

2023年3月28日

APPENDIXE D

SampleID	Site	Time_month	Treatment	Biochar_t_ha	Lime_t_ha	Legume	pH	AP_mg_kg	SOC_percent	Porosity_percent	Cd_mg_kg	Cd_residual_percent	Shannon_diversity	Acidobacteria_percent	Actinobacteria_percent	Cost_yuan_ha
1	P1	0	Initial	0	0	none	5.2	8.5	1.2	34.5	0.32	15.2	2.85	13.2	7.9	0
2	P2	0	Initial	0	0	none	4.8	7.8	0.9	34.5	0.45	15.2	2.85	11.5	8.3	0
3	P3	0	Initial	0	0	none	5.4	9.3	1.4	34.5	0.25	15.2	2.85	14.8	7.6	0
4	P4	0	Initial	0	0	none	4.6	6.5	0.7	34.5	0.53	15.2	2.85	9.2	8.1	0
5	P5	0	Initial	0	0	none	5.6	10.1	1.6	34.5	0.18	15.2	2.85	16.3	7.8	0
6	P6	0	Initial	0	0	none	4.9	7.3	0.8	34.5	0.49	15.2	2.85	10.4	8.5	0
7	P7	0	Initial	0	0	none	5.3	8.2	1.1	34.5	0.35	15.2	2.85	12.8	8	0
8	P8	0	Initial	0	0	none	5.1	7.6	0.9	34.5	0.41	15.2	2.85	11	8.4	0
9	P9	0	Initial	0	0	none	5	7.1	0.8	34.5	0.47	15.2	2.85	10.1	7.9	0
10	P10	0	Initial	0	0	none	5.2	8.8	1.3	34.5	0.29	15.2	2.85	13.5	8.2	0
11	P4	12	Optimal_Combo	8	3	紫云英	7.52	15.28	2.31	65.3	0.08	79.1	4.07	20.8	13.7	3550
12	P4	12	Optimal_Combo	8	3	紫云英	7.48	15.14	2.29	65.2	0.08	78.5	4.03	20.3	13.6	3550
13	P4	12	Optimal_Combo	8	3	紫云英	7.53	15.35	2.33	65.5	0.07	79.5	4.09	21	13.8	3550
14	P4	12	Optimal_Combo	8	3	紫云英	7.49	15.09	2.28	65.1	0.08	78.8	4.04	20.5	13.5	3550
15	P4	12	Optimal_Combo	8	3	紫云英	7.55	15.41	2.35	65.6	0.07	80.2	4.11	21.2	13.9	3550
16	P4	12	Biochar_Lime_Opt	8	3	紫云英	7.29	14.48	2.12	62.9	0.11	72.6	3.94	19.5	12.9	3250
17	P4	12	Biochar_Lime_Opt	8	3	紫云英	7.31	14.55	2.14	63.1	0.1	73	3.96	19.7	13	3250
18	P4	12	Biochar_Lime_Opt	8	3	紫云英	7.28	14.42	2.1	62.7	0.11	72.4	3.92	19.3	12.8	3250
19	P4	12	Biochar_Lime_Opt	8	3	紫云英	7.33	14.6	2.15	63.3	0.1	73.5	3.98	19.9	13.1	3250
20	P4	12	Pareto_10_3.5_Milkvetch	10	3.5	紫云英	7.58	15.48	2.41	66.1	0.08	80.3	4.12	21.3	14	3550
21	P4	12	Pareto_10_3.5_Milkvetch	10	3.5	紫云英	7.62	15.62	2.44	66.4	0.07	81	4.15	21.6	14.2	3550
22	P4	12	Pareto_10_3.5_Milkvetch	10	3.5	紫云英	7.55	15.42	2.39	66	0.08	79.8	4.1	21.1	13.9	3550
23	P4	12	Pareto_10_3.5_Milkvetch	10	3.5	紫云英	7.6	15.55	2.42	66.3	0.07	80.7	4.13	21.5	14.1	3550
24	P4	12	Traditional_Lime_4.5	0	4.5	none	6.79	12.58	1.51	44.8	0.27	47.8	3.12	13.3	9.2	1800
25	P4	12	Traditional_Lime_4.5	0	4.5	none	6.82	12.65	1.53	45	0.26	48.2	3.14	13.5	9.3	1800
26	P4	12	Traditional_Lime_4.5	0	4.5	none	6.75	12.5	1.49	44.6	0.28	47.5	3.1	13.1	9.1	1800
27	P2	12	Optimal_Combo	8	3	紫云英	7.5	15.2	2.3	65.2	0.08	79	4.06	20.6	13.7	3550
28	P2	12	Optimal_Combo	8	3	紫云英	7.51	15.22	2.31	65.3	0.08	79.2	4.07	20.7	13.8	3550
29	P2	12	Optimal_Combo	8	3	紫云英	7.47	15.1	2.27	65	0.09	78.5	4.03	20.2	13.5	3550
30	P2	12	Optimal_Combo	8	3	紫云英	7.54	15.3	2.33	65.5	0.07	79.8	4.09	21	13.9	3550
31	P2	12	Biochar_Lime_Opt	8	3	紫云英	7.3	14.5	2.13	63	0.11	72.8	3.95	19.6	13	3250
32	P2	12	Biochar_Lime_Opt	8	3	紫云英	7.32	14.58	2.15	63.2	0.1	73.2	3.97	19.8	13.1	3250
33	P2	12	Biochar_Lime_Opt	8	3	紫云英	7.27	14.45	2.11	62.8	0.11	72.5	3.93	19.4	12.9	3250
34	P2	12	Biochar_Lime_Opt	8	3	紫云英	7.34	14.62	2.16	63.4	0.1	73.6	3.99	20	13.2	3250
35	P2	12	Pareto_10_3.5_Milkvetch	10	3.5	紫云英	7.59	15.5	2.42	66.2	0.08	80.5	4.13	21.4	14.1	3550
36	P2	12	Pareto_10_3.5_Milkvetch	10	3.5	紫云英	7.63	15.64	2.45	66.5	0.07	81.2	4.16	21.7	14.3	3550
37	P2	12	Pareto_10_3.5_Milkvetch	10	3.5	紫云英	7.56	15.44	2.4	66.1	0.08	80	4.11	21.2	14	3550
38	P2	12	Traditional_Lime_4.5	0	4.5	none	6.8	12.6	1.52	44.9	0.27	48	3.13	13.4	9.3	1800
39	P2	12	Traditional_Lime_4.5	0	4.5	none	6.83	12.68	1.54	45.1	0.26	48.4	3.15	13.6	9.4	1800
40	P2	12	Traditional_Lime_4.5	0	4.5	none	6.76	12.52	1.5	44.7	0.28	47.6	3.11	13.2	9.2	1800
41	P6	12	Optimal_Combo	8	3	紫云英	7.49	15.18	2.29	65.1	0.08	78.9	4.05	20.4	13.6	3550
42	P6	12	Optimal_Combo	8	3	紫云英	7.52	15.25	2.32	65.4	0.08	79.4	4.08	20.8	13.8	3550
43	P6	12	Optimal_Combo	8	3	紫云英	7.46	15.08	2.26	64.9	0.09	78.3	4.02	20.1	13.4	3550
44	P6	12	Optimal_Combo	8	3	紫云英	7.53	15.32	2.34	65.5	0.07	79.6	4.1	20.9	13.9	3550
45	P6	12	Biochar_Lime_Opt	8	3	紫云英	7.29	14.47	2.12	62.8	0.11	72.5	3.94	19.5	12.9	3250
46	P6	12	Biochar_Lime_Opt	8	3	紫云英	7.31	14.56	2.14	63.1	0.1	73.1	3.96	19.7	13.1	3250
47	P6	12	Biochar_Lime_Opt	8	3	紫云英	7.28	14.43	2.1	62.7	0.11	72.3	3.92	19.3	12.8	3250
48	P6	12	Pareto_10_3.5_Milkvetch	10	3.5	紫云英	7.6	15.52	2.43	66.3	0.08	80.6	4.14	21.5	14.2	3550
49	P6	12	Pareto_10_3.5_Milkvetch	10	3.5	紫云英	7.64	15.66	2.46	66.6	0.07	81.4	4.17	21.8	14.4	3550
50	P6	12	Pareto_10_3.5_Milkvetch	10	3.5	紫云英	7.57	15.46	2.41	66.2	0.08	80.2	4.12	21.3	14.1	3550

51	P6	12	Traditional_Lime_4.5	0	4.5	none	6.81	12.62	1.52	45	0.27	48.1	3.13	13.5	9.3	1800
52	P6	12	Traditional_Lime_4.5	0	4.5	none	6.84	12.7	1.54	45.2	0.26	48.5	3.15	13.7	9.4	1800
53	P9	12	Optimal_Combo	8	3	紫云英	7.5	15.21	2.31	65.3	0.08	79.1	4.07	20.6	13.7	3550
54	P9	12	Optimal_Combo	8	3	紫云英	7.51	15.23	2.32	65.4	0.08	79.3	4.08	20.7	13.8	3550
55	P9	12	Optimal_Combo	8	3	紫云英	7.48	15.12	2.28	65	0.09	78.6	4.04	20.3	13.5	3550
56	P9	12	Optimal_Combo	8	3	紫云英	7.53	15.31	2.34	65.6	0.07	79.7	4.1	21	13.9	3550
57	P9	12	Biochar_Lime_Opt	8	3	紫云英	7.3	14.51	2.13	63	0.11	72.7	3.95	19.6	13	3250
58	P9	12	Biochar_Lime_Opt	8	3	紫云英	7.32	14.59	2.15	63.2	0.1	73.3	3.97	19.8	13.2	3250
59	P9	12	Biochar_Lime_Opt	8	3	紫云英	7.27	14.46	2.11	62.8	0.11	72.4	3.93	19.4	12.9	3250
60	P9	12	Biochar_Lime_Opt	8	3	紫云英	7.34	14.63	2.16	63.4	0.1	73.7	3.99	20	13.3	3250
61	P9	12	Pareto_10_3.5_Milkvetch	10	3.5	紫云英	7.61	15.54	2.44	66.4	0.08	80.8	4.15	21.6	14.3	3550
62	P9	12	Pareto_10_3.5_Milkvetch	10	3.5	紫云英	7.65	15.68	2.47	66.7	0.07	81.6	4.18	21.9	14.5	3550
63	P9	12	Pareto_10_3.5_Milkvetch	10	3.5	紫云英	7.58	15.48	2.42	66.2	0.08	80.4	4.13	21.4	14.2	3550
64	P9	12	Traditional_Lime_4.5	0	4.5	none	6.82	12.64	1.53	45.1	0.27	48.2	3.14	13.5	9.3	1800
65	P9	12	Traditional_Lime_4.5	0	4.5	none	6.85	12.72	1.55	45.3	0.26	48.6	3.16	13.7	9.5	1800
66	P1	12	Biochar_Lime_Opt	8	3	紫云英	7.29	14.49	2.12	62.9	0.11	72.6	3.94	19.5	12.9	3250
67	P1	12	Biochar_Lime_Opt	8	3	紫云英	7.31	14.57	2.14	63.1	0.1	73.2	3.96	19.7	13.1	3250
68	P1	12	Biochar_Lime_Opt	8	3	紫云英	7.28	14.44	2.1	62.7	0.11	72.4	3.92	19.3	12.8	3250
69	P1	12	Biochar_Lime_Opt	8	3	紫云英	7.33	14.61	2.15	63.3	0.1	73.5	3.98	19.9	13.2	3250
70	P1	12	Biochar_Lime_Opt	8	3	紫云英	7.27	14.42	2.09	62.6	0.12	72.2	3.91	19.2	12.7	3250
71	P1	12	Pareto_6_2.5_Alfalfa	6	2.5	苜蓿	7.01	13.52	1.91	60.1	0.18	68.2	3.81	17.6	11.2	2850
72	P1	12	Pareto_6_2.5_Alfalfa	6	2.5	苜蓿	7.03	13.58	1.93	60.3	0.17	68.6	3.83	17.8	11.3	2850
73	P1	12	Pareto_6_2.5_Alfalfa	6	2.5	苜蓿	7	13.48	1.9	60	0.18	68	3.8	17.5	11.1	2850
74	P1	12	Pareto_6_2.5_Alfalfa	6	2.5	苜蓿	7.05	13.65	1.94	60.5	0.17	69	3.85	18	11.5	2850
75	P1	12	Chinese_milkvetch	0	0	紫云英	6.21	13.12	1.92	48.7	0.12	65.4	3.64	14.7	9.8	950
76	P1	12	Chinese_milkvetch	0	0	紫云英	6.18	13.08	1.9	48.5	0.12	65.1	3.62	14.5	9.7	950
77	P1	12	Chinese_milkvetch	0	0	紫云英	6.23	13.15	1.93	48.8	0.11	65.6	3.66	14.8	9.9	950
78	P1	12	Chinese_milkvetch	0	0	紫云英	6.19	13.1	1.91	48.6	0.12	65.3	3.63	14.6	9.7	950
79	P7	12	Biochar_Lime_Opt	8	3	紫云英	7.3	14.5	2.13	63	0.11	72.8	3.95	19.6	13	3250
80	P7	12	Biochar_Lime_Opt	8	3	紫云英	7.32	14.58	2.15	63.2	0.1	73.2	3.97	19.8	13.1	3250
81	P7	12	Biochar_Lime_Opt	8	3	紫云英	7.27	14.45	2.11	62.8	0.11	72.5	3.93	19.4	12.9	3250
82	P7	12	Biochar_Lime_Opt	8	3	紫云英	7.34	14.62	2.16	63.4	0.1	73.6	3.99	20	13.2	3250
83	P7	12	Pareto_6_2.5_Alfalfa	6	2.5	苜蓿	7.02	13.55	1.92	60.2	0.18	68.4	3.82	17.7	11.3	2850
84	P7	12	Pareto_6_2.5_Alfalfa	6	2.5	苜蓿	7.04	13.6	1.93	60.4	0.17	68.8	3.84	17.9	11.4	2850
85	P7	12	Pareto_6_2.5_Alfalfa	6	2.5	苜蓿	7.01	13.5	1.91	60.1	0.18	68.1	3.81	17.6	11.2	2850
86	P7	12	Chinese_milkvetch	0	0	紫云英	6.2	13.11	1.91	48.6	0.12	65.3	3.63	14.6	9.7	950
87	P7	12	Chinese_milkvetch	0	0	紫云英	6.22	13.14	1.92	48.7	0.12	65.5	3.65	14.7	9.8	950
88	P7	12	Chinese_milkvetch	0	0	紫云英	6.17	13.07	1.9	48.4	0.12	65	3.61	14.4	9.6	950
89	P8	12	Biochar_Lime_Opt	8	3	紫云英	7.29	14.48	2.12	62.9	0.11	72.6	3.94	19.5	12.9	3250
90	P8	12	Biochar_Lime_Opt	8	3	紫云英	7.31	14.56	2.14	63.1	0.1	73.1	3.96	19.7	13.1	3250
91	P8	12	Biochar_Lime_Opt	8	3	紫云英	7.28	14.43	2.1	62.7	0.11	72.3	3.92	19.3	12.8	3250
92	P8	12	Biochar_Lime_Opt	8	3	紫云英	7.33	14.6	2.15	63.3	0.1	73.5	3.98	19.9	13.2	3250
93	P8	12	Pareto_6_2.5_Alfalfa	6	2.5	苜蓿	7.03	13.57	1.93	60.3	0.18	68.5	3.83	17.8	11.3	2850
94	P8	12	Pareto_6_2.5_Alfalfa	6	2.5	苜蓿	7.05	13.62	1.94	60.5	0.17	68.9	3.85	18	11.5	2850
95	P8	12	Pareto_6_2.5_Alfalfa	6	2.5	苜蓿	7.02	13.52	1.92	60.2	0.18	68.2	3.82	17.7	11.2	2850
96	P8	12	Chinese_milkvetch	0	0	紫云英	6.21	13.13	1.92	48.7	0.12	65.4	3.64	14.7	9.8	950
97	P8	12	Chinese_milkvetch	0	0	紫云英	6.19	13.09	1.91	48.5	0.12	65.2	3.62	14.5	9.7	950
98	P8	12	Chinese_milkvetch	0	0	紫云英	6.23	13.16	1.93	48.8	0.11	65.7	3.66	14.9	9.9	950
99	P10	12	Biochar_Lime_Opt	8	3	紫云英	7.3	14.51	2.13	63	0.11	72.7	3.95	19.6	13	3250
100	P10	12	Biochar_Lime_Opt	8	3	紫云英	7.32	14.59	2.15	63.2	0.1	73.3	3.97	19.8	13.2	3250

101	P10	12	Biochar_Lime_Opt	8	3	紫云英	7.27	14.46	2.11	62.8	0.11	72.4	3.93	19.4	12.9	3250
102	P10	12	Biochar_Lime_Opt	8	3	紫云英	7.34	14.63	2.16	63.4	0.1	73.7	3.99	20	13.3	3250
103	P10	12	Pareto_6_2.5_Alfalfa	6	2.5	苜蓿	7.02	13.54	1.92	60.2	0.18	68.3	3.82	17.7	11.2	2850
104	P10	12	Pareto_6_2.5_Alfalfa	6	2.5	苜蓿	7.04	13.59	1.93	60.4	0.17	68.7	3.84	17.9	11.4	2850
105	P10	12	Pareto_6_2.5_Alfalfa	6	2.5	苜蓿	7.01	13.49	1.91	60	0.18	68	3.8	17.5	11.1	2850
106	P10	12	Chinese_milkvetch	0	0	紫云英	6.2	13.12	1.91	48.6	0.12	65.3	3.63	14.6	9.7	950
107	P10	12	Chinese_milkvetch	0	0	紫云英	6.22	13.15	1.92	48.7	0.12	65.5	3.65	14.8	9.8	950
108	P10	12	Chinese_milkvetch	0	0	紫云英	6.18	13.08	1.9	48.5	0.12	65.1	3.61	14.5	9.6	950
109	P3	12	Biochar_8	8	0	none	7.09	12.82	1.62	55.3	0.14	68.6	3.46	16.9	8.4	2850
110	P3	12	Biochar_8	8	0	none	7.11	12.85	1.63	55.5	0.13	68.9	3.48	17.1	8.5	2850
111	P3	12	Biochar_8	8	0	none	7.08	12.78	1.61	55.2	0.14	68.4	3.45	16.8	8.3	2850
112	P3	12	Biochar_8	8	0	none	7.12	12.88	1.64	55.6	0.13	69.1	3.49	17.2	8.6	2850
113	P3	12	Biochar_8	8	0	none	7.07	12.75	1.6	55.1	0.14	68.2	3.44	16.7	8.2	2850
114	P3	12	Lime_3	0	3	none	6.21	11.42	1.61	42.4	0.19	53.9	3.46	12.4	10.6	1200
115	P3	12	Lime_3	0	3	none	6.19	11.38	1.6	42.2	0.19	53.6	3.44	12.2	10.5	1200
116	P3	12	Lime_3	0	3	none	6.23	11.45	1.62	42.5	0.18	54.2	3.48	12.5	10.7	1200
117	P3	12	Lime_3	0	3	none	6.18	11.35	1.59	42.1	0.2	53.4	3.43	12.1	10.4	1200
118	P3	12	Soybean	0	0	大豆	5.82	10.52	1.51	45.1	0.21	48.2	3.11	12.6	8.9	800
119	P3	12	Soybean	0	0	大豆	5.79	10.48	1.5	45	0.21	48	3.09	12.4	8.8	800
120	P3	12	Soybean	0	0	大豆	5.83	10.55	1.52	45.2	0.2	48.5	3.12	12.7	9	800
121	P3	12	Soybean	0	0	大豆	5.8	10.5	1.51	45.1	0.21	48.1	3.1	12.5	8.9	800
122	P5	12	Biochar_8	8	0	none	7.1	12.83	1.62	55.4	0.14	68.7	3.47	17	8.5	2850
123	P5	12	Biochar_8	8	0	none	7.12	12.86	1.63	55.5	0.13	69	3.48	17.2	8.6	2850
124	P5	12	Biochar_8	8	0	none	7.09	12.79	1.61	55.3	0.14	68.5	3.46	16.9	8.4	2850
125	P5	12	Biochar_8	8	0	none	7.13	12.89	1.64	55.7	0.13	69.2	3.49	17.3	8.7	2850
126	P5	12	Lime_3	0	3	none	6.22	11.43	1.61	42.5	0.19	54	3.47	12.5	10.7	1200
127	P5	12	Lime_3	0	3	none	6.2	11.4	1.6	42.3	0.19	53.8	3.45	12.3	10.6	1200
128	P5	12	Lime_3	0	3	none	6.24	11.46	1.62	42.6	0.18	54.3	3.48	12.6	10.8	1200
129	P5	12	Lime_3	0	3	none	6.19	11.37	1.59	42.2	0.2	53.5	3.44	12.2	10.5	1200
130	P5	12	Soybean	0	0	大豆	5.83	10.53	1.52	45.2	0.21	48.3	3.12	12.7	9	800
131	P5	12	Soybean	0	0	大豆	5.8	10.49	1.5	45	0.21	48.1	3.1	12.5	8.9	800
132	P5	12	Soybean	0	0	大豆	5.84	10.56	1.52	45.3	0.2	48.6	3.13	12.8	9.1	800
133	P5	12	Soybean	0	0	大豆	5.81	10.51	1.51	45.1	0.21	48.2	3.11	12.6	8.9	800
134	P1	12	Chinese_milkvetch	0	0	紫云英	6.19	13.1	1.91	48.5	0.12	65.3	3.63	14.6	9.7	950
135	P1	12	Chinese_milkvetch	0	0	紫云英	6.21	13.13	1.92	48.7	0.12	65.5	3.65	14.7	9.8	950
136	P7	12	Chinese_milkvetch	0	0	紫云英	6.22	13.14	1.92	48.7	0.12	65.6	3.64	14.8	9.8	950
137	P7	12	Chinese_milkvetch	0	0	紫云英	6.2	13.11	1.91	48.6	0.12	65.4	3.63	14.6	9.7	950
138	P8	12	Chinese_milkvetch	0	0	紫云英	6.18	13.08	1.9	48.5	0.12	65.2	3.62	14.5	9.6	950
139	P8	12	Chinese_milkvetch	0	0	紫云英	6.22	13.15	1.93	48.8	0.11	65.7	3.66	14.9	9.9	950
140	P10	12	Chinese_milkvetch	0	0	紫云英	6.21	13.12	1.92	48.6	0.12	65.4	3.64	14.7	9.8	950
141	P10	12	Chinese_milkvetch	0	0	紫云英	6.19	13.1	1.91	48.5	0.12	65.3	3.63	14.6	9.7	950
142	P2	12	Traditional_Lime_4.5	0	4.5	none	6.78	12.55	1.5	44.7	0.27	47.7	3.11	13.2	9.1	1800
143	P4	12	Traditional_Lime_4.5	0	4.5	none	6.77	12.53	1.49	44.6	0.28	47.6	3.1	13.1	9	1800
144	P6	12	Traditional_Lime_4.5	0	4.5	none	6.79	12.57	1.51	44.8	0.27	47.9	3.12	13.3	9.2	1800
145	P9	12	Traditional_Lime_4.5	0	4.5	none	6.8	12.59	1.52	44.9	0.27	48	3.13	13.4	9.3	1800
146	P3	12	Biochar_8	8	0	none	7.1	12.81	1.61	55.2	0.14	68.5	3.46	16.9	8.4	2850
147	P5	12	Biochar_8	8	0	none	7.11	12.84	1.62	55.4	0.13	68.8	3.47	17.1	8.5	2850
148	P3	12	Lime_3	0	3	none	6.2	11.39	1.6	42.3	0.19	53.7	3.45	12.3	10.5	1200
149	P5	12	Lime_3	0	3	none	6.21	11.41	1.61	42.4	0.19	53.9	3.46	12.4	10.6	1200
150	P3	12	Soybean	0	0	大豆	5.81	10.5	1.5	45	0.21	48	3.1	12.5	8.8	800

151	P5	12	Soybean	0	0	大豆	5.82	10.52	1.51	45.1	0.21	48.2	3.11	12.6	8.9	800
152	P1	12	Pareto_6_2.5_Alfalfa	6	2.5	苜蓿	7	13.47	1.89	60	0.18	68	3.8	17.5	11.1	2850
153	P1	12	Pareto_6_2.5_Alfalfa	6	2.5	苜蓿	7.03	13.56	1.92	60.3	0.17	68.6	3.83	17.8	11.3	2850
154	P7	12	Pareto_6_2.5_Alfalfa	6	2.5	苜蓿	7.01	13.51	1.91	60.1	0.18	68.2	3.81	17.6	11.2	2850
155	P7	12	Pareto_6_2.5_Alfalfa	6	2.5	苜蓿	7.04	13.6	1.93	60.4	0.17	68.8	3.84	17.9	11.4	2850
156	P8	12	Pareto_6_2.5_Alfalfa	6	2.5	苜蓿	7.02	13.53	1.92	60.2	0.18	68.3	3.82	17.7	11.2	2850
157	P8	12	Pareto_6_2.5_Alfalfa	6	2.5	苜蓿	7.05	13.61	1.94	60.5	0.17	68.9	3.85	18	11.5	2850
158	P10	12	Pareto_6_2.5_Alfalfa	6	2.5	苜蓿	7.01	13.5	1.9	60	0.18	68.1	3.81	17.6	11.1	2850
159	P10	12	Pareto_6_2.5_Alfalfa	6	2.5	苜蓿	7.03	13.57	1.93	60.3	0.17	68.5	3.83	17.8	11.3	2850
160	P2	12	Biochar_Lime_Opt	8	3	紫云英	7.31	14.53	2.13	63.1	0.11	72.9	3.96	19.7	13	3250
161	P2	12	Biochar_Lime_Opt	8	3	紫云英	7.28	14.44	2.1	62.8	0.11	72.3	3.92	19.4	12.8	3250
162	P4	12	Biochar_Lime_Opt	8	3	紫云英	7.32	14.57	2.14	63.2	0.1	73.1	3.97	19.8	13.1	3250
163	P4	12	Biochar_Lime_Opt	8	3	紫云英	7.29	14.49	2.12	62.9	0.11	72.7	3.94	19.5	12.9	3250
164	P6	12	Biochar_Lime_Opt	8	3	紫云英	7.33	14.6	2.15	63.3	0.1	73.4	3.98	20	13.2	3250
165	P6	12	Biochar_Lime_Opt	8	3	紫云英	7.3	14.52	2.13	63	0.11	72.8	3.95	19.6	13	3250
166	P9	12	Biochar_Lime_Opt	8	3	紫云英	7.31	14.55	2.14	63.1	0.11	73	3.96	19.7	13.1	3250
167	P9	12	Biochar_Lime_Opt	8	3	紫云英	7.28	14.47	2.11	62.8	0.11	72.5	3.93	19.4	12.9	3250
168	P1	12	Biochar_Lime_Opt	8	3	紫云英	7.32	14.59	2.15	63.2	0.1	73.3	3.97	19.8	13.2	3250
169	P1	12	Biochar_Lime_Opt	8	3	紫云英	7.29	14.5	2.12	62.9	0.11	72.6	3.94	19.5	12.9	3250
170	P7	12	Biochar_Lime_Opt	8	3	紫云英	7.31	14.54	2.14	63.1	0.11	72.9	3.96	19.7	13.1	3250
171	P7	12	Biochar_Lime_Opt	8	3	紫云英	7.28	14.46	2.11	62.8	0.11	72.4	3.93	19.4	12.8	3250
172	P8	12	Biochar_Lime_Opt	8	3	紫云英	7.32	14.58	2.15	63.2	0.1	73.2	3.97	19.8	13.2	3250
173	P8	12	Biochar_Lime_Opt	8	3	紫云英	7.29	14.51	2.13	63	0.11	72.7	3.94	19.5	13	3250
174	P10	12	Biochar_Lime_Opt	8	3	紫云英	7.31	14.56	2.14	63.1	0.1	73.1	3.96	19.7	13.1	3250
175	P10	12	Biochar_Lime_Opt	8	3	紫云英	7.28	14.48	2.12	62.8	0.11	72.5	3.93	19.4	12.9	3250
176	P3	12	Biochar_8	8	0	none	7.09	12.8	1.61	55.2	0.14	68.5	3.45	16.8	8.4	2850
177	P3	12	Biochar_8	8	0	none	7.11	12.83	1.62	55.4	0.13	68.7	3.47	17	8.5	2850
178	P5	12	Biochar_8	8	0	none	7.1	12.82	1.62	55.3	0.14	68.6	3.46	16.9	8.5	2850
179	P5	12	Biochar_8	8	0	none	7.12	12.85	1.63	55.5	0.13	68.9	3.48	17.1	8.6	2850
180	P3	12	Lime_3	0	3	none	6.19	11.38	1.6	42.3	0.19	53.6	3.44	12.2	10.5	1200
181	P3	12	Lime_3	0	3	none	6.21	11.42	1.61	42.4	0.19	53.9	3.46	12.4	10.7	1200
182	P5	12	Lime_3	0	3	none	6.2	11.4	1.6	42.3	0.19	53.7	3.45	12.3	10.6	1200
183	P5	12	Lime_3	0	3	none	6.22	11.44	1.61	42.5	0.18	54.1	3.47	12.5	10.8	1200
184	P3	12	Soybean	0	0	大豆	5.8	10.48	1.5	45	0.21	48	3.09	12.4	8.8	800
185	P3	12	Soybean	0	0	大豆	5.82	10.51	1.51	45.1	0.21	48.2	3.11	12.6	8.9	800
186	P5	12	Soybean	0	0	大豆	5.81	10.5	1.5	45	0.21	48.1	3.1	12.5	8.8	800
187	P5	12	Soybean	0	0	大豆	5.83	10.53	1.52	45.2	0.2	48.3	3.12	12.7	9	800
188	P1	12	Chinese_milkvetch	0	0	紫云英	6.2	13.11	1.91	48.6	0.12	65.3	3.63	14.6	9.7	950
189	P1	12	Chinese_milkvetch	0	0	紫云英	6.18	13.07	1.89	48.4	0.12	65	3.61	14.4	9.6	950
190	P7	12	Chinese_milkvetch	0	0	紫云英	6.21	13.12	1.92	48.6	0.12	65.4	3.64	14.7	9.8	950
191	P7	12	Chinese_milkvetch	0	0	紫云英	6.19	13.09	1.91	48.5	0.12	65.2	3.62	14.5	9.7	950
192	P8	12	Chinese_milkvetch	0	0	紫云英	6.22	13.14	1.92	48.7	0.12	65.5	3.65	14.8	9.8	950
193	P8	12	Chinese_milkvetch	0	0	紫云英	6.2	13.11	1.91	48.6	0.12	65.3	3.63	14.6	9.7	950
194	P10	12	Chinese_milkvetch	0	0	紫云英	6.21	13.13	1.92	48.7	0.12	65.5	3.64	14.7	9.8	950
195	P10	12	Chinese_milkvetch	0	0	紫云英	6.19	13.09	1.91	48.5	0.12	65.2	3.62	14.5	9.7	950
196	P2	12	Optimal_Combo	8	3	紫云英	7.5	15.19	2.3	65.2	0.08	79	4.05	20.5	13.6	3550
197	P4	12	Optimal_Combo	8	3	紫云英	7.52	15.26	2.32	65.4	0.07	79.3	4.08	20.7	13.8	3550
198	P6	12	Optimal_Combo	8	3	紫云英	7.49	15.16	2.28	65.1	0.08	78.8	4.04	20.4	13.5	3550
199	P9	12	Optimal_Combo	8	3	紫云英	7.51	15.22	2.31	65.3	0.08	79.2	4.06	20.6	13.7	3550
200	P9	12	Optimal_Combo	8	3	紫云英	7.53	15.28	2.33	65.5	0.07	79.5	4.09	20.8	13.9	3550

APPENDIXE E

Treatment	Replicate	Period	Bacterial_Chao1	Fungal_Shannon	pH	SOM_gkg	TN_gkg	TP_gkg	AN_mgkg	OP_mgkg
CF	1	Growth	1124.56	5.44	5.12	2.71	0.48	1.45	55.12	4.61
CF	1	Incorporation	393.12	3.43	5.12	2.71	0.48	1.45	55.12	4.61
CF	2	Growth	1089.34	5.47	4.56	2.48	0.62	0.88	55.92	4.32
CF	2	Incorporation	368.91	3.38	4.56	2.48	0.62	0.88	55.92	4.32
CF	3	Growth	1105.78	5.46	4.83	2.69	0.44	1.27	54.78	4.48
CF	3	Incorporation	396.45	3.47	4.83	2.69	0.44	1.27	54.78	4.48
CK	1	Growth	1154.56	4.63	5.01	3.53	0.56	1.03	52.56	4.29
CK	1	Incorporation	578.34	3.16	5.01	3.53	0.56	1.03	52.56	4.29
CK	2	Growth	1142.31	4.58	5.05	3.21	1.12	0.71	54.12	4.32
CK	2	Incorporation	601.23	3.09	5.05	3.21	1.12	0.71	54.12	4.32
CK	3	Growth	1167.89	4.71	4.97	3.89	0.23	1.32	51.23	4.27
CK	3	Incorporation	559.12	3.21	4.97	3.89	0.23	1.32	51.23	4.27
HAF	1	Growth	1734.05	7.19	3.17	18.86	2.64	6.14	32.91	7.36
HAF	1	Incorporation	688.7	3.94	3.17	18.86	2.64	6.14	32.91	7.36
HAF	2	Growth	1601.23	7.01	3.32	19.45	2.65	6.2	31.98	7.5
HAF	2	Incorporation	623.45	3.82	3.32	19.45	2.65	6.2	31.98	7.5
HAF	3	Growth	1845.67	7.38	3.01	18.12	2.63	6.09	33.45	7.23
HAF	3	Incorporation	743.12	4.05	3.01	18.12	2.63	6.09	33.45	7.23
MG	1	Growth	1760	5.19	2.02	71.81	1.47	6.12	25.36	1.82
MG	1	Incorporation	552.89	3.49	2.02	71.81	1.47	6.12	25.36	1.82
MG	2	Growth	1823.45	5.28	2.31	71.02	0.92	6.78	24.98	2.12
MG	2	Incorporation	489.23	3.61	2.31	71.02	0.92	6.78	24.98	2.12
MG	3	Growth	1698.12	5.09	1.89	72.45	1.98	5.56	25.78	1.56
MG	3	Incorporation	623.45	3.38	1.89	72.45	1.98	5.56	25.78	1.56
MH	1	Growth	1978.34	5.75	3.22	38.66	0.68	4.28	14.7	2.81
MH	1	Incorporation	499.93	3.48	3.22	38.66	0.68	4.28	14.7	2.81
MH	2	Growth	2012.34	5.82	2.98	39.12	1.12	4.89	13.98	3.12
MH	2	Incorporation	478.23	3.52	2.98	39.12	1.12	4.89	13.98	3.12
MH	3	Growth	1945.67	5.68	3.45	38.23	0.32	3.89	15.23	2.56
MH	3	Incorporation	521.34	3.45	3.45	38.23	0.32	3.89	15.23	2.56
MO	1	Growth	2235.82	5.66	5.27	20.77	1.74	2.23	25.47	2.31
MO	1	Incorporation	517.3	2.67	5.27	20.77	1.74	2.23	25.47	2.31
MO	2	Growth	2289.34	5.71	4.89	21.23	1.23	2.56	24.98	2.56
MO	2	Incorporation	489.23	2.45	4.89	21.23	1.23	2.56	24.98	2.56
MO	3	Growth	2189.34	5.62	5.67	20.23	2.23	1.98	25.98	2.12
MO	3	Incorporation	545.67	2.89	5.67	20.23	2.23	1.98	25.98	2.12
OMF	1	Growth	2017	9.59	4.15	10.44	1.71	1.18	18.34	2.49
OMF	1	Incorporation	234.41	4	4.15	10.44	1.71	1.18	18.34	2.49
OMF	2	Growth	1956.78	9.67	4.23	9.98	1.32	0.89	17.89	2.67
OMF	2	Incorporation	212.34	3.92	4.23	9.98	1.32	0.89	17.89	2.67
OMF	3	Growth	2089.34	9.51	4.07	10.89	2.12	1.56	19.12	2.34
OMF	3	Incorporation	256.78	4.08	4.07	10.89	2.12	1.56	19.12	2.34
RG	1	Growth	1464.64	5.57	5.44	8.23	6.47	2.12	87.33	6.46
RG	1	Incorporation	455.1	2.89	5.44	8.23	6.47	2.12	87.33	6.46
RG	2	Growth	1398.23	5.12	5.21	8.01	7.12	2.56	85.98	6.67
RG	2	Incorporation	489.34	3.01	5.21	8.01	7.12	2.56	85.98	6.67
RG	3	Growth	1512.34	5.89	5.67	8.45	5.98	1.89	88.23	6.23
RG	3	Incorporation	423.45	2.78	5.67	8.45	5.98	1.89	88.23	6.23
RH	1	Growth	1446.11	5.78	7.23	20.14	5.66	4.22	30.63	6.92
RH	1	Incorporation	4565.73	3.69	7.23	20.14	5.66	4.22	30.63	6.92
RH	2	Growth	1498.23	5.89	7.01	19.89	5.12	4.56	29.98	7.12
RH	2	Incorporation	4623.45	3.56	7.01	19.89	5.12	4.56	29.98	7.12
RH	3	Growth	1398.34	5.67	7.45	20.45	6.23	3.98	31.23	6.78
RH	3	Incorporation	4512.34	3.82	7.45	20.45	6.23	3.98	31.23	6.78
RO	1	Growth	2015.5	5.6	2.75	10.85	3.71	2.23	82.73	2.42
RO	1	Incorporation	530.23	3.75	2.75	10.85	3.71	2.23	82.73	2.42
RO	2	Growth	1898.34	5.78	2.45	11.23	4.23	1.89	83.45	2.67
RO	2	Incorporation	489.34	3.82	2.45	11.23	4.23	1.89	83.45	2.67
RO	3	Growth	2123.45	5.45	3.01	10.45	3.23	2.56	81.98	2.23
RO	3	Incorporation	569.78	3.68	3.01	10.45	3.23	2.56	81.98	2.23

APPENDIXE F


深圳中检联检测有限公司
时 间: 2022.11.29 10:00
经纬度: 22.754860 N,114.016360 E


深圳中检联检测有限公司
时 间: 2022.11.29 10:47
地 点: 深圳市 · 明华工业园
经纬度: 22.754951 N,114.019198 E


深圳中检联检测有限公司
时 间: 2022.11.29 11:42
经纬度: 22.751594 N,114.022452 E


深圳中检联检测有限公司
时 间: 2022.11.29 14:34
经纬度: 22.751798 N,114.021576 E


深圳中检联检测有限公司
时 间: 2022.11.29 15:42
经纬度: 22.753262 N,114.020136 E


深圳中检联检测有限公司
时 间: 2022.11.28 16:22
经纬度: 22.754112 N,114.018864 E

APPENDIXE G

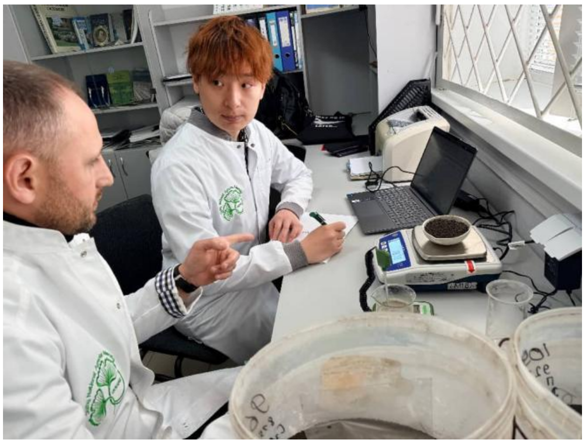
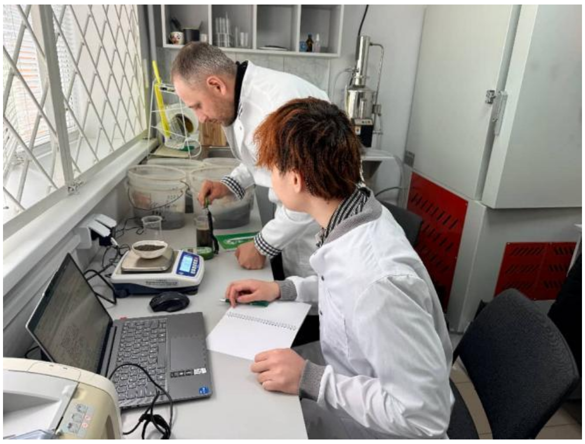


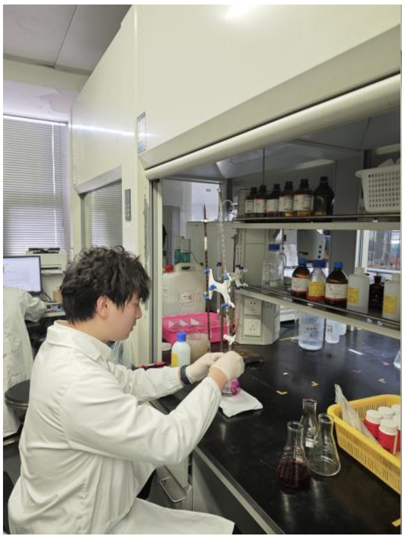

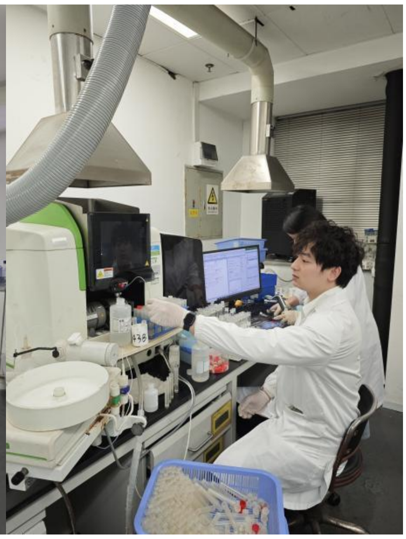

APPENDIXE H

研究成果应用证明

兹有黄超林同志，于 2022 年至 2026 年在苏梅国立农业大学（Sumy National Agrarian University）攻读博士学位，其博士学位论文题目为《广东省退化土地修复中的农林复合业特征》（Agroforestry features of restoration of degraded lands in the conditions of the Guangdong province）。

该论文围绕广东省土地修复、农林业等开展系统性研究，形成了具有较高学术价值与实践应用价值的研究成果。经深圳市标准技术研究院实际应用，纳入员工专业培训课程。

研究成果应用内容真实、成效客观，符合博士学位论文成果应用的相关要求，特此确认。

深圳市标准技术研究院

Certificate of Research Application

Huang Chaolin pursued a doctoral degree at Sumy National Agrarian University from 2022 to 2026. The title of his doctoral dissertation is "Agroforestry features of restoration of degraded lands in the conditions of the Guangdong province."

This dissertation conducts systematic research on land restoration and agroforestry in Guangdong Province, yielding research outcomes of high academic and practical value. Following practical application by the Shenzhen Institute of Standards and Technology, the findings have been incorporated into the institute's professional training curriculum for employees.

The content of the research application is authentic, and the results are objective, meeting the relevant requirements for the application of doctoral dissertation outcomes. This is hereby confirmed.

Shenzhen Institute of Standards and Technology